Transition Metal Catalyzed Hydroborations with Pinacolborane: New Applications and Mechanistic Investigations

by

Yonek Bryan Hleba

A thesis submitted to the Department of Chemistry

in conformity with the requirements for

the degree of Doctor of Philosophy

Queen's University

Kingston, Ontario, Canada

August 2007

Abstract

A methodology for the catalytic asymmetric hydroboration of vinylarenes with pinacolborane has been developed. Use of pinacolborane in hydroboration, especially catalytic asymmetric hydroboration grants direct access to chiral boronate esters, without the cryogenic temperatures required for catalytic hydroboration with catecholborane and the subsequent transesterification with excess pinacol. These chiral boronate esters were then subjected to a homologation/oxidation sequence previously refined in our labs to prepare Naproxen™ in 66% yield and 88% enantiopurity from its corresponding vinyl arene precursor.

A survey of metal catalysts, solvents and ligands revealed remarkable changes in regioselectivity with changes in metal. Rhodium catalysts in combination with pinacolborane were able to provide regioselectivity for the secondary branched isomer equivalent to those obtained with catecholborane. Iridium catalysts showed a near perfect regioselectivity for the primary linear isomer. With respect to the choice of chiral ligand, complete reversal in the enantiomer obtained was observed with the choice of hydroborating reagent from catecholborane to pinacolborane.

In order to understand the regioselectivity observed under iridium catalysis, deuterium labeling studies were undertaken. A synthesis of the deuterated hydroboration reagent pinacolborane was first completed. From the results of these studies, in combination with published thermodynamic data, a mechanism for the iridium catalyzed hydroboration of alkenes was proposed.

Acknowledgements

First and foremost, I owe my deepest gratitude and thanks to my supervisor Dr. Cathleen Crudden. Her inspiration, guidance and support have been invaluable to me in my research and her encouragement has taught me the patience and perseverance to bring out the best in my efforts.

The environment in the lab cannot be underestimated in its contributions to an enjoyable and productive working atmosphere. I am indebted to the past members of the lab, Dr. Austin Chen for teaching me the art and appreciation of organic synthesis and to Dr. Daryl Allen for imparting the skills and steady hand to manipulate sensitive materials required for catalysis. As I leave the lab, I know that the next generation, Kevin McEleney, Steve Dickson, Jeremy Praetorius, Jon Webb, Jenny Du, Ben Glasspoole and Chris Lata will each make their own mark on the history of the Crudden lab. They have made the excitement and tribulations of research more than worth the endeavor.

The unquestioning and unflinching support of my parents, John and Elaine has been a constant comfort. I know that without them, I could not have come as far as I have. The simple support of my family has allowed me to achieve so much. Even my siblings, Anya and Michael allowed me to take pride in my work, since they asked me how my research into flubber was progressing.

It is said that behind even good man you will find a great woman. That statement is nothing but truth. I am incredibly fortunate to have my girlfriend, Anna Lisa Gill, who has always been there for me. Her encouragement and role as “my better half” are immeasurable.

My sincere thanks go to Dr. L. Calhoun (UNB) and Dr. F. Sauriol (Queen's) for assistance with NMR experiments. Dr. B. Keller, Dr. Y. She and Jie Sui performed mass spectrometry analysis.

The memory of Phyllis Taylor, a fellow chemist who influenced my early exposure to science and nature, has been a personal guardian angel and whose hidden hand has aided me in ways I cannot fully comprehend.

Recreation outside of the lab, mainly cards and fishing I have enjoyed the company of Chris Ablan, Eric Anctil, John Brownie, David Heldebrant, Mark Moran, Greg Potter, Ryan Simms, and Goran Stojcevic. While at times, playing poker with these clowns was infuriating and costly to say the least, I wouldn't have it any other way.

Lastly, I am thankful for the financial assistance of UNB and Queen's, Shire Biochem (formerly Biochem Pharma) and NSERC.

"Luck is probability taken personally"

-Penn Jillette

Statement of Originality

The research contained in this thesis was carried out by the author in the Department of Chemistry at Queen's University and the University of New Brunswick under the guidance and supervision of Dr. Cathleen M. Crudden.

This work reports on the hydroboration of alkenes with pinacolborane, catalyzed by rhodium and iridium transition metals. The effects of substrate, ligand and reaction conditions are discussed. This work also describes the results obtained from deuterium labeling experiments of alkenes obtained from the use of deuteriopinacolborane with rhodium and iridium metal catalysts. The relevance they provide towards the understanding of the mechanism of transition metal hydroboration is highlighted.

Table of Contents

List of Figures

List of Tables

List of Equations

List of Schemes

List of Abbreviations

Ar	aryl
9-BBN	9-borabicyclo[3.3.1]nonane
BDPP	2,4-bis(diphenylphosphino)pentane
BINAP	2,2’-bis(diphenylphosphino)-1,1’-binaphthyl
BINAPHOS	(2-(diphenylphosphino)-1,1’-binaphthalene-2’-yl)-(1,1’-binaphthalene-2,2’-yl)phosphate
B:L	branched-to-linear
COD	1,5-cyclooctadiene
D	deuterium
DBU	1,8-dizazbicyclo[5.4.0]undec-7-ene
DIOP	2,3-*O*-isopropylidene-2,3-dihydroxy-1,4-bis(diphenylphosphino)butane
DIPA	diisopropylamine
DME	1,2-dimethoxyethane
DMF	*N*,*N*-dimethylformamide
DPPB	1,4-bis(diphenylphosphino)butane
DPPE	1,2-bis(diphenylphosphino)ethane
DPPF	1,1’-bis(diphenylphosphino)ferrocene
DPPP	1,3-bis(diphenylphosphino)propane
ee	enantiomeric excess
equiv	equivalents
Et	ethyl

GC	gas chromatography
HBpin	pinacolborane; 4,4,5,5-tetramethyl-1,3,2-dioxaborolane
HBcat	catecholborane; 1,3,2-benzodioxaborole
HPLC	high pressure liquid chromatography
HRMS	high resolution mass spectrometry
Hz	hertz
IR	infrared spectroscopy
J	coupling constant
L	ligand
LDA	lithium diisopropylamide
Me	methyl
NBD	2,5-norbornadiene
NMR	nuclear magnetic resonance spectroscopy
NSAID	non-steroidal anti-inflammatory drug
Ph	phenyl
PHENAP	6-(2'-diphenylphosphino-1'-naphthyl)phenanthridine
PMA	phosphomolybdic acid
ppm	parts per million
Pr	propyl
Prophos	1,2-bis(diphenylphosphino)propane
psi	pounds per square inch
PYPHOS	(2-(2'-diphenylphosphino-4',6'-di-*tert*-butyl-1'-phenyl)-3-methylpyridine)
QUINAP	1-(2-diphenylphosphino-1-naphthyl)isoquinoline

QUINAZOLINAP rac	(2-substituted-quinazolin-4-yl-2-(diphenylphosphino)naphthalene racemic
rbf	round-bottom flask
RT	retention time
S	solvent
TBD	1,5,7-triazabicyclo[4.4.0]dec-5-ene
TEA	triethylamine
THF	tetrahydrofuran
TLC	thin layer chromatography
TMEDA	*N,N,N',N'*-tetramethylethylenediamine
TMS	trimethylsilane
Tol	toluene or tolyl
UV	ultraviolet
w/v	weight over volume
v/v	volume over volume, volume to volume

Chapter 1

Hydroboration – Scope and Mechanism

1.1 Background of Uncatalyzed Hydroboration

Hydroboration, followed by an oxidation, converts an alkene into an alcohol by the net addition of water across the carbon-carbon double bond[1-3]. Its two general features are that the addition occurs in a *cis*-fashion, with the boron atom preferentially attached to the less substituted carbon[1]. Having said this, complete selectivity for the least sterically crowded carbon, giving rise to the anti-Markovnikov product is rare with the outcome generally controlled by the steric and electronic factors of both the hydroboration reagent and substrate alkene. The simplest borane reagent, diborane (B_2H_6) is a colourless, toxic gas that exists as a dimer, with two three-atom, two-electron bonds. Borane is a strong Lewis acid and any Lewis base (ethers, amines or sulfides) with a lone pair of electrons rapidly forms a stable complex with BH_3, and it is these borane reagents $BH_3{\cdot}SMe_2$ and $BH_3{\cdot}$THF that are most familiar to organic chemists. **Figure 1.1** shows some of the common hydroboration reagents and their regioselectivity in the hydroboration of styrene. Also note the influence of the *para*-substituent on the regioselectivity for the hydroboration with $BH_3{\cdot}$THF. The characteristic anti-Markovnikov orientation that leads to boron becoming bonded to the less substituted carbon atom of the alkene results from a combination of steric and electronic effects. **Table 1.1** illustrates the effects of sterics with the bulkier hydroboration reagents, where the addition of the second or third alkyl group would cause considerable steric repulsion if the boron were added to the internal carbon.

Figure 1.1: Common hydroboration reagents

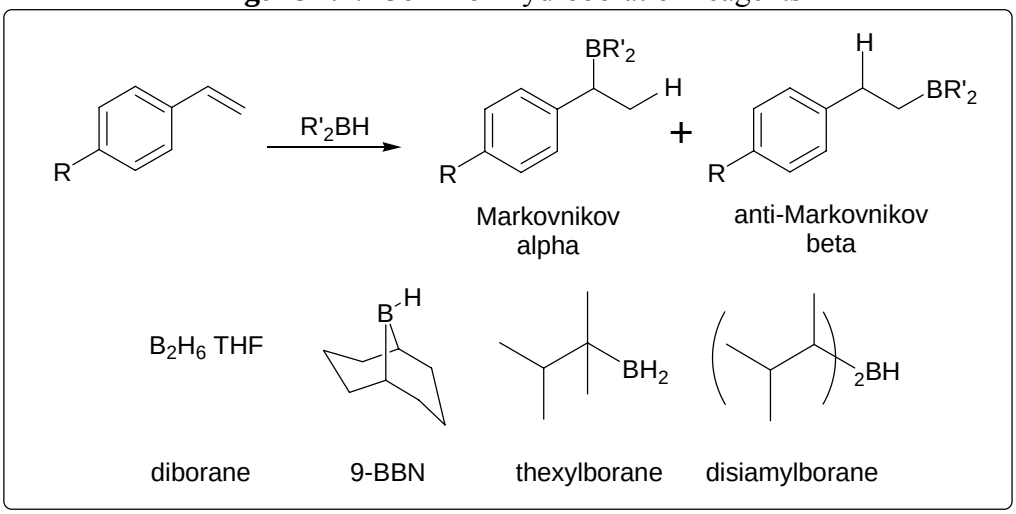

Table 1.1: Outcome of the hydroboration of styrene with hydroboration reagents[3-6]

Reagent	R = H α:β	R = CH_3O α:β	R = Cl α:β	R = CF_3 α:β
BH_3·THF	20:80	7:93	27:73	34:66
Thexylborane	6:94			
Disiamylborane	2:98			
9-BBN	1:99			

The regioselectivity of hydroboration with borane can be explained by examining the two possible transition states. Borane is an electrophilic reagent and is attacked by the π-electrons of the alkene. This leaves the carbon of the alkene electron-deficient. If boron then becomes bound to the terminal carbon, the carbon with the R group, the more substituted carbon is then electron-deficient in the transition state (**Figure 1.2**, eq 1). However, if boron is bound to the carbon with the R group, then the terminal carbon is then electron-deficient in the transition state (**Figure 1.2**, eq 2).

Since alkyl substitution at the electron-deficient carbon has a stabilizing effect, the transition state of eq 1 has lower energy than the transition state of eq 2. This then influences the rate of reaction, with the reaction with a lower energy transition state having a larger rate. This results in the hydroboration being regioselective as the reaction in eq 1 is faster than in eq 2.

Figure 1.2: Regioselectivity determined by transition state

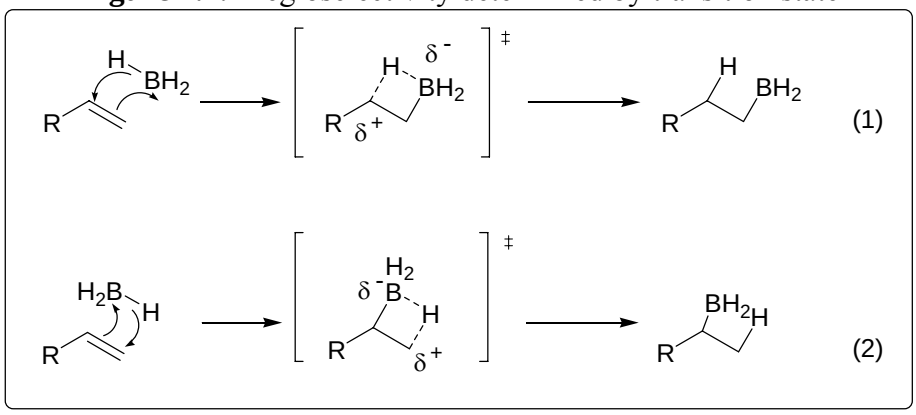

1.2 Mechanism of Uncatalyzed Hydroboration

Studies of the mechanism of the hydroboration reaction were initially complicated by the fact that donor solvents (THF, diethyl ether) brought about a strong rate enhancement compared to the gas phase reaction. Brown and Zweifel proposed a four-centered transition state based on the hydroboration of *para*-substituted styrenes with $BH_3 \cdot THF$[4]. They found that the direction of approach to the double bond and the regioselectivity of addition were influenced by both electronic and steric factors. The erosion of the anti-Markovnikov regioselectivity can be explained by the effect of the *para*-substituent on the transition state. The phenyl group is able to stabilize a positive charge in the benzylic position by supplying electron density; it can also stabilize a negative charge in the benzylic position by absorbing electron density. As can be seen in **Figure 1.3**, **Transition state 1** is stabilized by an electron-donating substituent (*para*-methoxy) and destabilized by an electron-withdrawing substituent (*para*-trifluoromethyl). The reverse case holds for **Transition state 2**. The outcome of these electronic effects is illustrated in the results of **Table 1**.

Figure 1.3: Influence of *para*-substituent on the BH_3 hydroboration of styrene derivatives

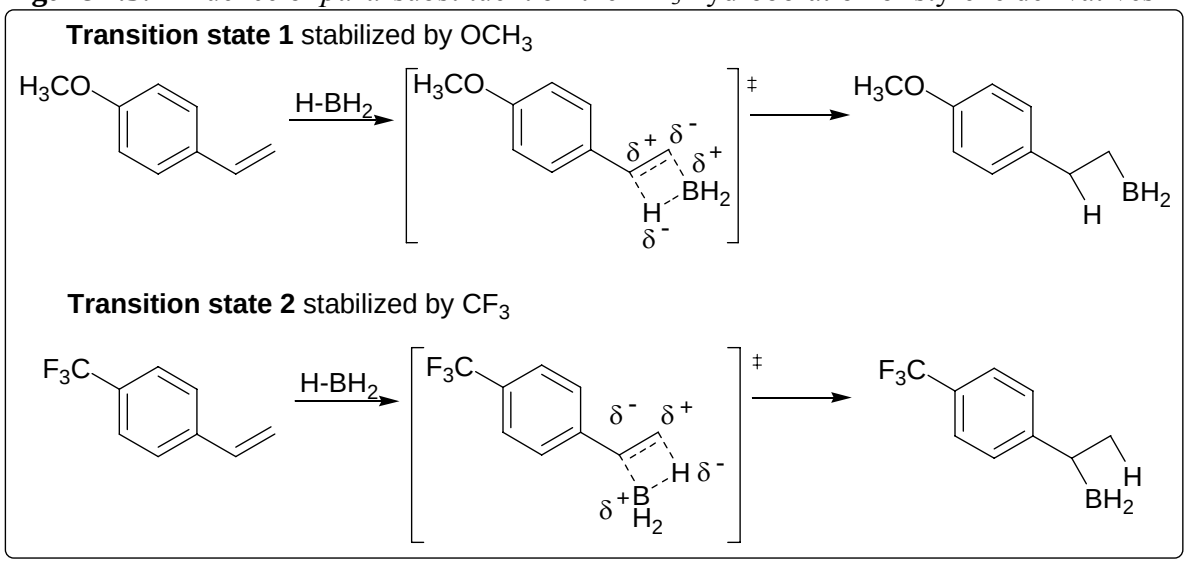

1.3 Background of Transition Metal Catalyzed Hydroboration

Männig and Nöth's initial paper[7] describing the use of the rhodium catalyst, tris(triphenylphosphine)chlororhodium (I), $RhCl(PPh_3)_3$, Wilkinson's catalyst, to catalyze the addition of catecholborane to carbon-carbon double bonds was well timed in the 1980s, coinciding with the explosion of enantioselective organic syntheses and enantioselective transition metal-catalyzed reactions. The realization that the catalyzed process showed markedly different chemoselectivity and regioselectivity compared to the uncatalyzed transformation was central to the further application and development of catalyzed hydroborations. It should be noted that Sneddon and co-workers had earlier reported the Ir- and Co-catalyzed addition of pentaborane (B_5H_9) to alkynes, which was the first true example of metal catalyzed hydroborations[8, 9].

In terms of *d*-block transition metals utilized to catalyze hydroboration, rhodium (Rh) is most frequently used. Iridium (Ir), a third row transition metal, directly below Rh was initially of limited scope, but has recently shown promise[10, 11]. Other transition

metals such as Ti[12-14], Zr[15-17], Co[8, 9, 18-20], Ni[19-23], Pd[24, 25], Ru[26] and Nb[27] have been tested with some interesting results, and these will be discussed in relation to the work presented here where necessary. As well, several lanthanides (*f*-block transition metals) have been used. These studies have focused on the use of Sm[28-30], but Sc[28-30], Pr[30], Lu[30], Eu[30], Nd[29, 30], and Y[29] have all shown activity. The mechanism of lanthanide catalyzed hydroboration operates by a metathesis pathway as opposed to the oxidative addition then reductive elimination cycle of Rh or Ir catalyzed reactions. These mechanisms are discussed below.

1.3.1 Rhodium

Rhodium was one of the first metals to be used as a homogeneous catalyst, making it one of the most well understood and widely used. Cornerstone industrial chemical processes utilizing rhodium catalysts are the Monsanto acetic acid process and Union Carbide hydroformylation[31]. While one of the rarest elements found in the earth's crust, it has wide use in organic chemistry for hydrogenation[32, 33], hydroformylation[32, 33], hydroboration[32], hydrosilylation[32, 33], cycloadditions[32] and carbene transfer[32].

The wide use of rhodium catalysts is attributed to the ease of oxidative addition to the four coordinate square planar rhodium (I) d^8 electron configuration to the octahedral coordination rhodium (III) d^6, which readily undergoes the reverse reaction of reductive elimination back to rhodium (I). This reversibility of these reactions between the Rh(I)/Rh(III) manifold is the crux of the ability of organorhodium compounds to catalyze such a wide variety of reactions. An excellent review on platinum group metals (Ru, Os,

Rh, Ir, Pd, Pt) in catalysis has recently appeared, focusing on their refinement from ores, and the preparation of catalysts and their applications to organic synthesis[31].

With regards to hydroboration, rhodium is the metal of choice, stemming from Männig and Nöth's report[7] using Wilkinson's catalyst, $RhCl(PPh_3)_3$ which showed exclusive hydroboration of the alkene bond in a variety of enones. The preference of reaction at the alkene in preference to the generally more reactive carbonyl group, accomplished at ambient temperature was one of the highlights of the first catalytic hydroboration reaction (**Figure 1.4**).

Figure 1.4: The first catalytic hydroboration with Wilkinson's catalyst

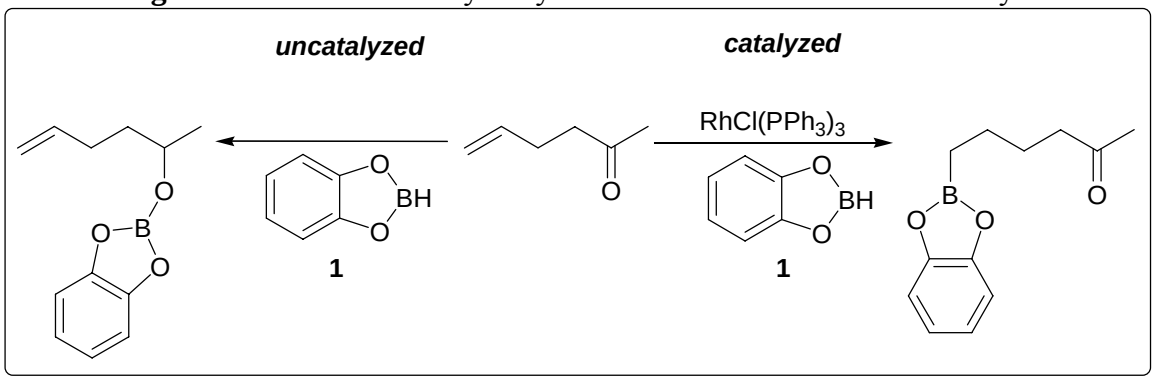

Other notable milestones around this time include the isolation of $Rh(H)Cl(BO_2C_6H_4)(PPh_3)_2$, the oxidative addition product of catecholborane (**1**) to Wilkinson's catalyst[34] in stoichiometric reactions to generate the same observed hydroboration products, the activation of another Lewis acidic borane, 2,2,4-trimethyl-1,3,2-dioxaborinane (**4**) in catalytic hydroboration (albeit less effectively) and the identification of other potential transition metals catalysts $[Rh(COD)Cl]_2$, $[RhCl(CO)(XPh_3)_2]$ X = P, As and $[HRuCl(CO)(PPh_3)_3]$ for this important reaction.

1.3.2 Wilkinson's Catalyst, $RhCl(PPh_3)_3$

Wilkinson's catalyst bears special mention for several reasons. The mechanism of catalytic hydroboration was elucidated under the influence of Wilkinson's catalyst[35-37] along with the competing side-reactions of dehydrogenative borylation[38] and degradation of catecholborane[39] that accompanied its use.

Wilkinson's catalyst is a "jack of all trades", able to catalyze a wide variety of reactions including hydroboration[7, 37, 40], hydrosilylation[33], hydrogenation[33], hydroformylation[32, 33] and the reverse reaction of decarbonylation[41], oxidation of alkanes[42, 43], isomerizations of alkenes[33], and C-H bond activation[44] with new uses continually being discovered.

Wilkinson's catalyst is synthesized from refluxing ethanol with excess PPh_3 using $RhCl_3 \bullet xH_2O$ as the rhodium source[45]. However, this rhodium salt precursor is a mixture of oxochloro and chlorohydroxo complexes in multiple (III/IV) oxidation states[31]. The initial report by Wilkinson[45] included remarks on an observed paramagnetic impurity and Ogle and Hubbard[46] reported the isolation and characterization of the proposed impurity as the square-planar yellow *trans*-$RhCl_2(PPh_3)_2$. This impurity could arise from the reduction of a Rh(IV) species during synthesis, but this proposed Rh(II) complex does not exhibit air-sensitivity or the typical colours (blue-green or red-purple) associated with paramagnetic Rh(II)[47]. Dunbar suggested after X-ray crystallographic studies and modeling, along with NMR studies that the route of synthesis by Ogle and Hubbard using $[Rh(COD)Cl]_2$ likely had acetaldehyde impurities from the synthesis in ethanol, and the $RhCl(PPh_3)_3$ produced in the reaction of $[Rh(COD)Cl]_2$ with PPh_3 would form *trans*-$RhCl(CO)(PPh_3)_2$ and it is was X-ray structure refinement on a disordered crystal that

neglected included CO in the refinement, leading to mistakes distinguishing between CO and Cl.

Also of critical importance is the use of an anaerobic atmosphere during the synthesis and storage of Wilkinson's catalyst. Oxidized catalyst has been shown to be responsible for observed differences in regioselectivity[35] and deuterium distribution[35, 48], with oxidized catalyst showing preference for the linear isomer with non-selective deuterium distribution, while catalyst prepared and stored under inert atmosphere yields near perfect branched selectivity and deuterium incorporation[35]. The effects of exposure to oxygen in solution have been well documented[49, 50]. The most thorough investigation of Wilkinson's catalyst by Carvalho[51] using X-ray photoelectron spectroscopy revealed that all commercial samples and those synthesized by Wilkinson's procedure all contained a mixture of Rh(I)/Rh(III) species in a 3:2 ratio and that exposure to oxygen lead to oxidation of Rh(I) to Rh(III). Further exploration with the use of this Rh(I)/Rh(III) mixture showed that hydrogenation of cyclohexene occurred at 60% the rate of pure Rh(I) Wilkinson's catalyst prepared from $[RhCl(C_2H_4)_2]_2$ and PPh_3. Finally, the Rh(III) species was determined not to be $RhCl_3(PPh_3)_3$ but a Rh(III) oxygen complex.

Clearly any studies to understand the mechanism of rhodium-catalyzed hydroboration should be carefully designed and executed to avoid these issues.

1.3.2 Iridium

In comparison to rhodium, there are few examples of the application of iridium catalysts to hydroboration. Ir(I) complexes such as *trans*-$IrCl(CO)(PPh_3)_2$ named Vaska's complex after its discoverer, are the most widely known and studied because they readily

undergo oxidative addition to stable Ir(III) complexes[51-56]. However, these Ir(III) compounds revert to Ir(I) by reductive elimination much less readily than the comparable Rh (III) analogue, restricting the use of an Ir(I)/Ir(III) manifold for catalysis. The reasons for d^6 Ir(III) complexes to slowly reductively eliminate back to d^8 Ir(I) can be attributed to high Ir-ligand bond strengths, the coordinatively saturated nature of the Ir(III) octahedral complex and the interaction of positive charge on the metal with π-bonding ligands (CO, PR_3), where as electrons are removed in forming the complex, the ability of the metal to be able to back-donate to the anti-bonding π*-orbitals is reduced, resulting in the increase of the bond order of the ligand.

A striking example of this is $IrCl(PPh_3)_3$, the iridium analogue of Wilkinson's catalyst. This compound cannot be made by heating $IrCl_3$ with excess PPh_3, using the phosphine as a reducing agent, as hydride complexes are formed that do not eliminate HCl[57]. This formation of stable hydride complexes is characteristic of iridium[58]. Instead, the desired species is made by displacing the alkene from the dimer of $[Ir(COD)Cl]_2$. However this does not act as a hydrogenation catalyst[57] since the strong Ir-H bonds do not permit hydride transfer to the coordinated alkene and the formed hydride complex, $Ir(H)_2Cl(PPh_3)_3$ does not dissociate, resulting in no vacant coordination site capable of binding an alkene.

With respect to hydroboration, iridium has not been widely employed. Evans investigated the scope and synthetic applications of $[Ir(COD)(PCy_3)(py)]PF_6$, Crabtree's catalyst, in amide-directed hydroborations[40]. The addition of catecholborane to *trans*-$IrCl(CO)(PPh_3)_2$ was investigated by Baker and Marder[59] and the addition to $IrCl(COE)(PMe_3)_3$ was studied by Knorr[60]. In all cases, the corresponding iridium boryl

compounds were stable enough to be isolated, but these compounds were either ineffective as catalyst precursors for the hydroboration of vinylarenes[59] or were exceedingly sluggish, requiring approximately 2 days to achieve greater than 6 turnovers[60] for the hydroboration of disubstituted alkynes. Iridium compounds not containing CO ligands of the type "$IrCl(PPh_3)(COE)_n$" were observed to be active catalysts, selective for the linear isomer in vinylarene hydroborations[59]. $[Ir(COD)Cl]_2/P^iPr_3$ was again investigated for the selective hydroboration of terminal alkynes, but showed poor selectivity regardless of the hydroborating reagent used[61]. More recently, Miyaura reported the use of $[Ir(COD)Cl]_2$ with diphosphines to give high linear selectivity with stryene[11], after the publication of our results with iridium catalyzed hydroboration[10]. Gratifyingly, they observed identical selectivity.

From the results of Marder and Baker[59] which produced the first structurally characterized metal-carbonyl boryl complex *trans*-$IrHCl(CO)(BO_2C_6H_4)(PPh_3)_2$, Hartwig undertook calorimetric and computational studies to determine the bond dissociation energies (BDEs) of the Ir-H and Ir-B bonds[62]. Using calorimetry, they determined that the sum of the Ir-H and Ir-B bond energies was 126.4 kcal/mol. From the known compound *trans*,*cis*-$[Ir(CO)(PPh_3)_2Cl(H)_2]$ is was known that the sum of Ir-H bonds was 120 kcal/mol or 60 kcal/mol per Ir-H bond. Applying this to the iridium boryl complex allowed for an estimate of 66 kcal/mol for the Ir-B bond in $IrHCl(CO)(BO_2C_6H_4)(PPh_3)_2$. This result demonstrated that the Ir-B bond (66 kcal/mol) is stronger than the Ir-H bond (60 kcal/mol). For comparison, the Ir-C bond in a typical iridium-methyl containing complex such as *trans*-$[Ir(CO)(PPh_3)_2(Cl)(CH_3)]$ is 35 kcal/mol. The combination of the computational studies and the calorimetric work are summarized in **Table 1.2**.

These values allowed for the calculations of ΔH for the steps of iridium catalyzed hydroboration (**Table 1.2**). It can be seen that alkene insertion into the iridium hydride is less favourable thermodynamically (rxn 2, **Table 1.2**) than alkene insertion into the iridium-boron bond (rxn 3, **Table 1.2**). This small difference in energy is given as one of the key reasons for the competition between these two processes[62]. Reductive elimination from the iridium boryl complex (rxn 4, **Table 1.2**) leading to C-B bond formation is exothermic, much more than the reductive elimination from the iridium hydride (rxn 5, **Table 1.2**) which generates a C-H bond. While it seems that one thermodynamic pathway would be preferred over another, notice that the sum from the alkene insertion into the Ir-H bond (rxn 2) and subsequent reductive elimination to give the C-B bond (rxn 4) gives a ΔH = -9 kcal/mol. The calculation of the alkene insertion into the Ir-B bond (rxn 3) with reductive elimination to give the C-H bond (rxn 5) also occurs exothermically with ΔH = -9 kcal/mol. It has been suggested that the strength of the Ir-B bond provides the necessary driving force for this reaction[62], but with identical ΔH sum of reactions, kinetic factors or solvent effects can favour one pathway process over another. For catalysis to occur, the energic barriers must not have high free energy of activation or have highly stable intermediates.

Table 1.2: Calculated ΔH values based on BDEs[62] for iridium catalyzed hydroboration

reaction number	simplified primary reaction	ΔH (kcal/mol)*
1	[Ir] + $H(BO_2C_6H_4)$ → [Ir](H) $(BO_2C_6H_4)$	-15
2	[Ir](H) $(BO_2C_6H_4)$ + CH_2CH_2 → [Ir]$(CH_2CH_3)(BO_2C_6H_4)$	2
3	[Ir](H) $(BO_2C_6H_4)$ + CH_2CH_2 → [Ir](H)$(CH_2CH_2BO_2C_6H_4)$	-6
4	[Ir]$(CH_2CH_3)(BO_2C_6H_4)$ → [Ir] + $CH_3CH_2(BO_2C_6H_4)$	-11
5	[Ir](H)$(CH_2CH_2BO_2C_6H_4)$ → [Ir] + $CH_3CH_2(BO_2C_6H_4)$	-3
6	$H(BO_2C_6H_4)$ + CH_2CH_2 → $CH_3CH_2(BO_2C_6H_4)$	-24

* based the following BDE data: C=C 163, C-C 88, C-H 98, H-$(BO_2C_6H_4)$ 111, C-$(BO_2C_6H_4)$ 113, H-[Ir] 60, C-[Ir] 35, B-[Ir] 66, [Ir] = *trans*-$[IrCl(CO)(PPh_3)_2]$

The implications of this will be further discussed in Chapter 3.2 Proposed Mechanistic Cycle of Iridium (I) Catalyzed Hydroborations.

1.4 Mechanism of Rhodium-Catalyzed Hydroboration

The accepted mechanism of the rhodium-catalyzed hydroboration is shown in **Figure 1.5**. This was established on the basis of studies of the reactions of catecholborane with Wilkinson's catalyst[36] and is consistent with the observed formation of vinylboronates and alkanes during the reaction and the results of deuterium incorporation and product distribution. This mechanism is further supported by Ziegler's density functional theory calculations[63].

The first step in the catalytic cycle is the loss of a phosphine from Wilkinson's catalyst to give solvent complex **A**, which then undergoes oxidative addition with the hydroborating reagent to give the known rhodium boryl species **B**[34]. Complexation of free alkene gives key intermediate **C** that now has three pathways available. Alkene insertion with hydride placement at the internal carbon leads to rhodium alkyl boryl species **G** which can then undergo reductive elimination to give the C-B bond of the linear boronate product **H** and regenerate solvent complex **A**. If alkene insertion occurs with hydride placement at the terminal carbon, this gives rhodium alkyl boryl species **D**, which is proposed to be stabilized by a π-benzyl interaction, shown in the inset as **E**, favouring the formation of the branched isomer **F**. The formation of the π-benzyl complex **E** was initially proposed to occur only with the use of cationic rhodium sources[64] but it was later shown that other rhodium catalysts under anaerobic conditions

and free of impurities also reacted with high branched selectivity[35, 37]. Reductive elimination from **D** gives **F**, regenerating starting complex **A**. Compound **C** can

Figure 1.5: Mechanism of Rhodium-Catalyzed Hydroboration

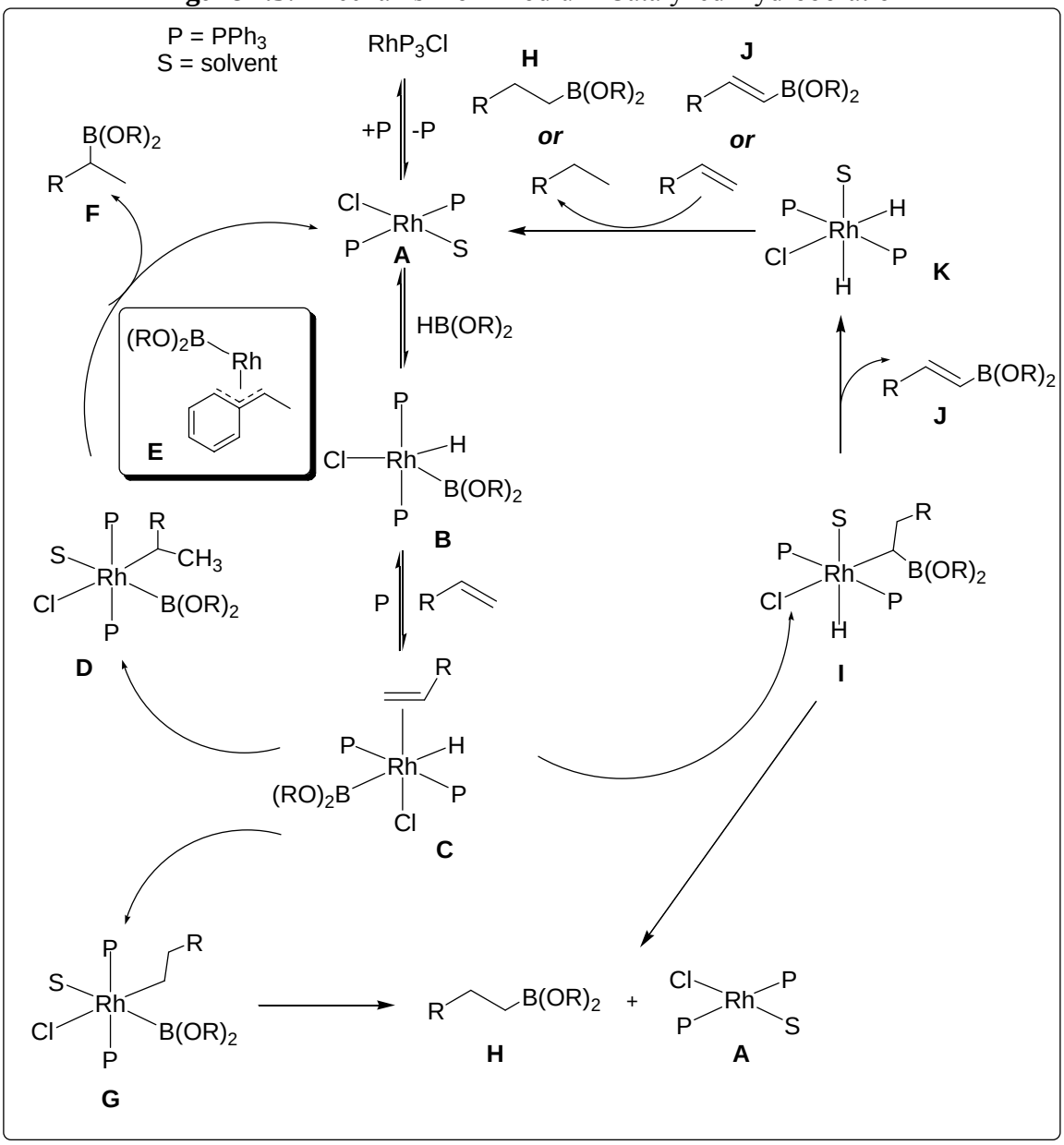

also undergo insertion of the alkene into the rhodium-boron bond to give **I**. From here two pathways can occur – standard reductive elimination to produce the linear isomer **H** again or a ß-hydride elimination to give the vinylboronate **J**. The catalytic species remaining (**K**) is a rhodium dihydride, a potent hydrogenation catalyst, which can

hydrogenate any vinylboronate **J** to linear isomer **H** or lead to the non-productive consumption of starting alkene to give alkane. It is this pathway that is responsible for the loss of one equivalent of alkene in the synthesis of vinylboronates[65, 66].

It should be noted that the pathway **C-I-K-A** often occurs in tandem with catecholborane degradation and the use of unreactive substrates where catalyst mediated degradation becomes significant[36, 39]. For further discussion, please refer to Chapter 1.5.2 Degradation of Catecholborane.

The complex nature of this mechanism and accompanied side-reacations was elucidated in a series of seminal papers[36-39]. The goal in the hydroboration of vinyl arenes is to achieve high branched selectivity with resulting boronate ester **F**, and furthermore to induce enantioselectivity when chiral ligands are employed. This goal can only be attained through pathway **C-D-A**, while the linear isomer **H** can be prepared via three routes by rhodium-boryl insertion (**C-I-H**), rhodium-hydride insertion (**C-G-H**) and from β-hydride elimination to produce vinylboronate ester **J** (**C-I-J**) followed by hydrogenation.

1.5 Hydroboration Reagents

Of all the hydroboration reagents in both catalyzed and uncatalyzed hydroborations, catecholborane (**1**) is by far the most commonly employed. Of the other dialkoxyboranes known, only pinacolborane (**2**) has achieved widespread use. Representative hydroboration reagents are shown in **Figure 1.6**.

Figure 1.6: Hydroboration reagents

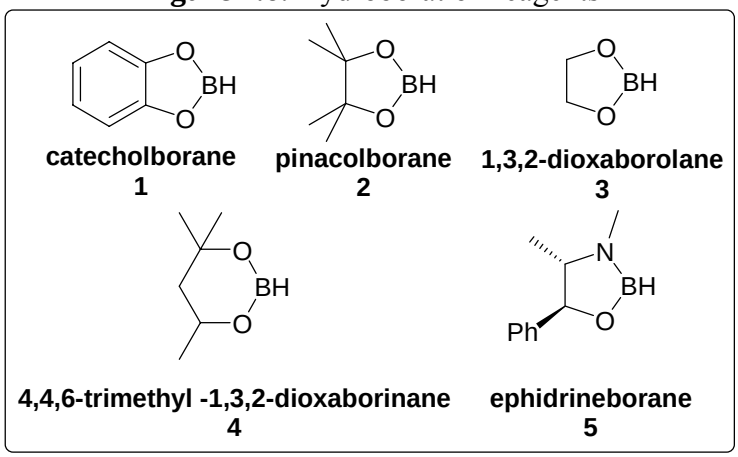

The first described cyclic dialkoxyborane **3**[67] readily undergoes disproportionation (**Figure 1.7**) at room temperature to $B_2(OCH_2CH_2O)_3$ and BH_3, rendering it unsuitable for hydroboration.

Figure 1.7: Disproportionation of a dialkoxyborane

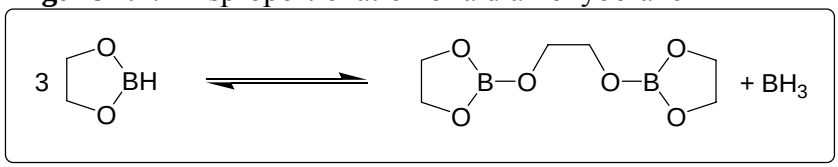

4,4,6-Trimethyl-1,3,2-dioxaorinane **4** was the first stable cyclic dialkoxyborane[68] resistant to disproportionation, and was able to hydroborate simple terminal alkenes[68, 69] at 100ºC over 3 to 4 days and allenes[70] at 130ºC over 24 hours. Note that in both cases the hydroboration is conducted at high temperature, a signature reaction condition for uncatalyzed hydroboration conditions. Although it was shown to be active in catalytic hydroborations by Männig and Nöth[7, 34], continued use of **4** was eclipsed by catecholborane **1**.

1.5.1 Catecholborane (1,3,2-Benzodioxaborole), 1

Catecholborane (HBcat, **1**) was first described by H.C. Brown and was shown to be an effective mono-hydroborating reagent for alkenes[71, 72] and alkynes[72, 73] at 100ºC and 70ºC respectively. Easily prepared from catechol and BH_3·THF and isolated by distillation, it allowed access to alkyl- and alkenylcatecholboronates (**Figure 1.8**), which on hydrolysis gave the corresponding alkane- and alkeneboronic acids. Catecholborane exhibits a preference for addition to the terminal carbon with high regioselectivity (usually >95%) in near quanititative yields when a 10% excess is employed[72].

Figure 1.8: Synthesis of catecholborane and its application in hydroboration

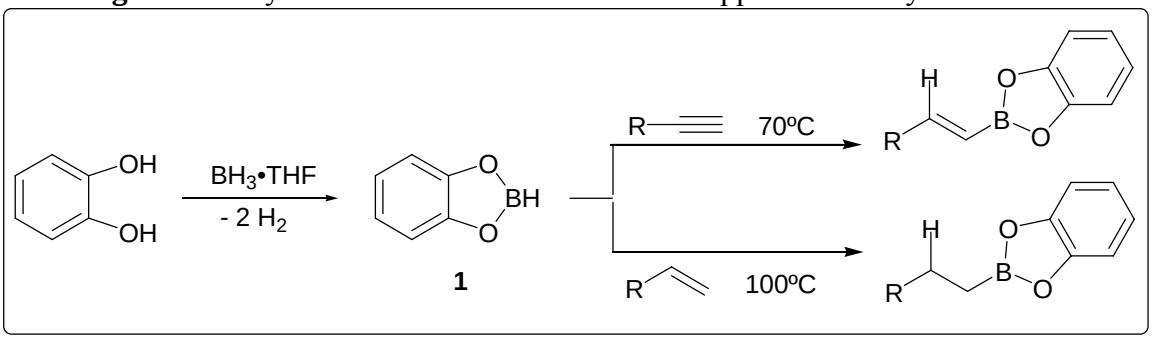

While it was not the first dialkoxyborane to be prepared, it was the first that was stable towards disproportionation *and* able to perform hydroboration under reasonable conditions. For comparison, borinane **4** shows greatly reduced reactivity relative to HBcat[71]. The reduced reactivity of **4** is due to the π-bonding between boron and oxygen and localization of electrons within the three atom O-B-O framework. However, with HBcat, where oxygen is bound to the benzene ring, the increased rate of reaction is due to the fact that the lone pair of electrons on oxygen are in conjugation with the benzene ring, making π-bonding between oxygen and boron less influential[74].

Since its introduction, HBcat has been widely used in hydroboration, especially of alkynes to give vinyl boronate products that are valuable reagents in Suzuki coupling reactions[75] and for numerous synthetic transformations, most notably in oxazaborolidine catalyzed reductions of ketones to give chiral alcohols in high enantiomeric excesses[76]. Its application in the hydroboration reaction has been reviewed[74, 77] and an improved synthesis, suitable for large scale has been disclosed by Brown[78].

1.5.2 Degradation of Catecholborane

Despite its widespread use in hydroboration, catecholborane is not a perfect reagent. The catecholboronate esters obtained are not stable to traditional purification techniques such as column chromatography and distillation yields glassy solids that are unstable to air and moisture[20, 21].

Catecholborane is also somewhat sensitive to disproportionation (**Figure 1.9**) and it is known that commercial samples contain $B_2(O_2C_6H_4)_3$[39, 78], simply known as B_2cat_3. This process also leads to the production of BH_3, which can lead to uncatalyzed hydroboration, or in combination with metal catalysts lead to isomerization and uncontrolled hydroborations leading to a gross mixture of products[79]. To overcome this, it is recommended that neat catecholborane be used and that it is freshly distilled under reduced pressure prior to use. The presence of these decomposition products in solution has further deleterious effects, as is most noticeable in THF solutions of catecholborane. On the basis of similarity with BH_3, decomposition by ring-opening of THF[80] could occur by two mechanistic routes. The unimolecular pathway is believed to occur with the THF coordinated to catecholborane adding into the hydrogen-boron bond in a four-center

transition state with concomitant carbon-oxygen bond scission. The alternative is a bimolecular pathway, where free catecholborane then attacks a THF molecule coordinated to another Lewis acidic catecholborane molecule. The resulting butoxylcatecholborates, (BuO)BCat, are known to undergo redistribution with catecholborane[71, 81], but slowly at ambient temperature ($t_{1/2}$ ~ 1 day).

Figure 1.9: Disproportionation of catecholborane

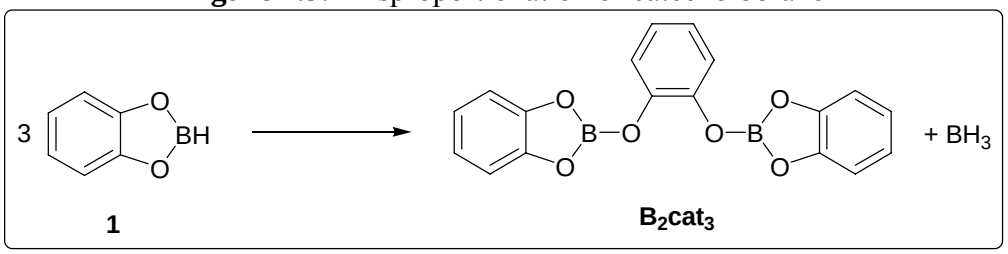

Further complications arise when the hydroboration is conducted under the influence of transition metal catalysis. Free phosphine (PPh_3) induces degradation of catecholborane with a half-life of 4 hours to B_2cat_3 and BH_3[39]. If excess PPh_3 is present, it can act as a sink to remove the BH_3 as the Lewis acid-base adduct PPh_3•BH_3 and prevents the rapid uncatalyzed hydroboration of alkenes by BH_3.

In addition, the metal catalysts themselves provide several pathways for catecholborane degradation and consumption. From the catalytic cycle, the RhP_2ClS (P = PPh_3) catalytic intermediate **A** reacts with catecholborane to give the desired oxidative addition product **B** (eq A). In the presence of excess catecholborane, **A** further reacts to give the rhodium bis(boryl) complex and dihydrogen (eq B). The produced dihydrogen is in equilibrium with Wilkinson's catalyst and the dihydride intermediate **K** (eq C), which is catalytically active for the hydrogenation of alkene or vinylboronate. During the course of the reaction, it has been observed that addition of catecholborane is reversible with Wilkinson's catalyst, however increased amounts of **B** lead to an increase in the

bis(boryl) complex and dihydrogen which is trapped as the dihydride intermediate **K**. This formation of greater amounts of **K** relative to the bis(boryl) complex revealed a pathway that resulted in irreversible rhodium-mediated degradation of catecholborane (eq E), where the exact stoichiometry is unknown[39]. Iridium catalysts have also been shown to promote this degradation[59].

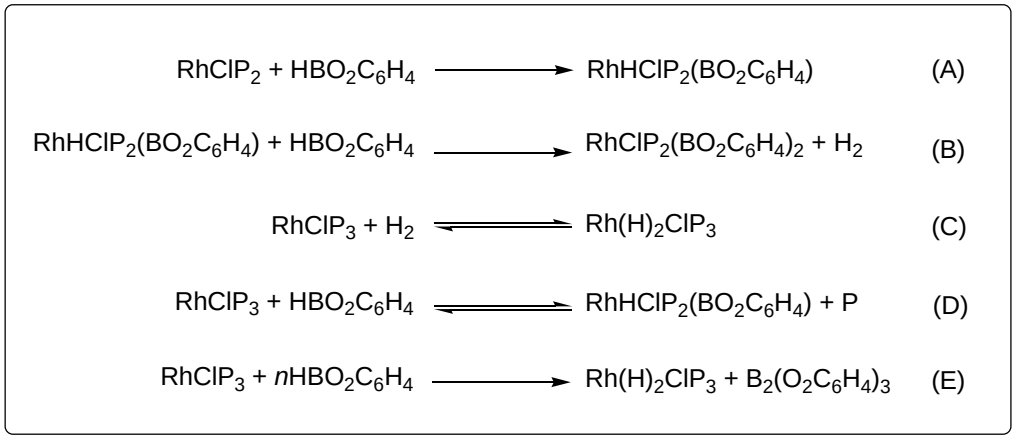

In general, for transition metal catalysts to promote this degradation, catecholborane much be present in excess relative to the catalyst, and an alkene substrate must not be present. In the presence of an alkene, the hydroboration reaction is more favourable than the aforementioned decomposition reactions, however, if a sterically hindered or slow reacting alkene is employed, these decomposition reactions can become important. In addition, free phosphine now present can induce phosphine promoted degradation[39].

1.5.3 Pinacolborane (4,4,5,5-Tetramethyl-1,3,2-dioxaborolane), 2

Pinacolborane was introduced as a hydroborating reagent by Knochel[82] and it was immediately recognized to have several advantages over catecholborane: it reacts under milder conditions with both alkynes and alkenes, it has high functional group tolerance,

higher regio- and stereoselectivity (*cis-trans* ratio in hydroboration of alkynes) and the resulting pinacolboronate esters are more stable. Knochel also noted that attempts at rhodium-catalyzed hydroboration with Wilkinson's catalyst, $RhCl(PPh_3)_3$ were unsuccessful, however, no further elaboration of the conditions attempted was provided.

Despite these advantages, pinacolborane was not widely employed and it was several years later that Srebnik reported the first transition metal-catalyzed hydroboration with pinacolborane, using a zirconocene catalyst, $HZrCp_2Cl$ (**Figure 1.10**) to aid in the addition to alkynes[15].

Figure 1.10: Catalyst selectivity in phenylethyne hydroboration[15, 17]

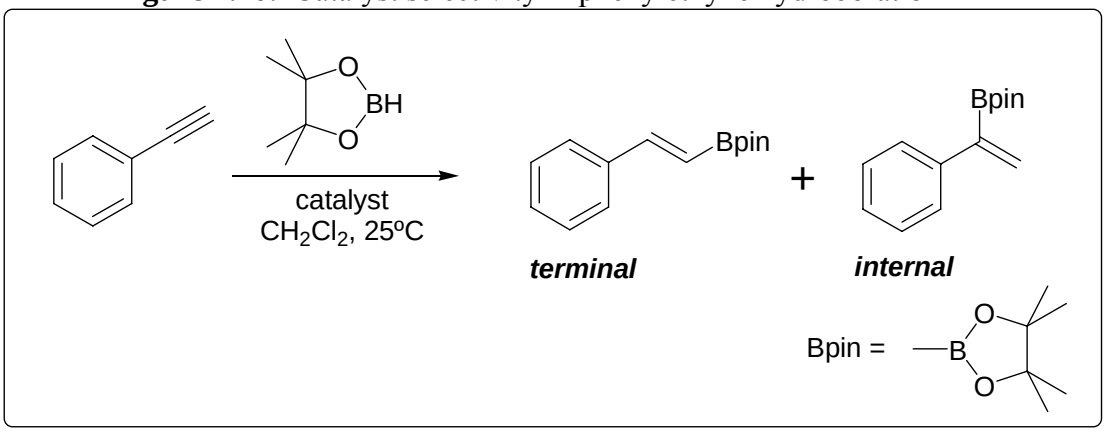

Table 1.3: Catalyst selectivity in phenylethyne hydroboration[15, 16]

catalyst	terminal:internal
$HZrCp_2Cl$	97:3
$RhCl(PPh_3)_3$	48:52
$RhCl(CO)(PPh_3)_2$	98:2
$NiClCpPPh_3$	98:2

The observed selectivities were similar to those seen by Knochel[82] with preference for the terminal vinyl boronate *trans* to the phenyl group. The non-selective results obtained with Wilkinson's catalyst may be due to the use of oxidized catalyst or exposure of the reaction to atmospheric oxygen[51, 83].

Srebnik extended the catalysis to alkenes, using rhodium in the form of Wilkinson's catalyst[17]. $HZrCp_2Cl$ was also found to be effective giving near exclusive

linear selectivity, but Wilkinson's gave superior yields in all cases. Wilkinson's catalyst also caused alkene isomerization of internal alkenes to terminal alkenes. This occurs by alkene insertion into the Rh-H bond of $RhHCl(PPh_3)_2(BO_2C_6H_4)$ followed by rapid ß-hydride elimination and re-insertion until the alkene bond is taken to a terminal position, followed by the comparatively slow reductive elimination to give the C-B bond. This apparent disadvantage has been used to give terminal pinacolboronate esters from a mixture of internal alkene, which are then subjected to homologation-oxidation to the corresponding aldehydes[83].

In the case of styrene (**Figure 1.11**), Wilkinson's catalyst gives an unattractive mixture of all three isomers. For a comparison with the results obtained in our labs, see Chapter 2.2 Development.

Figure 1.11: Catalyst selectivity in styrene hydroboration[16, 17]

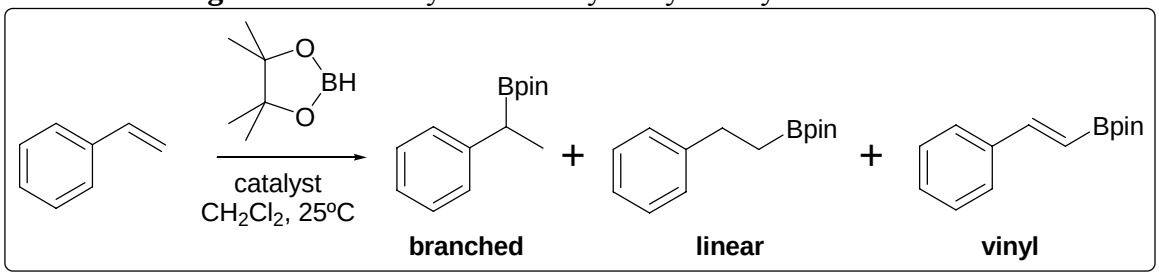

Table 1.4: Catalyst selectivity in styrene hydroboration[16, 17]

catalyst	branched:linear:vinyl
$RhCl(PPh_3)_3$	35:50:15
$RhCl(CO)(PPh_3)_2$	1:99:0
$NiClCpPPh_3$	1:99:0

trans-$RhCl(CO)(PPh_3)_2$ shows distinct preference for the linear isomer, which has also been reported by Sowa Jr.[84] for hydroborations run after catalyst pre-treatment under a CO atmosphere. Nickel-catalysis again shows high selectivity as in alkyne hydroboration, for the linear isomer. In all cases yields were near quanitative, but nickel-catalysis required an 18 hour reaction time versus 3 hours for rhodium.

Pinacolborane has also been used in selective vinylborane formation[65, 66] with contaminant production of alkane caused by hydrogenation of the alkene by a dihydride rhodium catalyst (**Figure 1.12**). Vinylborane formation, without the sacrificial hydrogenation has been achieved by the use of a rhodium catalyst, [$RhCl(CO)(PPh_3)_2$], that is active for dehydrogenative borylation of alkenes without consumption of half the alkene substrate by hydrogenation[85].

Figure 1.12: Vinylborane formation with alkene hydrogenation

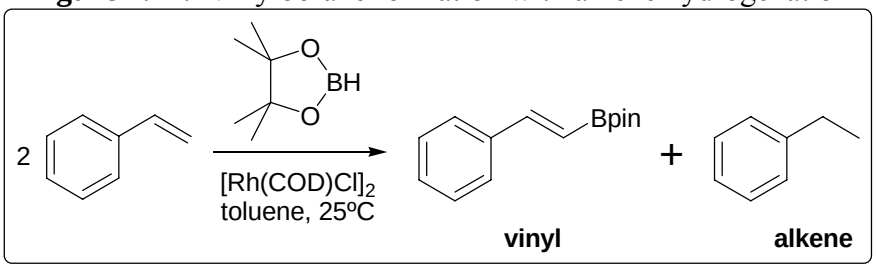

Borylation of aryl halides and triflates with pinacolborane has also been used to give arylboronates[86, 87] for use as partners in Suzuki-Miyaura coupling reactions[75],

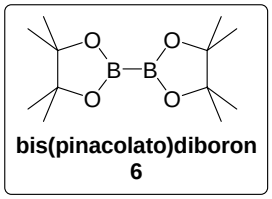

however this methodology has been supplanted by the use of the diboron reagent bis(pinacolato)diboron (B_2pin_2, **6**)[88] in combination with iridium-catalyzed C-H activation for borylation of arenes and heteroarenes[89] or the rhodium-catalyzed C-H activation and borylation of unfunctionalized alkanes[90].

1.6 Lewis Acidity and Reactivity of Hydroborating Reagents

In the initial reports of the respective hydroboration reagents **4**[68], catecholborane[71, 73] and pinacolborane[82] the authors make no comments on their Lewis acidity. Brown noted an increase in the rate of hydroboration with catecholborane

relative to **4**[69, 71] and attributed the increase to the resonance of the oxygen 2p electrons into the benzene ring, making the π-bonding between oxygen and boron less important[74].

The first mention of the importance of the Lewis acidity of the dialkoxyborane with respect to hydroboration was reported by Männig and Nöth in their seminal paper[7], where they noted that diazaborolidine and dialkylboranes could not be activated by rhodium complexes and suggested "that only sufficiently acidic borane components can be catalytically activated"[7] with no quantification given. Support for this was drawn from the work of Kono[34] where the rhodium adducts resulting from the addition of catecholborane and **4** were characterized.

Catecholborane was stated to be a stronger Lewis acid than pinacolborane[91], although both reagents lead to multiple products in attempts at rhodium catalyzed hydroborations of allylamines and allylimines. The lower reactivity and weak Lewis acidic nature of pinacolborane compared to catecholborane is again used to explain the observed product distribution in the metal catalyzed hydroboration of aminopropyl vinyl ethers[92].

The only report that correlates the Lewis acidity to a known physical characteristic is the further work of Nöth[93], where an examination of new hydroborating reagents and their application in rhodium catalyzed hydroboration was undertaken. By comparing the B-H stretching frequency and ^{11}B NMR signals of the dialkoxyboranes it was suggested that the B-H stretching frequency was a measurement of the ring strain in the hydroborating reagent and its Lewis acidity (**Figure 1.13**), exemplified by the tetrachlorocatecholborane **7**.

Figure 1.13: IR stretching frequencies of the B-H bond and ^{11}B NMR data

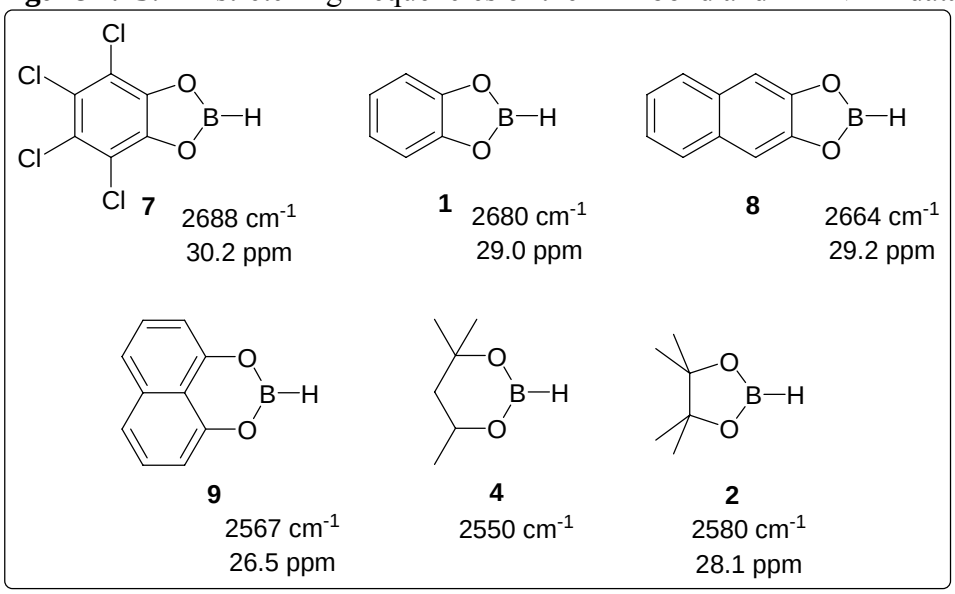

While the B-H stretching frequency may relate to the Lewis acidity, neither it nor the ^{11}B NMR signal correlates with the observed rates for rhodium catalyzed hydroboration of cyclopentene (**9** > **8** > **7** > **1**). The borane predicted to have the highest Lewis acidity (**7**) does not have the fastest rate, and is slower than a six-membered ring reagent (**9**) that with decreased ring strain is expected to have decreased Lewis acidity. This characteristic property has been shown to be true by Nozaki[94], where the reaction of boronate esters with amines was used to determine their Lewis acidity by the extent of complex formation. Five membered ring boronate esters showed binding to primary and secondary amines, while six membered rings did not show any significant interaction with primary amines in ^{1}H NMR studies.

Further hindering a general comparison of the Lewis acidity and reactivity is that Nöth did not include **4** or pinacolborane **2** in his study[93].

The observation that B-H bonds contained in a 5-membered ring (**1**, **7**, **8**) all have the higher IR stretching frequencies that Nöth correlated to their high observed Lewis acidity[93], but this does not match with their order of reactivity (**8** > **7** > **1**). It can also be

seen for all 5-membered systems that those in resonance with a π-system of the benzene ring also have a deshielded boron nucleus. In addition, 5-membered ring systems have higher ^{11}B signals and B-H stretching frequencies than the 6-membered cyclic systems (**2**,**4**,**9**).

Unfortunately this data gives little support to the claims of high Lewis acidity when comparing catecholborane to pinacolborane and the reactivity of boranes. It should be noted that all of these dialkoxyboranes are active in rhodium catalyzed hydroboration. Unfortunately, the regioselectivity cannot be compared between boranes, as Nöth conducted his study with Wilkinson's catalyst and cyclopentene as the standard alkene.

1.7 Miscellaneous Reagents for Promoting Hydroboration

Since catecholborane enjoyed such widespread use prior to Srebnik's report of rhodium-catalyzed hydroboration with pinacolborane, it is not surprising that research was done to enhance the reactivity of catecholborane. Two discoveries that are noteworthy are the use of $LiBH_4$[95] and *N*,*N*-dimethylacetamide ($CH_3CON(CH_3)_2$)[81] to enable the hydroboration of alkenes with catecholborane to be conducted at ambient temperature without a transition metal catalyst. While the yields and selectivities are identical to those obtained with uncatalyzed thermal hydroborations with catecholborane, the *N*,*N*-dimethylacetamide method has been employed where efficient, cost-effective one-pot conditions are required along with access to large quantities of ß-alkylcatecholboronates under metal free conditions[96]. The Lewis acid-base adduct *N*,*N*-dimethylaniline-borane can also activate catecholborane towards the hydroboration of alkynes under mild conditions, but proves ineffective towards alkenes[97].

Chapter 2

Scope of Transition Metal Catalyzed Hydroboration with Pinacolborane

2.1 Introduction

Since Srebnik's initial report[17] of rhodium-catalyzed hydroborations using pinacolborane, this reagent has received little attention, despite its noted stability towards air[82], lack of degradation in the presence of nucleophiles[17] (a major problem for catecholborane[36, 39]) and fact that the product pinacolboronate esters are air and moisture stable, and easily purified by chromatography[17, 82]. It is possible that the poor selectivity demonstrated in this first report has discouraged the use of pinacolborane, despite the ease of handling and the near quantitative yields generally obtained (**Equation 2.1**).

Equation 2.1: Catalyzed hydroboration with pinacolborane[16, 17]

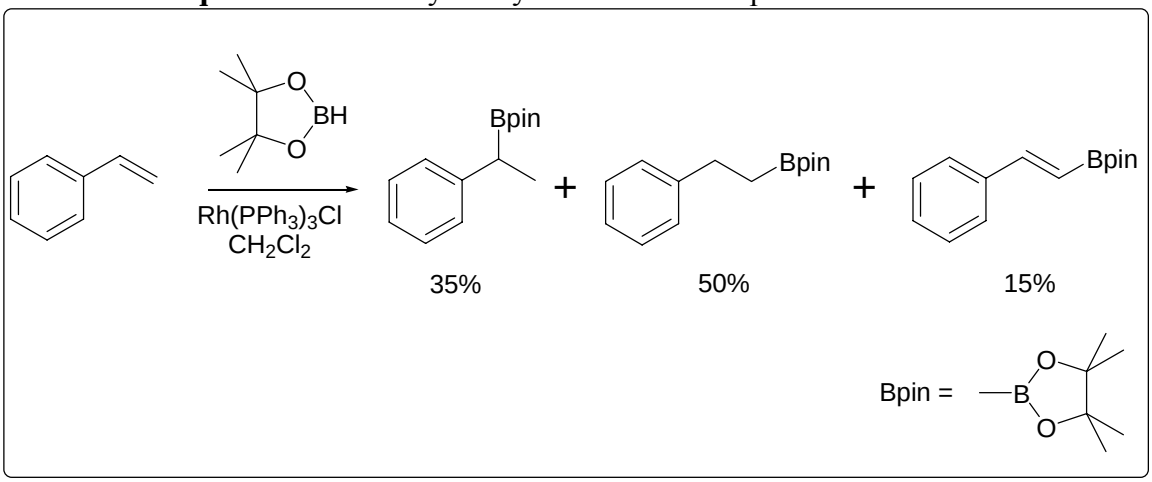

In 1999, Masuda and co-workers[65, 66] demonstrated that the phosphine ligand had a profound effect on the product distribution. For example, running the reaction with $[Rh(COD)Cl]_2$, without any added phosphine ligands lead to clean (or virtually exclusive) dehydrogenative borylation (**Equation 2.2**).

Unfortunately, this result is not as impressive as it seems. The 84% isolated yield with the shown composition is based on pinacolborane as the limiting reagent and does not reflect the fact that one full equivalent of ethylbenzene is generated for every equivalent of styrene that undergoes dehydrogenative borylation. This consumption of 1

equivalent of starting aryl alkene is a significant drawback if it is a valuable material, and thus strategies such as those developed by Marder and coworkers without using a sacrificial acceptor are of significant value[85]. A more serious drawback is the limited scope. Clean dehydrogenative borylation is only observed in the case of vinyl arenes, while aliphatic alkenes such as 1-hexene give the usual linear hydroboration product with traces of vinylboronates.

Equation 2.2: Dehydrogenative borylation to vinylboranes[65, 66]

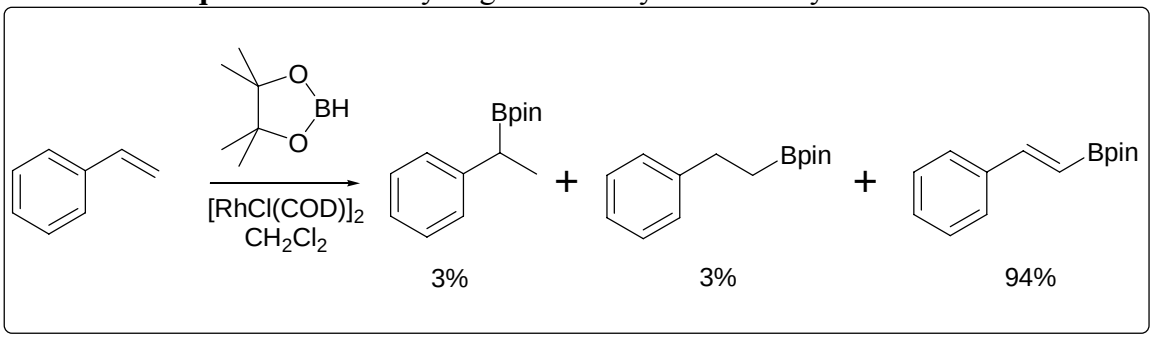

However, the use of cationic rhodium catalysts with bidentate ligands seemed to be a promising alternative based on J.M. Brown's work using hydroborating agents derived from ephedrineborane **5** and pseudoephedrineborane[98-100] (**Equation 2.3**). Although the strategy in this case is different, namely the use of chiral reagents to introduce chirality in the product, the improved product distribution relative to that observed with Wilkinson's catalyst and the similarity of these reagents to pinacolborane encouraged us to examine these same conditions with HBPin.

This result pointed to three key aspects to be explored with pinacolborane hydroborations in order to achieve high branched selectivity: the use of cationic rhodium catalysts which could be modulated using both mono- and bidentate phosphines, that high branched selectivity was possible with pinacolborane and that hydroborations could be

achieved at ambient temperatures, with the possibility of significant asymmetric induction.

Equation 2.3: Rhodium-catalyzed hydroboration with ephedrineborane[98]

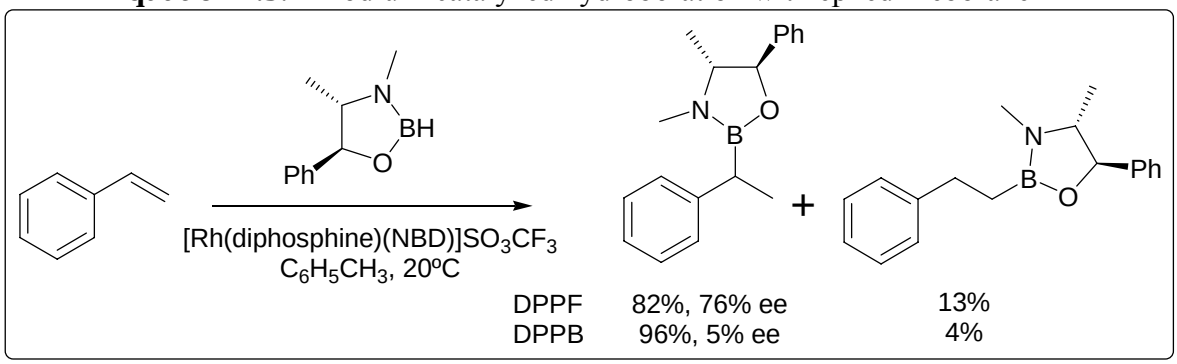

The versatility of organoboranes in organic synthesis has been demonstrated by H. C. Brown, for which he received a Nobel Prize in Chemistry in 1979, jointly with Georg Wittig. His emphasis on reactions to broaden the synthetic scope of hydroboration/organoborane transformation[101] has added greatly to the field of organic synthesis.

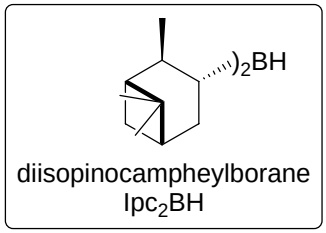

However, access to chiral boronic esters was extremely limited prior to Hayashi's seminal paper[64]. Brown obtained them by asymmetric hydroboration using the chiral hydroboration reagent diisopinocampheylborane (Ipc_2BH), followed by treatment of the hydroboration product with acetaldehyde to remove the chiral auxiliary to provide the boronic acid[101]. One drawback is the lack of atom economy as the use of Ipc_2BH requires two full equivalents of the alkene, α-pinene. Another route to these compounds was achieved by Matteson[102] by asymmetric homologation.

With catalytic asymmetric hydroboration now granting easy access to chiral boronic esters, it was suprising that the main use of the compounds was simple alkaline

oxidation (NaOH, H_2O_2) to furnish the chiral alcohols. Previous work in our lab[103] had focused on the use of Matteson homologation methods to extend the use and scope of these important chiral compounds. The key steps in this route were a regio- and enantioselective hydroboration, followed by a stereospecific carbon-carbon bond homologation paired with oxidation[103, 104] (**Figure 2.1**).

Figure 2.1: Hydroboration/homologation sequence

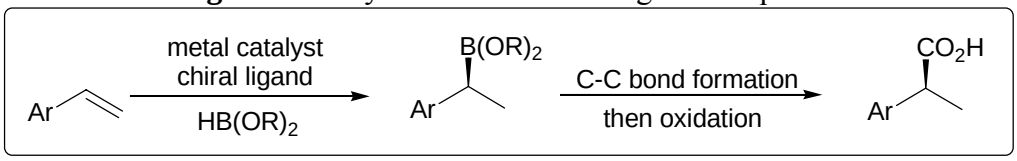

The class of NSAIDs (non-steroidal anti-inflammatory drugs) accessible through this route is the "Profens" that contain the 2-arylpropionic acid structure[104] (**Figure 2.2**).

Figure 2.2: 2-Arylpropionic acid framework NSAIDs, the Profens

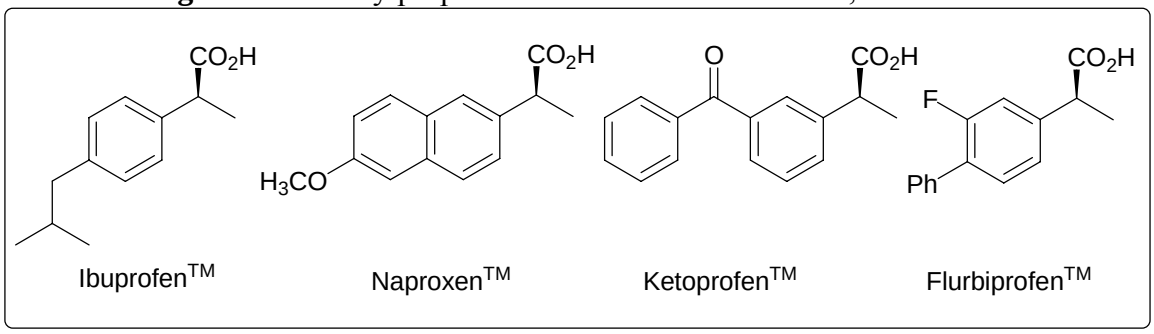

For the synthesis of Ibuprofen™, the asymmetric hydroboration was conducted using catecholborane with cationic Rh/BINAP at cryogenic temperature. For the homologation to be successful, it was found that a quench with pinacol was necessary to transesterify to the pinacolboronate ester[103]. The switch from catechol, with the extensive delocalization into the adjacent benzene ring, to a system where it is restricted to the immediate O-B-O framework in pinacol allowed the homologation to proceed in higher yield. The added advantage was that the pinacolboronate ester could be isolated and then subjected to the homologation with CH_2Cl_2/n-BuLi and oxidized by a modified

Lingren oxidation ($NaClO_4/NaH_2PO_4$)[105] procedure to the corresponding carboxylic acid. As well, the ester or the homologated ester could be oxidized with alkaline hydrogen peroxide to give the enantiomerically enriched alcohol and homologated alcohol respectively[103, 104]. This added to the scope of transformations to which enantiomerically enriched boronate esters could be subjected, which were previously restricted to oxidation to the alcohol and electrophilic amination to the primary amine[106, 107].

The interest in the synthesis of NSAIDs (non-steroidal anti-inflammatory drugs) is a highly active area of research. Mouzin[108] has reviewed the myriad of synthetic methods to obtain this carbon framework. NSAIDs are drugs with analgesic, antipyretic and anti-inflammatory effects, reducing pain, fever and inflammation[109]. All NSAIDs work by a similar mode of action: by cyclooxygenase inhibition they stop the arachidonic acid cascade to prostaglandins and thromboxane A_2 which are responsible for the inflammation mechanism[108]. There are three general classes of NSAIDs: salicylic acids, aryl acetic acids and α-aryl propionic acids. The addition of a methyl group into the aliphatic side chain of an aryl acetic acid to an aryl propionic acid leads to higher potency[108]. As well, the (*S*)-isomer is found to be the active form in both *in vitro* and *in vivo* for most aryl propionic acids[108]. While Naproxen is sold as the single (*S*)-enantiomer since (the (*R*) form leads to liver damage), ibuprofen is marketed as a racemic mixture, as an isomerase has been shown to convert the (*R*)-ibuprofen into the active (*S*)-enantiomer[109]. However in Europe, it is manufactured as a single enantiomer, since studies have indicated greater incorporation of the (*R*)-enantiomer into fatty tissues as glycolic esters.

2.2 Development

A variety of cationic rhodium complexes for use in catalysis can be obtained easily from the compound $[Rh(COD)_2]BF_4$ which was introduced by Schrock and co-workers in 1971[110-112]. This species is easily prepared and can be readily modified by the addition of the appropriate phosphine. However, complex mixtures are known to result from the combination of $[Rh(COD)Cl]_2$ and PPh_3 where displacement of the diene is incomplete after 24 hours[36]. The reactions of $[RhCl(C_2H_4)_2]_2$ and chelating diphosphine ligands are even more complex[113]. Our initial studies focused on monodentate phosphines and phosphites using $[Rh(COD)_2]BF_4$. Comparisons were made to the results obtained using Wilkinson's catalyst and similar transformations with HBcat[16, 17] (**Equation 2.4**).

Equation 2.4: Hydroboration with cationic rhodium and monodentate phosphorus ligands

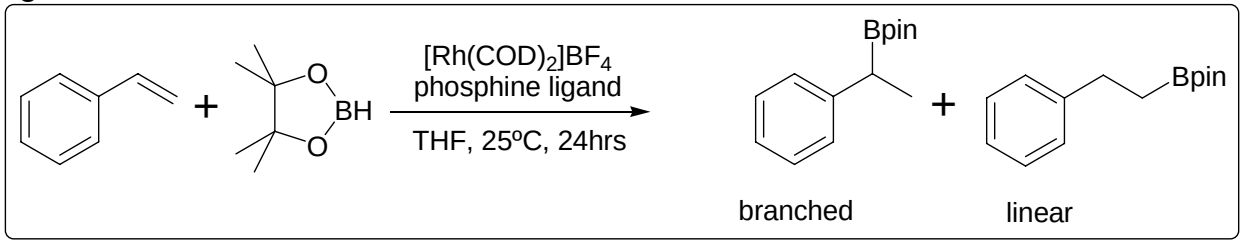

Table 2.1: Rhodium-catalyzed hydroboration with monodentate phosphorus ligands

Entry	$Rh:PR_3$	Ligand	B : L (vinyl)	Yield (%)[a]
1	1:2	PPh_3	84:16	65
2	1:4	PPh_3	80:13:7	74
3	1:2	$P(^tBu)_3$	57:43	18
4	1:4	$P(^tBu)_3$	63:37	47
5	1:2	$P(OPh)_3$	61:39	45
6	1:4	$P(OPh)_3$	23:77	14
7	----	$RhCl(PPh_3)_3$	64:16:20	23
8	----	$RhCl(PPh_3)_3$	35:50:15	99[b]

[a] obtained by ^1H NMR spectroscopy of the reaction mixture against a known amount of added internal standard (hexamethylbenzene), by comparison of the integration ratios
[b] reported result of Srebnik[17]

As can be seen in **Table 2.1** the use of monodentate ligands is accompanied by poor to moderate branched to linear selectivity and vinylborane formation. More disturbingly, our results differed from those of Srebnik, who reported a high yield with Wilkinson's catalyst and a product distribution favouring the linear isomer (compare entries 7 and 8)[17]. Increased bulk at phosphorus leads to poor selectivity (entry 2 vs 4) and so does a change in electronics from phosphine to phosphite (entry 2 vs 6). In these cases, poor yields are also obtained. The most striking difference is the results of cationic rhodium modified by PPh_3 versus Wilkinson's catalyst in terms of regio- and chemoselectivity[36, 38]. As noted previously (Chapter 1.3.2 Wilkinson's Catalyst) while Wilkinson's catalyst is a highly efficient catalyst for the hydroboration reaction, it is also known to often be contaminated with Rh(III) species[51], and may contain traces of Rh(II)[46] along with *trans*-$RhCl(CO)(PPh_3)_2$[47].

The differences between entries 2, 7 and 8 can be explained as follows. The comparison of 7 and 8 is likely due to the use of oxidized Wilkinson's catalyst in Srebnik's case, for reasons described below. The oxidized or "aged" material may contain triphenylphosphine oxide ($O=PPh_3$) in the case of entry 8 and may lead to higher activity but lower selectivity. Entry 7 is freshly prepared Wilkinson's catalyst (obtained from Daryl Allen), which shows higher branched selectivity, but is a less active catalyst, giving lower conversion over 24 hours. Our research group previously demonstrated that there were difficulties repeating the report of Srebnik during a study of the hydroboration of aliphatic internal olefins with HBPin and Wilkinson's catalyst[83]. In this study, it was found that the reported reaction[17] was carried out with oxidized catalyst which proceeded with a different rate and selectivity. The higher activity of the oxidized catalyst leads to

faster but less regioselective hydroboration, and it is known that rapid hydroboration of simple non-sterically hindered terminal alkenes reduces vinylborane formation[36]. It is also known that addition of excess phosphine ligand leads to increased vinylborane formation[38]. The differences seen in entries 2 versus 7 can be explained by the different catalyst precursors employed. The addition of PPh_3 to $[Rh(COD)_2]BF_4$ and $[Rh(\mu\text{-}Cl)(COD)]_2$ for *in situ* generation of the active catalyst does not give a "$RhCl(PPh_3)_2$" species but instead leads to $RhCl(COD)(PPh_3)$ initially, which reacts slowly with PPh_3, and gives incomplete conversion to Wilkinson's catalyst after 24 hours at 25ºC, even with 8 equivalents of PPh_3[36], making it a fundamentally different catalyst[51]. This change in the nature of the active catalyst results in increased yield and branched selectivity and reduced formation of vinylboronate, which can be seen by comparing entry 2 versus entry 7 (**Table 2.1**).

2.2.1 Use of Bidentate Phosphine Ligands

Bidentate phosphine ligands have been the keystone of catalysis with transition metals and methods to quantify their properties have long been desirable to explain observed trends, predict the effects of ligand modification and guide researchers towards finding successful catalysts for desired transformations. One parameter that is of critical importance in assessing ligand properties is the ligand bite angle[114], which is defined as

Equation 2.5: Hydroboration with cationic rhodium and bidentate phosphorus ligands

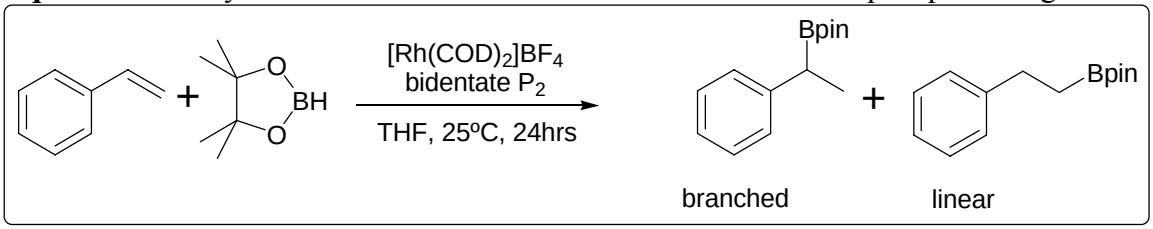

Table 2.2: Rhodium-catalyzed hydroboration with bidentate phosphorus ligands

Entry	Catalyst (% loading)	Ligand	L:M	B:L	Yield (%)[a]
1	$[Rh(COD)_2]BF_4$ (1%)	DPPB	1:1	95:5	62[b]
2	$[Rh(COD)_2]BF_4$ (5%)	DPPB	1:1	98:2	96
3	$[Rh(COD)_2]BF_4$ (5%)	DPPB	2:1	95:5	70
4	$[Rh(COD)_2]BF_4$ (5%)	DPPB	1.2:1	96:4	84
5	$[Rh(COD)Cl]_2$ (5%)	DPPB	1:1	84:16	63
6	$[Rh(COD)_2]BF_4$ (1%)	DPPP	1:1	69:31	79[b]
7	$[Rh(COD)_2]BF_4$ (5%)	DPPP	1:1	70:30	86
8	$[Rh(COD)_2]BF_4$ (1%)	DPPP	2:1	92:8	18[b]
9	$[Rh(COD)_2]BF_4$ (5%)	DPPP	2:1	98:2	56
10	$[Rh(COD)_2]BF_4$ (5%)	DPPE	1:1	73:27	82
11	$[Rh(COD)_2]BF_4$ (5%)	DPPE	2:1	-----	no rxn
12	$[Rh(COD)_2]BF_4$ (5%)			67:33	68[c]
13	$[Rh(COD)(DPPE)]BF_4$ (5%)		1:1	65:35	99[c]
14	$[Rh(COD)(DPPB)]BF_4$ (5%)		1:1	76:24	75[b]
15	$[Rh(COD)_2]BF_4$ (5%)	DPPF	1.2:1	73:27	85

[a] isolated yield after chromatography unless otherwise noted
[b] obtained by ^1H NMR
[c] obtained by ^1H NMR after 1 hour

Figure 2.3: Bidentate phosphines used in catalysis

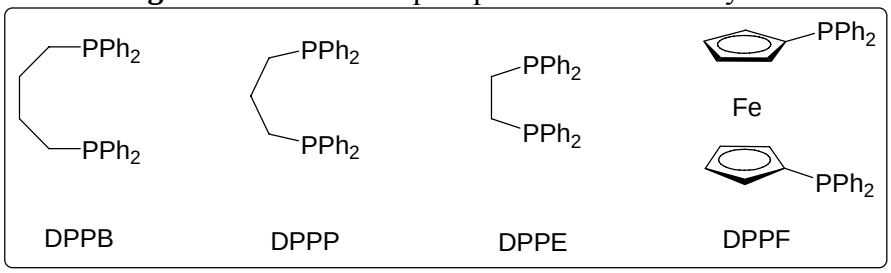

the ligand-metal-ligand angle of the bidentate ligand. The secondary parameter known as the flexibility range can be used to describe the rigidity of the ligand backbone and is defined as the range of bite angles accessible within 3 kcal/mol of the minimum energy (generally between 95º to 135º). These are the angles that can be adopted by a ligand to optimize its confirmation. **Table 2.3** shows the bite angles for those bidentate ligands used.

Table 2.3: Ligand bite angles[114] for bidentate phosphines

Entry	Bidentate ligand	Ligand bite angle (°)
1	DPPE	85
2	DPPP	91
3	DPPB	98
4	DPPF	96

From **Table 2.2** it can be seen that two key factors that influence the regioselectivity – the ligand bite angle and the ratio of rhodium-to-phosphine[115], while catalyst loading influences the yield. DPPB, with the largest bite angle, consistently gives high branched selectivity with cationic rhodium at all ratios and loadings (entries 1-4). An increase from 1 to 5 mol% catalyst loading increases the yield. DPPP (entry 9) performs well at 2:1 ligand:metal to give high branched selectivity, but suffers in yield compared to 1:1 (entry 7). Sanger has reported[116] that reactions of $[Rh(COD)Cl]_2$ under CO atmosphere with 2 equivalents of diphosphine P_2 (DPPP, DPPB) give equilibrium mixtures of $[\{Rh(CO)Cl(P_2)\}_2]$ and $[Rh(CO)(P_2)_2]Cl$. In our system, with an absence of CO, the likely species formed would be $[Rh(COD)(P_2)]BF_4$ and $[Rh(P_2)_2]BF_4$ and indeed these species have been observed[113].

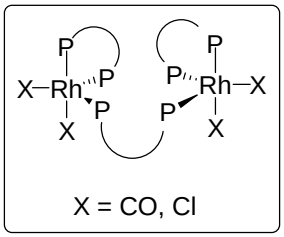

The increase in branched selectivity with DPPP may also be due to the formation of a bridged bimetallic species (inset), which Sanger has observed with the diphosphines DPPP and DPPB[116]. Further support for this can be seen comparing entry 14 against entry 2. The use of $[Rh(COD)(DPPB)]BF_4$ (entry 14) gives moderate selectivity (76:24) and yield (75%), while the combination of $[Rh(COD)_2]BF_4$ and DPPB give high selectivity (98:2) and yield (96%). Clearly a complex other than the expected $[Rh(COD)(DPPB)]BF_4$ is responsible for the high regioselectivity. DPPE gives only

moderate selectivity (entry 10) at 1:1. Increasing the ratio to 2:1 completely halts the catalysis, likely due to the strong chelating power of this ligand and its propensity to form stable complexes[114]. Preformed cationic $[Rh(COD)(DPPE)]^+$ (entry 13) shows similar selectivity to $[Rh(COD)_2]^+$ (entry 14), though it is unlikely that loss of DPPE from the preformed complex leads to the same active catalyst species given that DPPP and DPPB exhibit markedly higher selectivity for the branched isomer. DPPF, even with its large bite angle, only gives moderate selectivity (entry 15), possibly reflecting the rigidity of the ferrocene framework over the methylene CH_2 linkages.

The reduced selectivity of the neutral $[Rh(COD)Cl]_2$ and DPPB (entry 5) compared with cationic $[Rh(COD)_2]BF_4$ and DPPB (entry 2) is difficult to rationalize. Fernández has shown that the addition of halide ion to reaction mixtures for the asymmetric hydroboration of vinyl arenes has a positive effect on the observed enantioselectivity[117]. It has also been reported that cationic rhodium sources provide better yields than neutral sources[118], although no explanation is given. One possible factor is the *trans* effect the X-type chloride ligand could exert during the course of the catalysis[116, 119], compared to the spectator anion used with cationic rhodium (BF_4^-, PF_6^-, $CF_3\ SO_3^-$, ClO_4^-).

The decrease in ligand bite angle (DPPB > DPPP > DPPE), leading to constrained P-M-P angles in complexes has been implicated in slow migrations of subsituents on the metal center[114]. Wider angles allow the phosphine ligand to be coordinated *cis* to a migrating group and this configuration tends to widen the P-M-P angle[114], and in the process allowing the migrating group access to the desired site. Clearly, DPPB has the flexibility to achieve this, with a rhodium center containing a hydride, bulky

pinacolborate ligand and coordinated alkene. However, Sanger[116, 119, 120] has shown that diphosphines linked by four carbon atoms or more do not have simple bidentate complexation behaviour and do result in bridged bimetallic complexes.

2.2.2 Rhodium versus Iridium Catalysts

Rhodium is by far the most commonly utilized transition metal in catalytic hydroborations[7, 36, 37], and is used almost exclusively in asymmetric variants of this reaction. Iridium has been reported to catalyze the hydroboration of alkynes[61] with poor selectivity and with sluggish catalytic activity – at room temperature, six turnovers require approximately 2 days[82] and catalyze the hydroboration of alkenes[59].

Equation 2.6: Change in regioselectivity with the change in metal catalyst

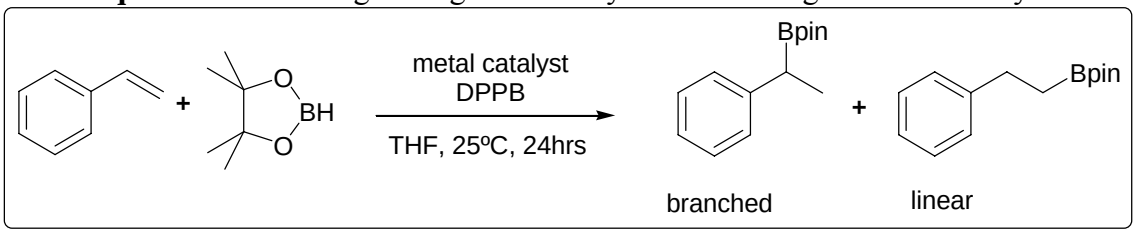

Table 2.4: Comparison of rhodium and iridium catalysts for the hydroboration of styrene

Entry	Catalyst	Ligand	L:M	B:L	Yield[a] (%)
1	$[Rh(COD)_2]BF_4$	DPPB	1:1	98:2	96
2	$[Rh(COD)Cl]_2$	DPPB	2:1	84:16	63
3	$[Ir(COD)_2]BF_4$	DPPB	1:1	0:100	68
4	$[Ir(COD)Cl]_2$	DPPB	1:1	0:100	99

[a] isolated yields after column chromatography

In our screening of catalysts for hydroboration (**Equation 2.8**, **Table 2.4**) we observed complete reversal of regioselectivity when iridium catalysts were used. This was regardless of the charge on the iridium complexes, suggesting that more complex phenomena were responsible for the change in regioselectivity. Changes in selectivities with changes in metal catalyst was also observed by Bonin[121] in the hydroboration of

bicyclic hydrazines where a change in enantioselectivity was seen on switching from rhodium to iridium catalyst. This was attributed to the insertion of alkene substrate into the Ir-B bond followed by reductive elimination rather than metal hydride insertion followed by reductive elimination of the boron substituent. In the first report of iridium catalyzed hydroborations, Westcott[59] observed high linear selectivities, but also the formation of alkane hydrogenation product. The presence of this indicates the formation of vinylboronate esters, arising via dehydrogenative borylation. Theoretical studies involving bond dissociation energies by Hartwig[62] show that insertion into the Ir-B bond is more favourable than insertion into the Ir-H bond by 8 kcal/mol. This is in contrast to rhodium, where the key step appears to be insertion into the Rh-H bond (**Figure 1.5**). Furthermore, taking into account Ziegler's DFT study[63], for the associative mechanism, initial hydride insertion is only slightly favoured over boron migration, as both have similar energy profiles. Considering the dissociative mechanism, the initial endothermic hydride migration has a lower barrier (8.5 kcal/mol) than initial endothermic boryl migration (19.5 kcal/mol).

Rhodium-catalyzed hydroborations with DPPB behaved as seen before with high branched selectivity for a variety of *para*-substituted styrenes in high yields, with the exception of 4-bromostyrene and no change in selectivity with respect to the electronics of the alkene (**Equation 2.7**, **Table 2.5**).

Figure 2.4: Postulated catalytic cycles for M-H and M-B insertion in hydroboration[121]

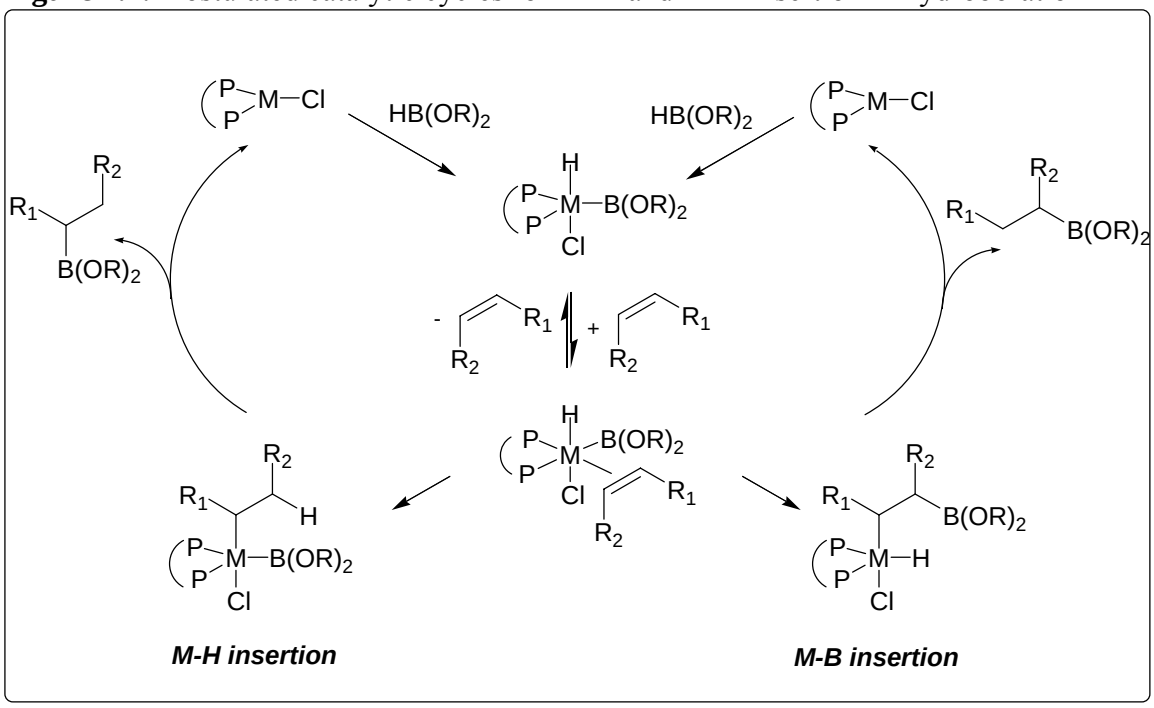

Equation 2.7: Scope of rhodium-catalyzed pinacolborane hydroborations

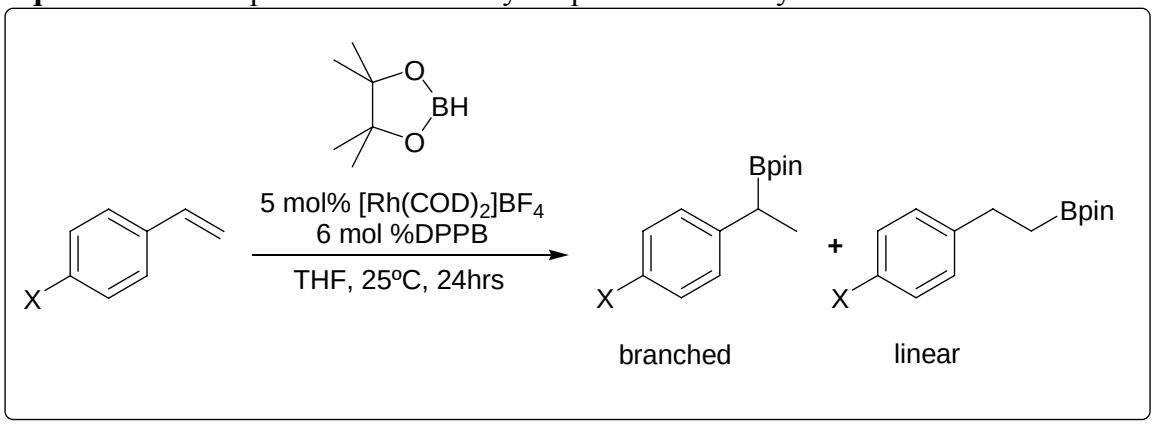

Table 2.5: Rhodium-catalyzed hydroborations of *para*-substituted styrenes

Entry	X	B:L	Isolated Yield (%)
1	H	98:2	96
2	OCH_3	97:3	99
3	CH_3	99:1	97
4	Cl	98:2	93
5	Br	72:28	39[a]

[a]poor yields and regioselectivity due to polymer formation of starting material

Equation 2.8: Scope of iridium-catalyzed pinacolborane hydroborations

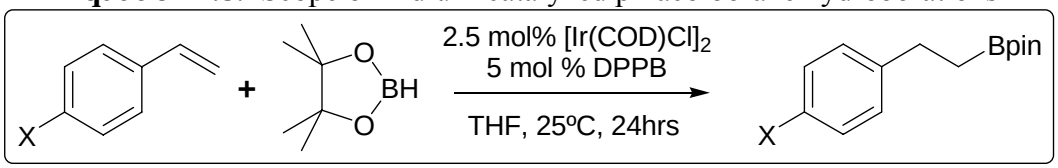

Table 2.6: Iridium-catalyzed hydroborations of *para*-substituted styrenes

Entry	Catalyst	X	B:L[a]	Yield (%)[b]
1	$[Ir(COD)_2]BF_4$	H	0:100	68
2	$[Ir(COD)Cl]_2$	H	0:100	99
3[c]	$[Ir(COD)Cl]_2$	H	0:100	99
4	$[Ir(COD)Cl]_2$	OCH_3	0:100	98
5	$[Ir(COD)Cl]_2$	CH_3	0:100	95
7	$[Ir(COD)Cl]_2$	Cl	0:100	99
8	$[Ir(COD)Cl]_2$	Br	0:100	99

[a] determined by ^{1}H NMR spectroscopy; [b] isolated yields after chromatography;
[c] conducted with 2.65 eq of DPPB

Iridium-catalyzed hydroborations with DPPB all gave near perfect selectivity for the linear isomer for a series of *para*-substituted styrenes, regardless of the electronics (**Equation 2.8**, **Table 2.6**). Yields were consistently higher with the use of the neutral iridium complex $[Ir(COD)Cl]_2$ with 2.0 to 2.65 equivalents of DPPB (entries 2 and 3) and this system was chosen for ease of reproducibility. The cationic iridium catalyst was successful (entry 1), but was extremely sensitive to oxygen and the ratio of bidentate phosphine used. Just after our work appeared, Miyaura[11] also reported high linear selectivity with neutral iridium catalysts and a wide range of selectivity for cationic iridium catalysts modified with mono- and bidentate phosphine ligands.

2.3 Stability of Pinacolborane

In the initial publication on the uncatalyzed hydroboration with pinacolborane[82] Knochel reported that the resulting boronate products from the hydroboration of alkenes and alkynes were highly stable and could be isolated by column chromatography.

Knochel also remarked that hydroboration of alkenes could not be accomplished with pinacolborane under the influence of Wilkinson's catalyst. Since the pinacolborane employed by Knochel was prepared from BH_3•SMe_2, it is possible that traces of remaining sulfide destroyed the catalytic activity. Four years later, Srebnik[17] showed that catalytic hydroboration was in fact possible with pinacolborane. Srebnik also stated that "careful examination of the reaction mixture failed to reveal any pinacolborane degradation products, indicating that it is much more stable than catecholborane in metal-catalyzed hydroborations". Unfortunately, no experimental details were given to support this statement.

Decomposition of catecholborane in the presence of metal catalysts[36] and nucleophiles[39] is well documented. In the presence of PPh_3, it has a half-life ($t_{½}$) of 4 hours (Chapter 1.5.2 Degradation of Catecholborane). Knowing that free phosphine is present during catalysts, either from exogenous addition or dissociation from metal centers, we studied the reaction of pinacolborane in the presence of phosphine.

Treatment of pinacolborane with 2 equivalents excess of PPh_3 and monitoring the reaction by ^{11}B NMR demonstrates the remarkable stability of pinacolborane. After 7 hours, only 5% of another boron containing species is present (**Figure 2.5**). The large doublet corresponds to the B-H signal of pinacolborane with twp other small peaks. The degradation product, $B_2(OC(CH_3)_2C(CH_3)_2O)_3$, B_2pin_3, that is the pinacol analogue of the most common product of degradation of HBcat, would appear at a chemical shift of 21.9 ppm[122]. While phosphine-borane adducts PR_3-BH_3 (R = Ph, Cy, iPr) are known to arise from the decomposition of catecholborane[39], the ^{11}B signal of these complexes appear as a quartet due to ^{11}B-^{31}P coupling. If the unknown species contains a B-H bond,

Figure 2.5: ^{11}B NMR ($C_6D_5CD_3$) of pinacolborane in the presence of excess phosphine

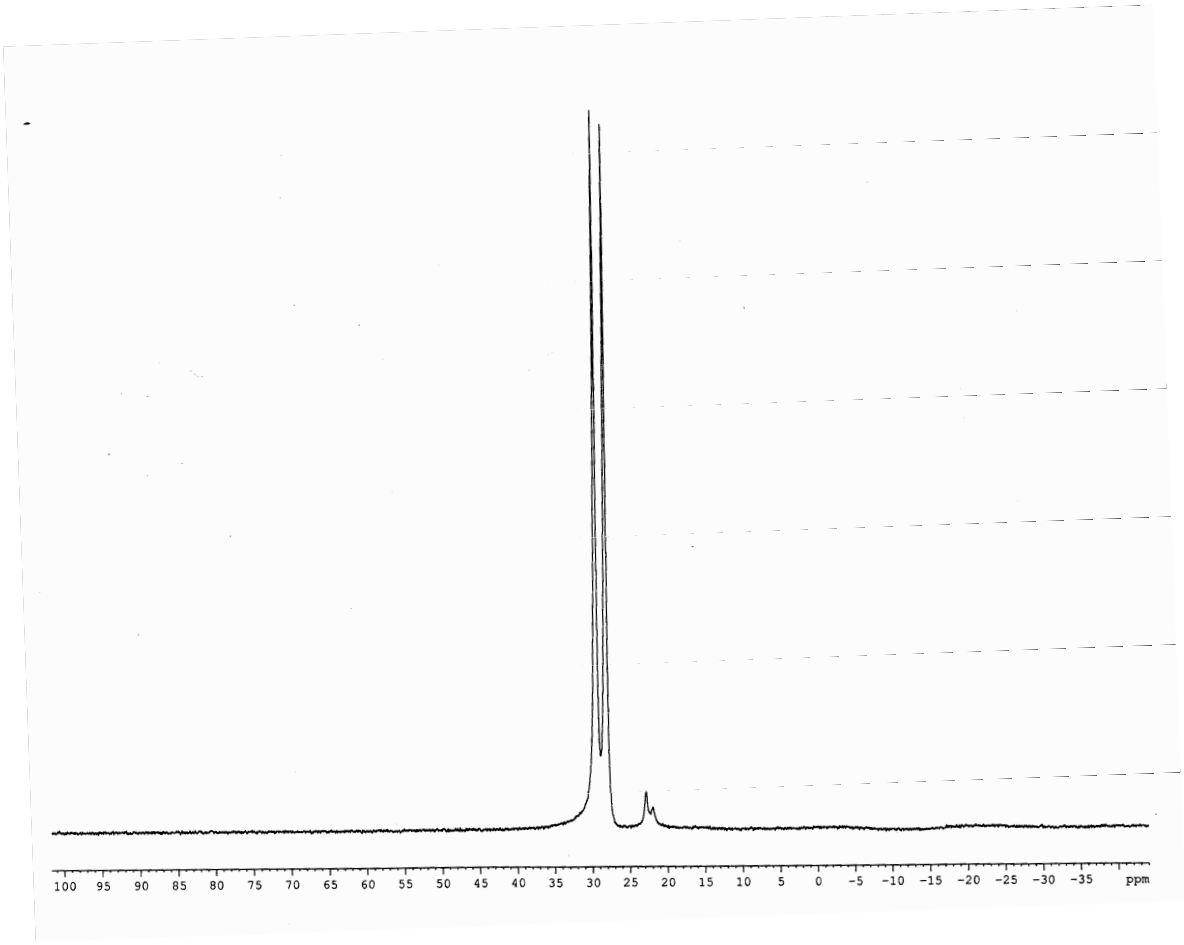

the resulting signal would be a quintet from ^{11}B-^{31}P and ^{11}B-^{1}H coupling[123]. Since no such complexity arises, the boron species does not seem to contain a B-H bond. As well, both signals are broad, a characteristic of boron bonded to three oxygen atoms. While PPh_3 slowly converts pinacolborane into B_2pin_3, the signals observed in the above spectrum likely correspond to a mixture of two boron containing species, B_2pin_3 and pinB-O-Bpin ("B-O-B"). This species may arise from water presence in the solvent. Note that there is no signal for a PPh_3-BH_3 adduct, that would accompany B_2pin_3 production, centered at -40 ppm[123].

It has been suggested that the observed stability of pinacolborane comes from its decreased Lewis acidity although there is little literature data to back up this claim[93] (Chapter 1.6 Lewis Acidity and Reactivity of Hydroborating Reagents). The higher Lewis acidity of catecholborane was considered a factor in its ease of activation compared to other hydroboration reagents by Nöth[7] and has also been implicated in lanthanide catalyzed hydroboration[30].

The decreased Lewis acidity of pinacolborane has been utilized by Westcott[91, 92] in the hydroboration of nitrogen and oxygen containing alkenes to generate higher yields and less side reactions than with catecholborane. Takacs observed that pinacolborane gives superior results in terms of yield and enantiomeric excess compared to catecholborane under cationic rhodium catalysis with phosphate/phosphoramidite monodentate ligands[124], attributing the results to the nature of the hydroborating reagent.

With little decomposition in the presence of excess phosphine, pinacolborane has a distinct advantage over catecholborane. The decomposition products BH_3 and H_2 are not formed, preventing complex mixtures of products due to reaction with the alkene substrate. Pinacolborane is also a liquid and can be stored at ambient temperatures, unlike catecholborane which requires cold storage, otherwise it disproportionates to B_2cat_2 and BH_3, making it a storage hazard.

2.4 Asymmetric Transition Metal Catalyzed Hydroboration

Since Hayashi's seminal report on asymmetric rhodium-catalyzed hydroboration[64], a wide variety of chiral phosphines both mono- and bidentate have been employed. Most are borrowed from the sister reaction, the asymmetric rhodium-

catalyzed hydrogenation of alkenes (BINAP **10**) of which there may be considerable mechanistic similarity. JOSIPHOS (**11**) was initially screened for both hydroboration, hydrogenation and allylic substitution reactions[125], and further modified to extend the results achieved in each area.

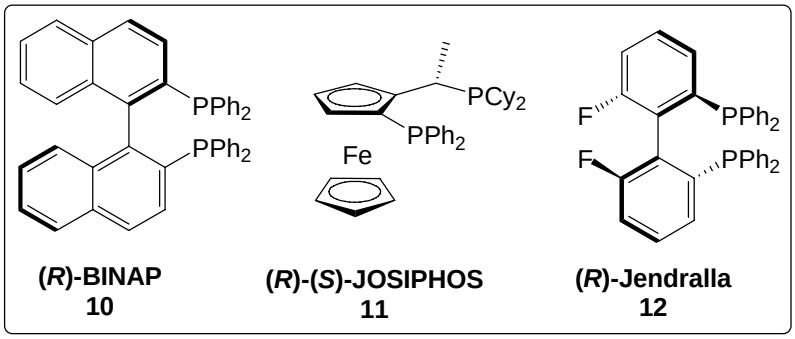

(*R*)-BINAP 10 **(*R*)-(*S*)-JOSIPHOS 11** **(*R*)-Jendralla 12**

Phosphites[126] and phosphoroamidites[124] were discovered by a "trial and error" approach following a screening of a wide library of ligands. J.M. Brown's highly successful P,N-ligand QUINAP (**13**)[127] was initially synthesized for allylic alkylations[128] and was the framework for further modifications in PHENAP(**15**)[129] and the QUINAZOLINAP(**14**)[130-132] series, and the basis for PYPHOS (**16**)[133].

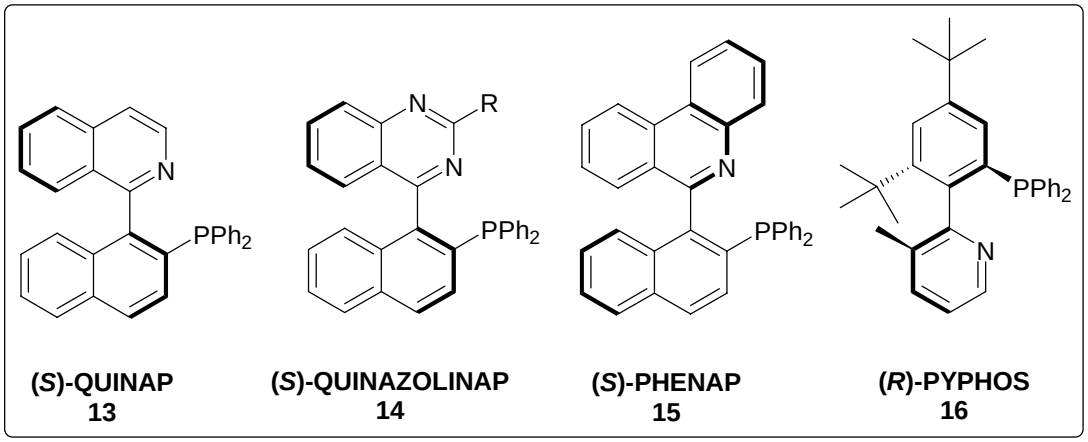

(*S*)-QUINAP 13 **(*S*)-QUINAZOLINAP 14** **(*S*)-PHENAP 15** **(*R*)-PYPHOS 16**

All of these ligands had been screened under rhodium catalysis utilizing catecholborane and typically conducted at or below 0ºC, with the exception of the P,N ligands. The use of pinacolborane had not been investigated and consequently, its

reactivity, regioselectivity and enantiomeric induction were unknown under the influence of chiral ligands. The effects of solvent and temperature also required investigation.

2.4.1 Screening of Chiral Ligands for Asymmetric Rhodium-Catalyzed Hydroboration

The ultimate goal of asymmetric transition-metal catalyzed hydroboration is to realize near total regio- and enantiocontrol, allowing access to compounds that can be further utilized in C-C bond forming reactions[134] and other functional group transformations[135].

The most significant results to this end have been obtained with Hayashi's use of BINAP[64] and J.M. Brown's use of QUINAP[127, 136], using catecholborane as the hydroborating reagent. The use of pinacolborane in hydroboration was later introduced by Knochel as described previously[82] highlighting the stability of the product boronate esters with catalysis being demonstrated by Srebnik[16, 17]. As catalysis was now possible under mild conditions, combining it with chiral ligands opened the possibility of direct access to highly enantiopure boronate esters. This would bypass the use of catecholborane requiring cryogenic temperatures followed by a transesterification with pinacol, a key feature in homologation studies[103].

Our investigation began with ligands that had previously been used in asymmetric rhodium-catalyzed hydroboration with catecholborane, now employing pinacolborane with styrene as a standard substrate.

Equation 2.9: Ligand screen for asymmetric rhodium catalyzed pinacolborane hydroborations

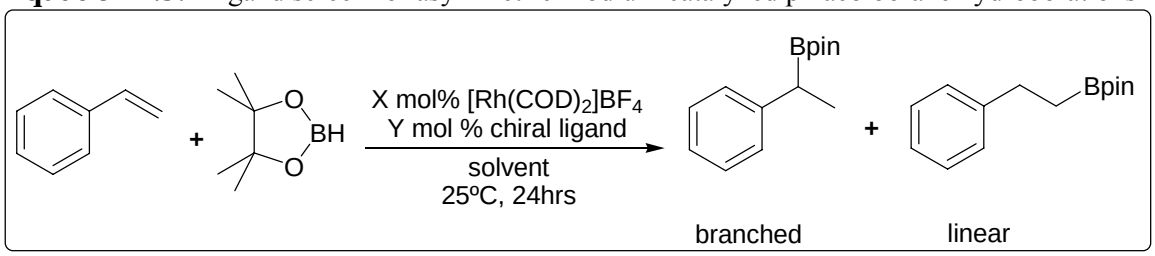

Table 2.7: Chiral ligands for asymmetric hydroboration

Entry	Catalyst Loading (%)	Ligand loading (%)	Ligand	Solvent	B:L	ee (%)	Yield (%)
1	1	1.3	(*S*)-BINAP	THF	56:44	41 (*R*)	30
2	1	1.3	(*S*,*S*)-BDPP	THF	91:9	34 (*S*)	74
3	5	6.5	(*S*)-(*R*)-JOSIPHOS	DCE	78:22	84 (*R*)	70
4	5	6.5	(*S*)-(*R*)-JOSIPHOS	THF	78:22	75 (*R*)	77
5	5	6.5	(*R*)-(*S*)-JOSIPHOS PPh_2-P^tBu_2	DCE	18:82	30 (*S*)	100
6	1	1	(*S*)-QUINAP	THF	66:34	82 (*S*)	30
7	5	6.5	(*R*)-methyl BoPhoz	THF	39:61	24 (*R*)	77
8	5	13	(*S*)-Beller	THF	43:57	2 (*S*)	41
9[a]	1.25	1.25	(*S*)-MOP	DME	65:35	0	79
10[a]	1.25	1.25	(*R*,*R*)-DIOP	DME	63:37	21 (*R*)	55

[a] conducted by Austin Chen

Figure 2.6: Ligands screened for asymmetric hydroboration

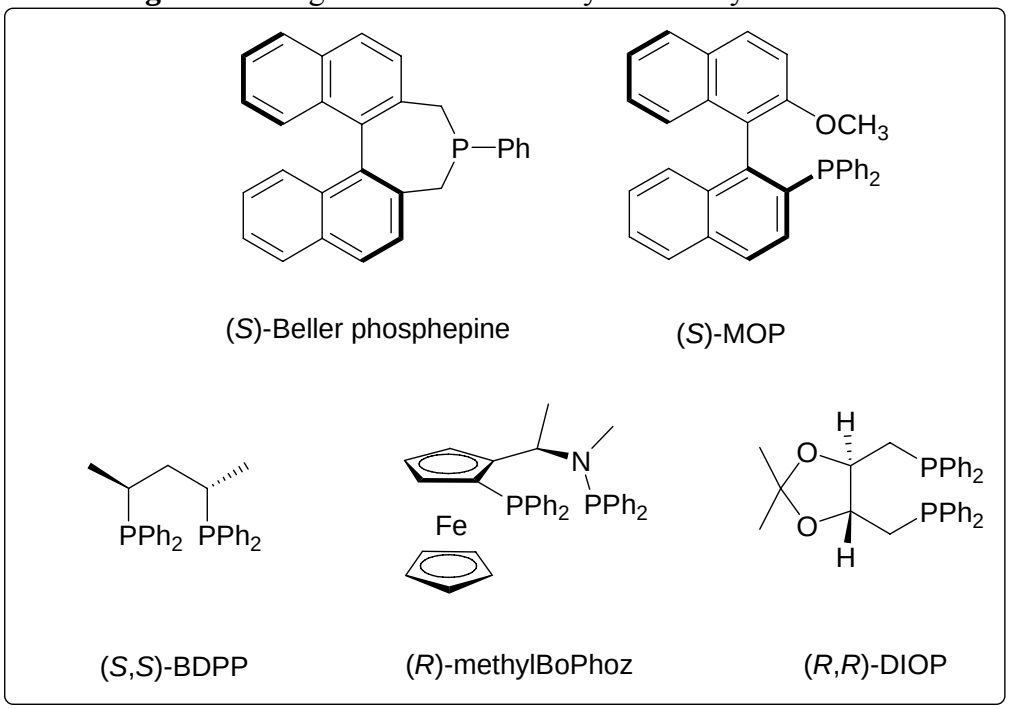

The performance of the diphosphine ligands BINAP (entry 1) and JOSIPHOS (entry 3) gave poor to moderate regioselectivity. BINAP at room temperature gave an enantio- and regioselectivity (41% ee, *R*, 56:44) even poorer than that achieved using catecholborane under the same conditions (57% ee, *R*, 99:1)[64] while JOSIPHOS achieves better enantioselectivity (84% ee, *R*, 78:22) with pinacolborane versus catecholborane at room temperature (60% ee, *R*, unknown regioselectivity)[125]. However, the most remarkable feature of the use of pinacolborane as the hydroborating reagent was that opposite enantiomer of the product was obtained using the same antipode of the chiral ligand for both BINAP and JOSIPHOS. Full comparisons of our results with BINAP and JOSIPHOS with literature values are given in **Tables 2.8**.

Table 2.8: BINAP and JOSIPHOS HBcat/HBpin rhodium-catalyzed hydroborations

	catalyst	ligand	reagent	T (ºC)	B:L	ee (%)	yield (%)
1[a]	$[Rh(COD)_2]BF_4$	(*R*)-BINAP	HBcat	-78	99:1	96 (*R*)	91
2[a]	$[Rh(COD)_2]BF_4$	(*R*)-BINAP	HBcat	25	99:1	57 (*R*)	90
3[b]	$[Rh(COD)_2]BF_4$	(*R*)-BINAP	HBcat	-65	99:1	93 (*R*)	99
4	$[Rh(COD)_2]BF_4$	(*S*)-BINAP	HBpin	25	56:44	41 (*R*)	30
5	$[Rh(COD)_2]BF_4$	(*R*)-BINAP	HBpin	25	53:47	33 (*S*)	30
6	$[Rh(COD)_2]BF_4$	(*S*)-BINAP	HBpin	0	16:74[c]	31 (*R*)	--
7[d]	$[Rh(NBD)_2]BF_4$	(*R*)-(*S*)-JOSIPHOS	HBcat	-78	99:1	92 (*R*)	65
8[d]	$[Rh(NBD)_2]BF_4$	(*R*)-(*S*)-JOSIPHOS	HBcat	25	----	60 (*R*)	--
9[d]	Ir species[e]	(*R*)-(*S*)-JOSIPHOS	HBcat	25	----	77 (*R*)	--
10	$[Rh(COD)_2]BF_4$	(*R*)-(*S*)-JOSIPHOS	HBpin	25	84:16	83 (*S*)	85
11	$[Rh(COD)_2]BF_4$	(*S*)-(*R*)-JOSIPHOS	HBpin	25	78:22	84 (*R*)	70
12	$[Rh(COD)_2]OTf$	(*S*)-(*R*)-JOSIPHOS	HBpin	25	83:17	79 (*R*)	87
13	$[Ir(COD)_2]BF_4$	(*S*)-(*R*)-JOSIPHOS	HBpin	25	3:97	7 (*R*)	72

[a] from Hayahi[64]
[b] from Crudden[103]
[c] 10% vinyl boronate was also observed
[d] from Togni[125]
[e] exact catalyst was not specified

Overall, the combination of BINAP and pinacolborane gives results inferior to BINAP and catecholborane and decreasing of the reaction temperature with

pinacolborane leads to a decrease in ee and formation of vinylboronate (entry 6). A plausible explanation for this decrease is the steric bulk of the four methyl groups of pinacolborane, compared to the planar catecholate of catecholborane, which also has the added ability of π-aryl stacking with both the substrate and chiral ligand. Ziegler's work on DFT calculations suggested that a favourable interaction could occur by chelation to the rhodium center with an oxygen adjacent to boron from the hydroborating reagent[63]. This is likely disrupted by the increased steric bulk of pinacolborane.

The reversal of asymmetric induction has been reported in hydrogenation with the change in metal (Rh and Ru)[137] and minor structural modifications of a chiral ligand[138]. With respect to hydroboration, Bonin has recently observed this reversal with a change of metal (Rh to Ir) for the hydroboration of symmetrical bicyclic hydrazines[121]. This was attributed to the insertion of alkene substrate into the Ir-B bond followed by reductive elimination rather than metal hydride insertion followed by reductive elimination of the boron substituent.

JOSIPHOS shows similar trends (**Table 2.8**), with the change in antipode of JOSIPHOS giving a complete switch in the enantiomer of the product obtained (entry 10 vs 11). The use of pinacolborane gives better results than catecholborane when conducted at room temperature (entry 11 vs 8), and comes close to the results obtained at cryogenic temperatures (entry 11 vs 7). Togni has observed that the use of JOSIPHOS ligands in palladium-catalyzed allylic amination were heavily influenced by the anion, with small, hard anions (F-) enhancing the ee, while non-coordinating anions (PF_6^-) were detrimental[139]. In our studies, little difference was observed between BF_4^- and OTf^- (entry 11 vs 12), however, Fernández has noted the beneficial neutralizing influence of

halide couterions on enantioselectivity[117]. Employing QUINAP (**13**), J.M. Brown's highly successful P,N-ligand[127] gives moderate regioselectivity with the enantioselectivity closely approaching that achieved with catecholborane (**Table 2.9**). No reversal of enantioinduction is seen with QUINAP, which is a less sterically demanding ligand, lending support to the notion that it is the unfavourable steric interactions between the bulky methyl groups of pinacolborane and the diphenylphosphino group of the chiral ligand that are the cause of the change in enantioselectivity. Recent work conducted in our lab (Chris Lata) also indicates that there may be a different mechanism at play between hydroborations with HBcat and HBpin since a Hammett comparison of substituted vinyl arenes gives σ values with opposite signs for the two boranes. Fernández has also conducted work on the influence of the change in hydroboration reagent[117, 140], further discussed in Chapter 2.4.5.

Table 2.9: QUINAP HBcat/HBpin rhodium-catalyzed hydroborations

	Catalyst	Ligand	Reagent	T (ºC)	B:L	ee (%)	Yield (%)
1[a]	[Rh(COD)((*S*)-QUINAP)]OTf		HBcat	20	97:3	88 (*S*)	69
2	$[Rh(COD)_2]BF_4$	(*S*)-QUINAP	HBpin	25	66:34	82 (*S*)	30[b]

[a] from Brown[127]; [b] isolated yield after column chromatography

BDPP and DIOP (**Figure 2.6**) were among the first chiral phosphine ligands investigated for asymmetric hydroborations[141, 142]. However, the combination of (*S*,*S*)-BDPP with catecholborane has not been previously applied to styrene, only to 2-phenylpropene (**Table 2.10**, entry 2), making a direct comparison of the results of (*S*,*S*)-BDPP with pinacolborane (**Table 2.10,** entry 1) impossible.

DIOP gives asymmetric induction in the same sense with different hydroborating reagents (**Table 2.10**, entry 3,4) and it has been suggested that in the absence of steric

effects, the backbone chirality of the ligand is the dominant factor[142]. Cyrogenic temperatures with HBcat (**Table 2.10**, entry 4) are again required but only achieve moderate enantioselectivity. The relatively small size of these two C_2-symmetric diphosphines could explain why no reversal of enantioinduction is observed, although comparison is not prudent with such low observed enantiomeric excesses.

Table 2.10: BDPP and DIOP HBcat/HBpin rhodium-catalyzed hydroborations

	Catalyst	ligand	reagent	T (ºC)	B:L	ee (%)	yield (%)[c]
1	$[Rh(COD)_2]BF_4$	(*S*,*S*)-BDPP	HBpin	25	91:9	34 (*S*)	74
2[a]	$[Rh(COD)Cl]_2$	(*S*,*S*)-BDPP	HBcat	-5	48:52	27 (*R*)	--
3	$[Rh(COD)_2]BF_4$	(*R*,*R*)-DIOP	HBpin	25	63:37	21 (*R*)	55
4[b]	$[Rh(COD)_2]BF_4$	(*R*,*R*)-DIOP	HBcat	-78	----	48 (*R*)	--

[a] substrate 2-phenylpropene[141]
[b] from Burgess[142]
[c] isolated yield after column chromatography

Two monodentate chiral ligands were also investigated: MOP[143], which is highly successful in palladium-catalyzed hydrosilylation of alkenes, and Beller's phosphine[143-146], that had given excellent results in hydrogenation (**Figure 2.6**).

Table 2.11: Chiral ligands for asymmetric hydroboration

Entry	Catalyst Loading (%)	Ligand loading (%)	Ligand	Solvent	B:L	ee (%)	Yield (%)[b]
1[a]	1.25	1.25	(*S*)-MOP	DME	65:35	0	79
2	5	13	(*S*)-Beller	THF	43:57	2 (*S*)	41
3	5	6.5	(*R*)-methyl BoPhoz	THF	39:61	24 (*R*)	77

[a] conducted by Austin Chen; [b] isolated yield after column chromatography

Unfortunately, both of these ligands gave near statistical branched-to-linear selectivity and virtually no asymmetric induction (**Table 2.11** entries 1 and 2). While it would seem that a chiral bidentate ligand is necessary for successful asymmetric induction, the poor results here may lie in the binaphthyl framework chosen. Chiral

monophosphites and phosphoramidites based on a TADDOL framework[124] have been shown to give excellent enantioselectivities with moderate branched selectivity.

The final ligand investigated was the novel P,N,P ligand BoPhoz[147] (**Table 2.11** entry 3). This phosphinoferrocenylaminophosphine was developed along the same lines as JOSIPHOS, to allow for flexibility and variation in the groups attached to phosphorus. These ligands proved to be highly successful in the hydrogenation of dehydro-α-amino acid and itaconic acid derivatives and α-ketoesters, showing extremely high turnover rates under very short reaction times at low catalyst loadings[147]. It was suggested that this resulted from the seven-membered rhodium-BoPhoz chelate, since it is known that seven-membered chelates tend to undergo internal reorganization more rapidly than their five-membered analogues, affording faster reactions[147]. Regrettably, this does not translate into successful hydroboration as the branched-to-linear ratio favours the linear isomer (39:61) with the secondary alcohol in 24% ee. The use of *R*-BoPhoz does not result in a reversal of enantioinduction and yields the *R* alcohol.

2.4.2 Solvent Screen

The results of the ligand screening showed that JOSIPHOS was the most successful ligand, giving the highest ee and second highest branched-to-linear ratio. With these results, a solvent screen was undertaken in an attempt to improve upon the results (**Table 2.12**). The main objective was to maximize the two outcomes of ee and branched-to-linear ratio.

Some interesting results can be observed from the solvent screen. Both 1,4-dioxane (entry 3) and toluene (entry 5), where the ligand and catalyst have poor solubility

and remain ostensibly heterogeneous, give considerably lower ee. Ethereal solvents perform well, but not as well as chlorinated solvents. 1,2-Dichloroethane is by far the best (entry 4) but note the results of chlorobenzene (entry 8) and toluene with minimal 1,2-dichloroethane to ensure a homogeneous solution (entry 7). The addition of the chlorinated solvent gives a higher branched-to-linear ratio and gives a considerable beneficial boost to the ee from 39% in toluene (entry 5) to 66% in the toluene:1,2-dichloroethane (entry 7). These results are quite close to those seen with chlorobenzene alone (entry 8).

1,2-Dichloroethane (entry 4) was chosen as the best solvent as it satisfied the objectives, providing the highest ee and branched-to-linear ratio, although at the expense of the yield.

Table 2.12: Solvent screen for asymmetric rhodium-catalyzed hydroborations

Entry	solvent	B:L	ee (%)[a]	yield (%)[b]
1	THF	78:22	75	77
2	DME	72:28	72	90
3	1,4-Dioxane	68:32	59	76
4	1,2-Dichloroethane, $(CH_2Cl)_2$	78:22	84	70
5	Toluene	48:52	39	45
6	CH_2Cl_2	83:17	77	69
7	Toluene, min $(CH_2Cl)_2$, 10:3	78:22	66	75
8	Chlorobenzene	77:23	71	75

[a] using (*S*)-(*R*)-JOSIPHOS gives *R* enantiomer in all cases
[b] isolated yields after chromatography

2.4.3 Substrate Scope

Having identified JOSIPHOS as the most successful ligand and 1,2-dichloroethane the optimal solvent, the scope of the reaction was investigated.

Equation 2.10: Substrate scope for asymmetric rhodium-catalyzed hydroborations

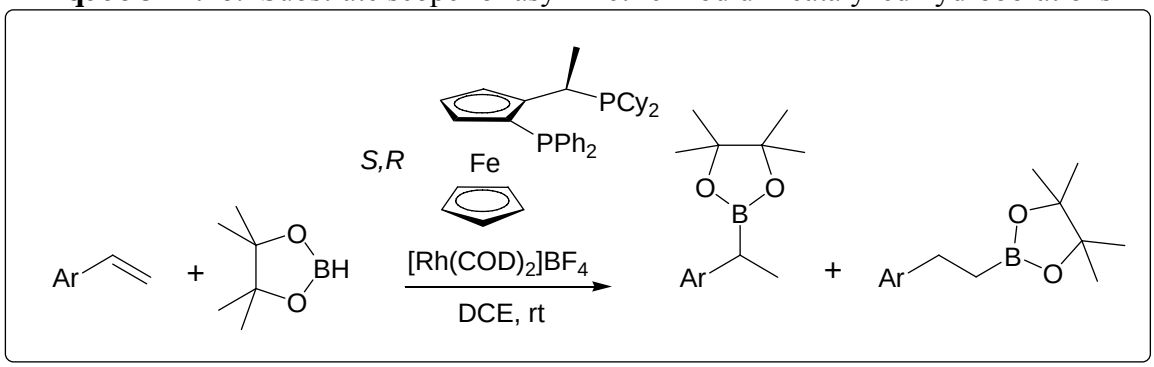

Table 2.13: Substrate scope for asymmetric rhodium-catalyzed hydroborations

entry	vinyl arene	B:L	ee (%)[a]	yield (%)[b]
1	styrene	83:17	84	87
2	4-methylstyrene	82:18	88	39
3	4-chlorostyrene	72:28	80	90
4	4-bromostyrene	83:17	84	87
5	4-methoxystyrene	83:17	76	69
6	2-vinylnaphthalene	95:5	86	67
7	6-methoxy-2-vinylnaphthalene	95:5	88	83
8	6-methoxy-5-nitro-2-vinylnaphthalene	91:9	84	51

[a] using (*S*)-(*R*)-JOSIPHOS gives *R* enantiomer in all cases
[b] isolated yields after chromatography

The series of 4-substituted styrenes has similar branched-to-linear ratios but showed no dependence on the electronics of the styrene with relation to the observed ee. In fact, 4-methoxystryene, the most electron rich substrate gives the lowest ee (76 %, entry 5). Other P,P ligands such as BINAP[64] and Knochel's cyclohexyldiphosphine[148] do not show any dependence on the electronics of the substrate either, in stark contrast to P,N ligands such as QUINAP[127, 136] and PYPHOS[133], which both show linear free energy relationships dependent on the electronic properties of the alkene substrate for hydroborations with HBcat. Fernández has shown that pinacolborane also exhibits this linear free energy relationship[117].

On expanding the scope to vinylnaphthalenes, uniformly high ee's are again obtained, with enhanced branched selectivity, as high at 95:5 in the case of 6-methoxy-2-vinylnaphthalene (entry 7) and vinylnaphthalene (entry 6). It is important to note that this former substrate is a precursor to Naproxen™ via our hydroboration/homologation approach (Chapter 2.5 Optimization en route to Naproxen™). The enhanced branched selectivity is likely due to the formation of the η^3-naphthyl complex **17** which is more stable than the η^3-benzyl complex **18** formed with styrenes[10]. Hayashi first proposed this complex **18**[64] to explain the difference in the regiochemistry of the metal-catalyzed hydroboration compared to the uncatalyzed reaction. Addition of the Rh-H bond across the carbon-carbon bond of the alkene gives complex **18** (**Figure 2.7**), with a potentially stabilizing interaction between the metal and the aryl group. Further discussion of the importance of these complexes can be found in Chapter 3.1.

Figure 2.7: η^3-Vinylarene rhodium complexes

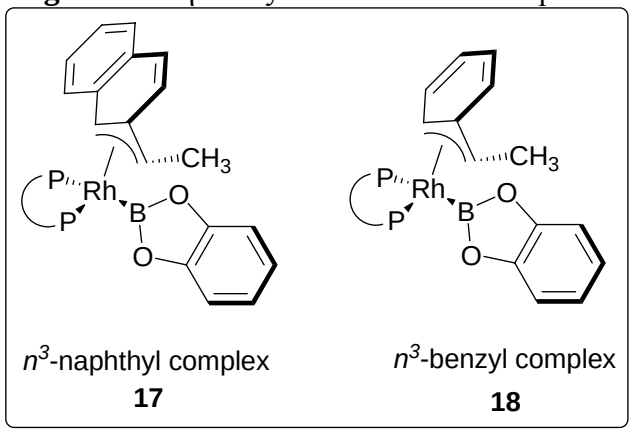

n^3-naphthyl complex **17**

n^3-benzyl complex **18**

2.4.2 Ligand Screen

After the initial report on JOSIPHOS[125] and subsequent modifications[149-151], the ligands and associated technologies were licensed to Solvias AG. Under Solvias' research and development wing, the JOSIPHOS family of ligands has been highly

successful in the industrial synthesis of (*S*)-metochlor, a grass herbicide and *d*-(+)-biotin an important food additive[152].

Solvias AG has a wide variety of ferrocene-based chiral ligands and is actively searching for new applications for them. They kindly provided ligands to screen from a variety of families of ligands (JOSIPHOS, WALPHOS, MANDYPHOS and TANIAPHOS). These ligands (**Figure 2.8** JOSIPHOS and WALPHOS; **Figure 2.9** MANDYPHOS, TANIAPHOS and SOLPHOS) were used under our optimized conditions for asymmetric hydroboration with pinacolborane, with the results shown in **Table 2.14**. For ease of reference, Solvias AG's research number denotes the ligands.

Table 2.14: Solvias AG ligand screen in asymmetric rhodium catalyzed hydroborations

Entry	ligand	yield [a]	B:L [b]	ee [b]
1	(*R*)-(*S*)-SL-J001-1	85	84:16	83 (*S*)
2	(*R*)-(*S*)-SL-J002-1	87	7:93	44 (*S*)
3	(*R*)-(*S*)-SL-J003-1	81	38:62	11 (*S*)
4	(*R*)-(*S*)-SL-J005-1	Incomplete conv	--	--
5	(*R*)-SL-A001-1	87	30:70	32 (*S*)
6	(*R*)-(*R*)-SL-W001-1	72	18:82	29 (*S*)
7	(*R*)-(*R*)-SL-W002-1	90	5:95	0
8	(*R*)-(*S*)-SL-M001-1	53	31:69	27 (*R*)
9	(*R*)-(*S*)-SL-M002-1	35	54:46	22 (*R*)
10	(*R*)-(*S*)-SL-T001-1	45	0:100	0
11	(*R*)-(*S*)-SL-T002-1	27	66:34	5 (*S*)

[a] isolated yields after chromatography
[b] determined by GC

Figure 2.8: JOSIPHOS and WALPHOS families

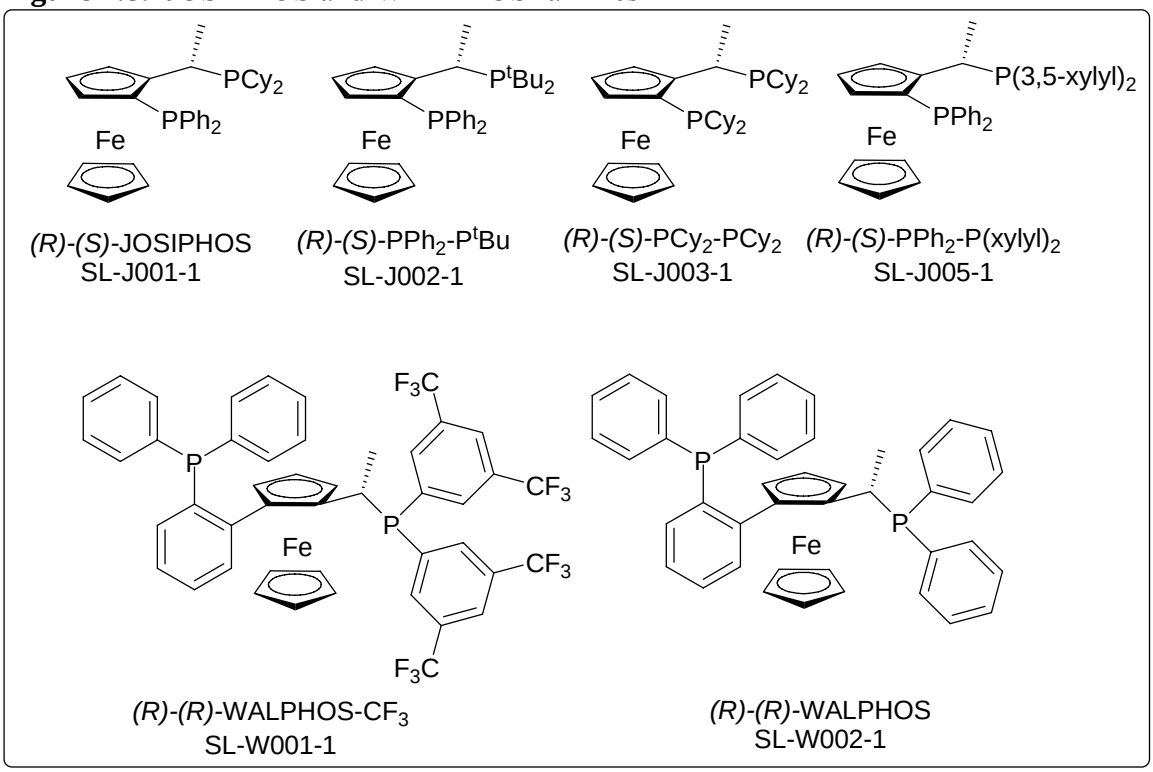

(R)-(S)-JOSIPHOS
SL-J001-1

(R)-(S)-PPh_2-P^tBu
SL-J002-1

(R)-(S)-PCy_2-PCy_2
SL-J003-1

(R)-(S)-PPh_2-$P(xylyl)_2$
SL-J005-1

(R)-(R)-WALPHOS-CF_3
SL-W001-1

(R)-(R)-WALPHOS
SL-W002-1

Figure 2.9: MANDYPHOS, TANIAPHOS and SOLPHOS families

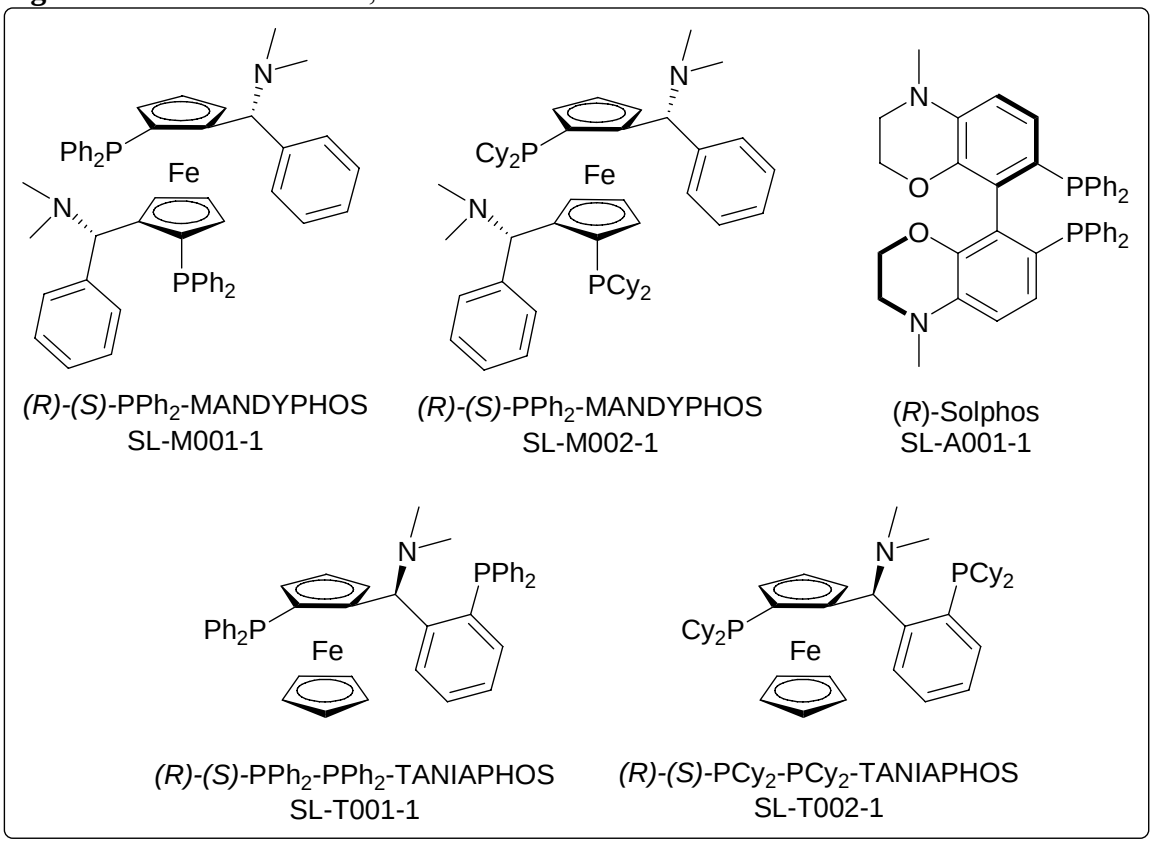

(R)-(S)-PPh_2-MANDYPHOS
SL-M001-1

(R)-(S)-PPh_2-MANDYPHOS
SL-M002-1

(*R*)-Solphos
SL-A001-1

(R)-(S)-PPh_2-PPh_2-TANIAPHOS
SL-T001-1

(R)-(S)-PCy_2-PCy_2-TANIAPHOS
SL-T002-1

Unfortunately, no other ligand tested performs better than standard JOSIPHOS (entry 1) to which the protocol was optimized. However, several trends can be gleaned from the data.

In the JOSIPHOS family (entries 1 to 4), increasing steric bulk on the chiral phosphine from cyclohexyl (entry 1) to *tert*-butyl (entry 2) to 3,5-xylyl (entry 4) leads to steep declines in the observed ee, to the point where the highly bulky 3,5-xylyl group effectively prohibits reaction altogether, likely due to sterics. Change in the bulk of the cyclopentadienylphosphine from phenyl to cyclohexyl (entries 1 versus 3) leads to the same decrease. The increased bulk adversely affects the branched-to-linear ratios, but in all cases the use of the (*R*)-(*S*) enantiomer gives the corresponding (*S*)-alcohol after alkaline oxidation.

(*R*)-Solphos (entry 5), a ligand with a morpholino-modified binaphthyl framework, gives results similar to those of BINAP with the (*R*) antipode yielding (*S*)-alcohol.

The WALPHOS family, with the additional bulk of a phenyl ring between the cyclopentadienyl ring and the diphenylphosphino group, gives high preference for the linear product (almost exclusively in entry 7), with the addition of highly electron withdrawing CF_3 groups (entry 6) giving only a slight improvement and minimal observed ee. Due to the novel nature of these ligands and their limited use in asymmetric catalysis, judgements on the reversal in enantioselectivity cannot be made, as they have not been tested with other hydroboration reagents (specifically HBcat).

The MANDYPHOS (entries 8,9) and TANIAPHOS (10,11) families are modified di- and mono-P, N ligands respectively and give uniformly poor branched-to-linear

selectivities, with MANDYPHOS showing a low observed ee and TANIAPHOS giving only the slightest enantioinduction.

2.4.3 P,P Ligands versus P,N Ligands and the Reversal of Enantioselectivity

This section highlights the central issue for any asymmetric reaction: a general solution rarely exists. Enantioselectivity is influenced by reaction conditions such as choice of solvent and temperature that can be tailored to a given situation, but the importance of these factors may not be great in a particular circumstance. As we have seen, ligand design is an ever-evolving field and reagent choice is often dictated by availability, stability and the researcher's personal preferences and experiences. The substrate is often restricted as the researcher wishes to effect a given transformation on a specific carbon framework. Changes in sterics and electronics are employed to gauge their influence on the course and outcome of the transformation from which inferences on the reaction course are based.

With respect to asymmetric hydroboration, there are a wide variety of ligands which fall into one of two general classifications. The first are the homotopic phosphorus-phosphorus (P,P) ligands such as BINAP[64, 153] and Knochel's cyclohexyl 1,2-diphosphanes[148] that give uniformly high enantiomeric excesses under cryogenic conditions. This occurs regardless of the electronics of the substrate in both cases, with Knochel's ligands overcoming the problem of sterics yielding successful hydroboration of *ortho*-substituted styrenes.

The second class of ligands are the heterotopic phosphorus-nitrogen ligands, first developed in the form of QUINAP[127], modified in the PHENAP series[132] and studied

with a smaller biphenyl frame in PYPHOS[133]. These ligands all share a dramatically decreased dependence on reaction temperature, supplying high enantiomeric excesses within a range of 0-25ºC and are influenced by the electronic nature of the alkene substrate, governed by linear free energy relationships. Typically electron rich vinyl arenes give higher enantioselecitivities.

Brown's proposal for the control of enantioselectivity[136] with QUINAP is based upon the X-ray crystal data of palladium-QUINAP complexes and the trends observed for a series of square-planar platinum complexes where electron-rich styrenes coordinate more strongly *trans* to pyridine that electron-poor styrenes[154]. This approach argues that the stereochemical control is governed by the configuration of the reactive Rh-H, whose transfer to the coordinated alkene defines the configuration of the new stereogenic centre[136]. Based on models of P-Rh-P complexes at the time, and later supported by Fernández and Bo[117, 140], it was deduced that styrene should coordinate *cis* to PPh_2, allowing for the preferred pathway with styrene binding *trans* to the isoquinoline nitrogen. This places the hydroborating reagent *cis* to N and *trans* to PPh_2 (**Figure 2.10**). This pathway is increasingly favoured as the styrene becomes more electron-rich, keeping it tightly bound in the chiral environment of the phosphine, which allows for discrimination between the two enantiotopic faces, key to the transfer of chirality. With an electron-poor styrene, the rationale is that this leads to decreased binding preference *trans* to the isoquinoline nitrogen, reflected in the decreased enantioselectivity. There is also the case where the styrene binds *trans* to the PPh_2, placing it *cis* to the sterically undemanding isoquinoline nitrogen where again it is removed from the chiral environment leading to decreased selectivity. It should be noted that in all cases the Rh-

H bond has the same configuration relative to the N-Rh-P plane in the penta-coordinate complex[136].

Figure 2.10: Model for enantioselectivity with QUINAP[136]

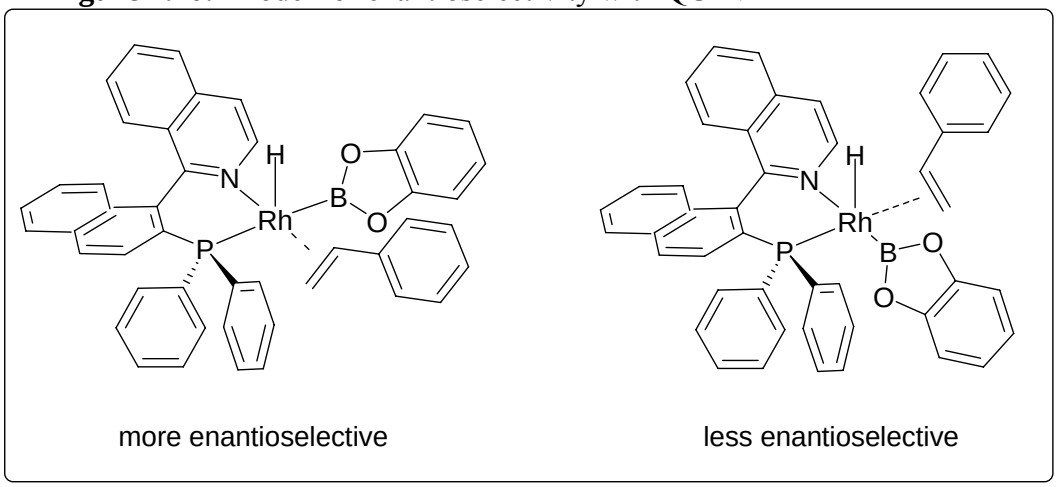

Chan[133] has proposed a different rationale for the results obtained with the ligand PYPHOS (**Figure 2.11**). Chan used the coordination of the vinylarene in the transition-state model to suggest that this may be the governing factor in the observed enantioselectivity for electron rich and poor vinylarenes. He proposed that vinylarenes with electron-donating substituents would lead to stronger coordination *trans* to the pyridyl ring of the ligand compared to vinylarenes with electron-withdrawing groups. This would lead to electron-rich vinyl arenes being closer to the rhodium center, resulting in improved stereochemical communication and give rise to a higher enantioselectivity, while electron-poor vinylarenes with their greater distance from the rhodium center, has two modes of coordination available as it is further away from the chiral environment and this leads to a lower observed ee in the product[133].

Note that in both models for PYPHOS and QUINAP, the key issue is to have the vinylarene coordinating *trans* to the nitrogen of the pyridine or isoquinoline group and the hydroborating reagent *cis* to the nitrogen.

Figure 2.11: Model for enantioselectivity with PYPHOS[133]

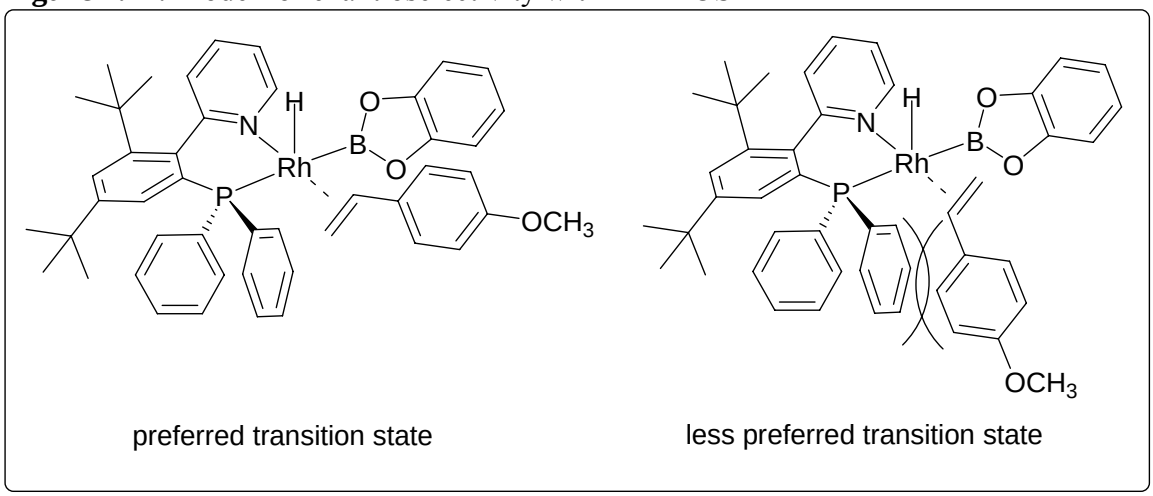

Both of these models were developed with the use of catecholborane as the hydroborating reagent. Catecholborane has enjoyed near exclusive use in catalytic asymmetric hydroborations until recently[10, 155], with several properties that aid its utility. It is a coplanar molecule, making it sterically undemanding, and possesses a cloud of π electrons from the benzene ring permitting stabilizing interactions, such as π-stacking, which can lead to lowering the energies of key transition states and influence the binding of vinyl arenes[63]. The five-membered ring heterocycle may be aromatic[93] and it is suggested to possess a high degree of Lewis acidity, allowing for ease of catalytic activation (Chapter 1.6)[7].

Fernández and Bo[117, 140] conducted multinuclear NMR studies with QUINAP and PYPHOS ligands and performed computational modeling by hybrid quantum mechanics/molecular mechanics (QM/MM) methods to interpret the observed trends and gain insight into the energetics of the proposed intermediates.

When subjected to multinuclear (^{1}H, ^{11}B, ^{31}P) NMR analysis, the signals resulting from the treatment of the pre-catalyst [Rh(COD)(R)-BINAP]BF_4 with catecholborane and styrene were suggested to be generated by the isomer (**19**) shown[140].

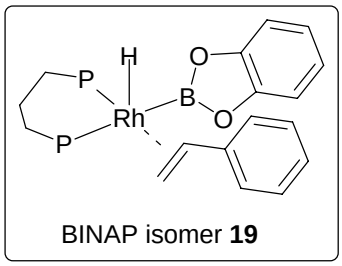

BINAP isomer **19**

However, when the pre-catalyst [Rh(COD)(R)-QUINAP]BF_4 was similarly treated, no hydride signals appeared in the upfield region of the ^{1}H NMR spectra, only a slight upfield shift in the ^{31}P NMR was seen and the signals due to H and B from free catecholborane were not observed, indicating that it was no longer free. They proposed that a three-center bonding interaction (**20**) between the Rh metal center and the B-H bond of the reagent had taken place[140]. They then assumed that the key intermediates were those proposed by Brown[136], by virtue of the similarity to the Rh-BINAP analogue.

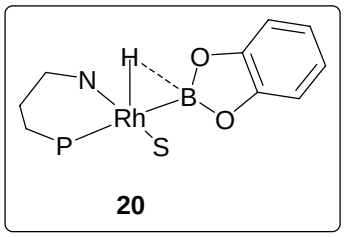

20

Our research has shown us that the use of pinacolborane as the hydroborating reagent leads to a complete reversal of enantioselectivity compared to the use of catecholborane with the same antipode of ligand, most dramatically with the ligand JOSIPHOS, but also seen with BINAP. However, this reversal was not seen with the use of QUINAP. A summary of these results is given in **Table 2.15**.

What can be taken from these evaluations is the recognition that two influencing factors are at work here: the ligand and the hydroborating reagent.

We had proposed[10] that with the switch from BINAP to QUINAP structural differences were responsible for the reversal in stereoinduction. Comparing QUINAP to BINAP, QUINAP is less sterically demanding as the bulk of the PPh_2 group is removed,

accompanied with a change in electronics from a symmetrical P,P system to unsymmetrical P,N.

Table 2.15: Comparison of ligand and hydroboration reagent

	catalyst	ligand	reagent	T (ºC)	B:L	ee (%)	yield (%)
1[a]	$[Rh(COD)_2]BF_4$	(*R*)-BINAP	HBcat	-78	99:1	96 (*R*)	91
2[a]	$[Rh(COD)_2]BF_4$	(*R*)-BINAP	HBcat	25	99:1	57 (*R*)	90
3	$[Rh(COD)_2]BF_4$	(*S*)-BINAP	HBpin	25	56:44	41 (*R*)	30
4[b]	$[Rh(NBD)_2]BF_4$	(*R*)-(*S*)-JOSIPHOS	HBcat	-78	99:1	92 (*R*)	65
5[b]	$[Rh(NBD)_2]BF_4$	(*R*)-(*S*)-JOSIPHOS	HBcat	25	----	60 (*R*)	--
6	$[Rh(COD)_2]BF_4$	(*R*)-(*S*)-JOSIPHOS	HBpin	25	84:16	83 (*S*)	85
7	$[Rh(COD)_2]BF_4$	(*S*)-(*R*)-JOSIPHOS	HBpin	25	78:22	84 (*R*)	70
8[c]	[Rh(COD)((*S*)-QUINAP)]OTf		HBcat	20	97:3	88 (*S*)	69
9	$[Rh(COD)_2]BF_4$	(*S*)-QUINAP	HBpin	25	66:34	82 (*S*)	30

[a] Hayashi[64] [b] Togni[125] [c] Brown[127]

On the basis of their spectroscopic studies, supported by QM/MM calculations that agreed with their results for the proposed intermediates, Fernández and Bo[140] made the assumption that the relative stability of the isomeric reaction intermediates was proportional to their population and so the most stable isomers lead to the observed reaction products. In general, they found that intermediates that would lead to the linear product where higher in energy relative to those that lead to the desirable branched product. When the ligand was (*R*)-QUINAP of the two most stable isomers leading to branched product, the pro-*R* and pro-*S* isomers, there was an energy difference of 4.1 kcal/mol. With (*R*)-BINAP, the difference between pro-*R* and pro-*S* was only 0.3 kcal/mol. Fernández and Bo explained that this small energy difference that was responsible for the lower stereodifferentiation of BINAP.

The crucial flaw in this proposal by Fernández and Bo is that it goes directly against the Curtin-Hammett principle which states that "for a reaction that has a pair of reactive intermediates or reactants that interconvert rapidly, each going irreversibly to a

different product, the product ratio will depend only on the difference in the free energy of the transition state going to each product, and not on the equilibrium constant between the intermediates". This oversight is not uncommon in asymmetric catalysis, the most notable example being the case of asymmetric hydrogenation where isolation of a "transient" rhodium intermediate by J. M. Brown[156] led to an incorrect assignment of the active catalytic species until it was[157] recognized that the minor rhodium species was sufficiently more reactive to H_2 and dominated the enantioselectivity of the reaction.

It is also important to consider the effect of π- π interactions, which they found to be present between the substrate and the ligand, the substrate and the hydroboration reagent, and the hydroboration reagent and the ligand - all of which are contributing towards the stability of the key reaction intermediates[140].

Fernández and Bo repeated the same QM/MM analysis for their results on the Rh/ligand/borane/styrene systems, evaluating the effect of the hydroborating reagent when the chiral ligand was held constant[117]. Their experimental results showed that catecholborane leads to higher branched selectivity and enantioselectivity compared to pinacolborane regardless of the ligand used, a trend that we observed for our data as well. They also observed the reversal in stereoinduction with the change of hydroborating reagent.

The results of the QM/MM calculations can be summarized as follows. For Rh/(*R*)-QUINAP/borane/styrene, for catecholborane the pro-*S* isomer energy is 4.1 kcal/mol for catecholborane compared to 1.9 kcal/mol for the pro-*S* isomer with pinacolborane. Thus both hydroboration reagents favoured the pro-*S* isomers. This leads to the same enantioinduction with (*R*)-QUINAP, but the decrease in energy with the

change of borane reagent from catecholborane to pinacolborane was taken as responsible for the decreased enantiomeric excess and branched selectivity observed[117].

For the Rh/R-BINAP/borane/styrene system, the most stable isomer was pro-*R* (0.3 kcal/mol) with catecholborane but was changed to pro-*S* (0.2 kcal/mol) with pinacolborane. The change in the most stable isomer was taken as responsible for the switch in enantioinduction, and the small difference in energy agreed with the low asymmetric induction[117]. This proposal is again in conflict with the Curtin-Hammett principle.

One should also be quick to notice that the change in hydroborating reagent from catecholborane to pinacolborane would result in the loss of stabilizing π- π interactions and this is the case when comparing the change in energy for Rh/R-QUINAP/borane/styrene system from catecholborane to pinacolborane (4.1 to 1.9 kcal/mol). However, QM/MM calculations showed a new stabilizing interaction between the substrate and one methyl group of pinacolborane (**Figure 2.12**), compensating for the loss of the π- π interactions[117].

Figure 2.12: π-π Interactions with HBcat and π-methyl interactions with HBpin[117]

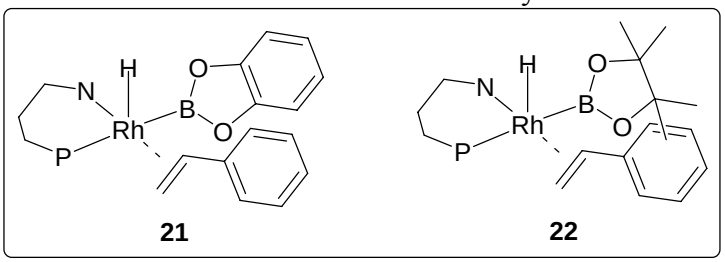

21 **22**

From these results, extrapolations to JOSIPHOS can be made. Comparing entries (**Table 2.15**, enteries 6 and 7), where the antipode of JOSIPHOS is changed and HBpin is the hydroboration reagent, both give similar branched-to-linear ratios and enantiomeric excesses that show complete reversal. This suggests that JOSIPHOS is able to

accommodate the increased steric bulk of pinacolborane, although no direct comparison can be made to catecholborane at similar temperatures (entry 5). More striking is the complete reversal of enantioinduction and its magnitude, leading to the argument that the differences between the diastereomeric transition states was large, with the two intermediate isomers leading to the different enantiomers. The sterics of the ligand has considerable influence (**Table 2.14** entries 1-4) on both branched-to-linear selectivity and enantiomeric excess, with increased bulk causing steep erosion.

It would be of interest to see the results of pinacolborane hydroborations under the influence of the chiral ligand PYPHOS. Its dependence on the electronics has been studied with catecholborane[133] and it has been extensively modelled[140], however it is unknown how well it could handle the increased sterics of pinacolborane and how great the effects of the electronic of the substrate would influence selectivities.

Jendrealla's ligand (**12**)[158] would provide insight into the comparison of reduced sterics from a binapthyl to a biphenyl system, along with a change in electronic factors with the addition of highly electron-withdrawing fluorine substituents[159]. Support for making the ligand electron-poor can be seen in the WALPHOS system (**Table 2.14** entries 6 and 7) where the addition of CF_3 groups on the phenyl rings of phosphorus gives an ee significantly higher, albeit with poor regioselectivity.

2.5 Optimization en route to Naproxen™

With favourable results obtained for the hydroboration of 6-methoxy-2-vinylnaphthalene (**Table 2.13**), the hydroboration was performed using the opposite enantiomer (*R*)-(*S*)-JOSIPHOS to furnish the (*S*)-boronate ester. Oxidation with alkaline H_2O_2 followed by

analysis of the branched alcohol (obtained free of the linear achiral alcohol) showed an 88% ee. Prior to further use, the (*S*)-boronate ester was obtained as the pure branched isomer by chromatography treatment on a Cyclograph™ centrifugal chromatography system (Analtech Inc). The (*S*)-boronate ester was then subjected to homologation[103] with 89% conversion as judged by ^{1}H NMR spectroscopy. This crude material was then carried forward under conditions of biphasic Lindgren oxidation[105] to give the desired carboxylic acid, Naproxen™, matching known spectra[160]. Reduction with BH_3•SMe_2 to the corresponding alcohol and chiral HPLC revealed an 88% ee, indicating total retention of configuration. The enantiomeric composition was authenticated by comparison to the alcohol obtained from the reduction of commercial (S)-Naproxen™.

Equation 2.11: Hydroboration/homologation reactions to Naproxen™

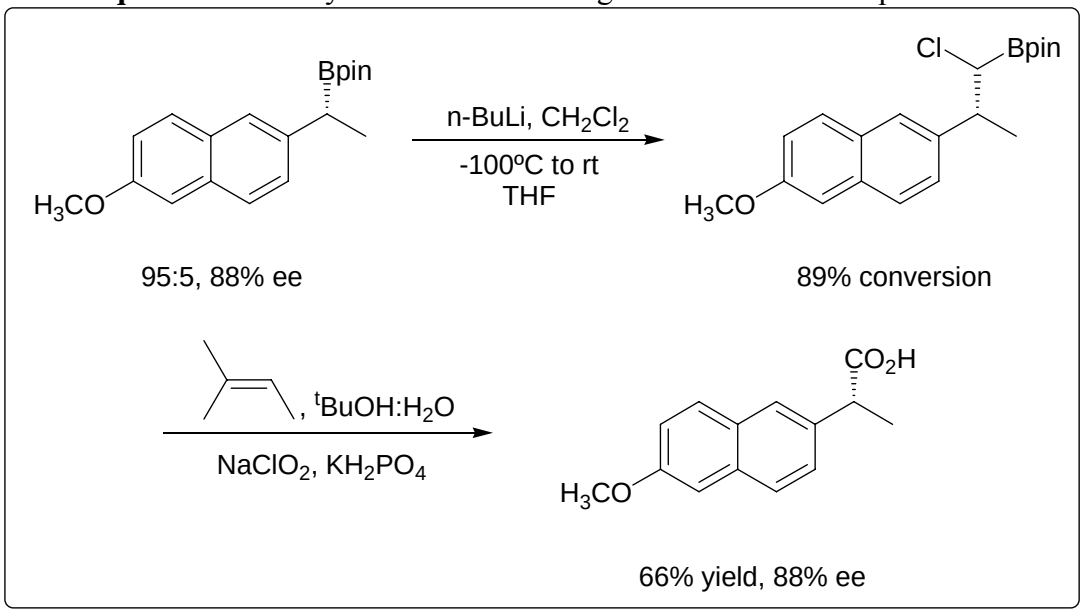

2.6 Conclusions

The investigations reported herein have broadened the scope of hydroboration by the addition of pinacolborane to the arsenal of reagents amenable to transition metal-

catalysis by merit of its increased stability. Complementary regioselectivity is observed with rhodium giving high branched selectivity, while iridium shows exclusive linear selectivity. When applied to asymmetric catalysis, the influence of the ligand and hydroborating reagent showed the dramatic influence of sterics and electronics that can be rationalized by the work of Fernández and Bo[117, 140]. However, these conclusions must be regarded with skepticism as they ignore the Curtin-Hammett principle, a key tenet of physical organic chemisty. The use of pinacolborane in hydroborations can be successfully applied to homologation chemistry[103, 104] circumventing a transesterification step, and generates the non-steroidal anti-inflammatory Naproxen™ in high enantiomeric excess.

Chapter 3

Mechanistic Insight into Transition Metal Catalyzed Hydroboration with Pinacolborane

3.1 Introduction and Comments

This chapter describes our mechanistic investigations of both rhodium- and iridium-catalyzed hydroborations. Important details of the mechanism of rhodium-catalyzed hydroborations have been elucidated by Baker, Marder and Evans[35-37], although questions still remain about the mechanism in the presence of different metals and different reagents. For example, iridium-catalyzed hydroborations have dramatically different regioselectivities from their rhodium counterparts[10, 11, 59] increasing the breadth of products that can be formed by metal-catalyzed hydroborations and will find doubtless use in organic synthesis.

This chapter will also draw upon work conducted in our lab by David Edwards concerning his investigations into rhodium-catalyzed hydroborations and mechanistic implications derived from this work. Due credit will be mentioned when referencing these results as they pertain to the discussions included here.

3.1.1 The Accepted Mechanistic Cycle of Rhodium (I) Catalyzed Hydroborations

In the literature covering rhodium (I) catalyzed hydroborations, there are two differing opinions on the nature of the intermediates involved and the key step in the reaction mechanism. This stems from Männig and Nöth's initial mechanistic proposal[7] of a dissociative mechanism (**Figure 3.1**) for the hydroboration reaction.

Figure 3.1: Männig and Nöth's mechanism for rhodium catalyzed hydroboration

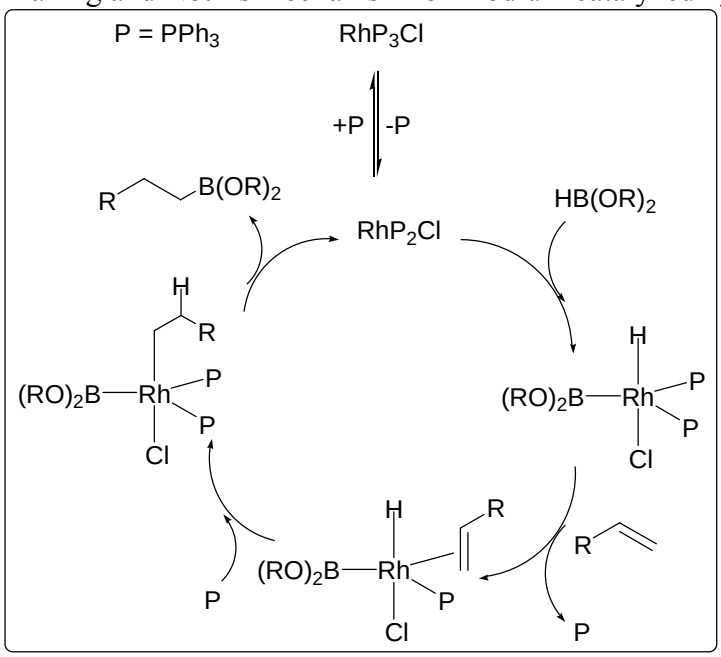

Research into the mechanistic pathway by Evans[35] supported the dissociative mechanism while work by Baker, Westcott and Marder[36] lead to the proposal of an alternative associative mechanism.

The differences between the two mechanistic pathways are subtle. The dissociative pathway of **Figure 3.1** occurs by ligand dissociation to give a vacant coordination site, oxidative H-B addition to the rhodium center, followed by alkene coordination that displaces a phosphine ligand, giving a penta-coordinate intermediate. Subsequent alkene insertion into the Rh-H bond occurs in tandem with phosphine binding and reductive C-B bond coupling completes the catalytic cycle. The associative pathway

proceeds by the same initial steps of ligand dissociation and oxidative H-B addition, but alkene coordination occurs without phosphine displacement, generating a hexa-coordinate intermediate (**23**). In both mechanisms, the next step is alkene insertion into the Rh-H bond or Rh-B bond. Insertion into the Rh-H bond gives the expected alkylboronate after reductive elimination, while insertion into the Rh-B leads to alkylboronate, or if β-hydride elimination occurs, vinylboronate ester formation. This is supported by the observed formation of these products[36] and theoretical calculations outlined below.

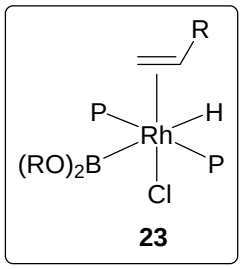

23

Theoretical studies by a number of researchers gave conflicting results and support for different mechanisms. Musaev[161] restricted his calculations to the investigation of the associative mechanism and concluded that the favoured pathway involved H-B bond addition to the rhodium center, followed by alkene co-ordination, migratory alkene insertion into the Rh-B bond and completed by reductive C-H bond formation as the rate-determining step. Schleyer[162] based their calculations on the dissociative mechanistic proposals of Nöth[7] and Evans[35] and ruled out the associative mechanism on the basis of experimental and computational evidence. Not surprisingly, this study confirmed that H (hydride) migration was preferred to BR_2 (boryl) migration in the key step. They supported this conclusion by drawing parallels to other rhodium-catalyzed reactions, such as the hydrosilylation of carbon-carbon double bonds.

To date, the most authoritative study has been conducted by Ziegler[63] which compared both the associative and dissociative mechanisms using density function theory (DFT) calculations at the BP86 level. Their calculations were based on the generic

reaction shown below using a model of Wilkinson's catalyst [$RhCl(PH_3)_3$] (**Equation (3.1)**).

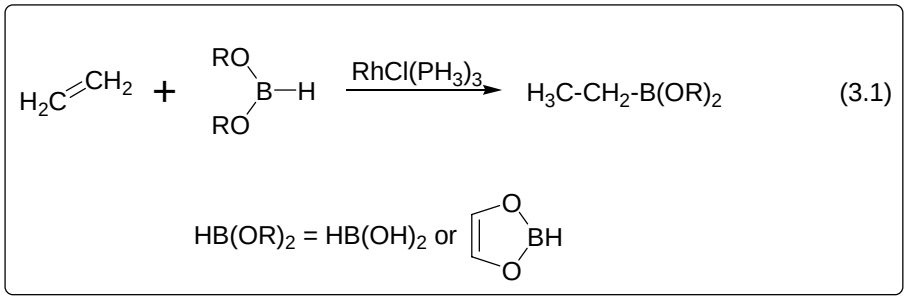

Ziegler's study concludes that either mechanism is feasible. For the associative mechanism, it was determined that the initial hydride migration was only slightly favoured over boron migration as both had similar energy profiles. In the case of the dissociative mechanism, initial boryl migration is endothermic with a high activation barrier (19.5 kcal/mol) relative to initial endothermic hydride migration (8.5 kcal/mol), however, reductive elimination to form the C-B bond of the boryl migration pathway is exothermic by 6.5 kcal/mol, compared to endothermic C-H bond formation (15.8 kcal/mol) which requires substantial reorientation of the boryl and alkyl units about the rhodium center. Ziegler's calculations also yielded two key conclusions. The first was that in either mechanism, the occurrence of a boryl migration would lead to the production of the side products of vinylboronates and alkanes. This is in agreement with observed production of these compounds[36]. In the second conclusion, Ziegler favours the associative mechanism, but allows for the possibility of a dissociative mechanism with bulky electron-withdrawing phosphine ligands[63].

The associative mechanism is often associated with the feasibility of boryl insertion where boryl migration must occur as the initial step, as seen in the rhodium

catalyzed diboration of alkenes[85, 163-166]. Morken has extended the scope of this reaction to an enantioselective variant (**Equation 3.2**)[165, 166] and proposed a general mechanism (**Figure 3.2**).

Equation 3.2: Rhodium catalyzed diboration of alkenes[165]

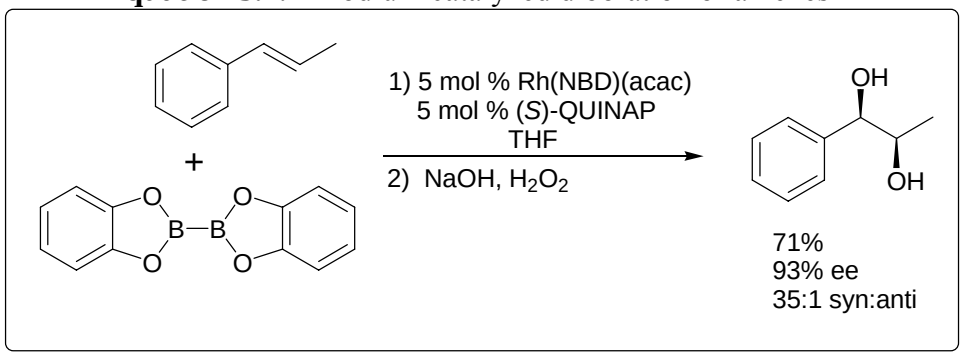

Figure 3.2: Mechanism for rhodium catalyzed diboration of alkenes[166]

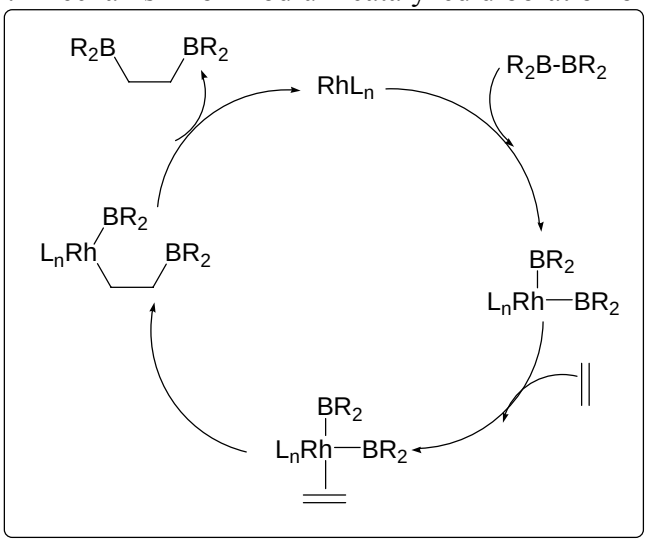

While this mechanism appears to be straightforward, there is evidence that the final reductive elimination to form the carbon-boron bond is in competition with β-hydride elimination and subsequent hydroboration. As shown in **Equation 3.3**, choices of ligand and catalyst have profound impact on the observed product ratios.

The use of Rh(I)/BINAP generates the desired 1,2-diol as the major product, but also affords the 1,3-diol that arises from β-hydride elimination followed by reinsertion

then reductive elimination. Dissociation of the complex results in an allylboronate species that is not observed, possibly because it is rapidly protonated upon

Equation 3.3: Rhodium-ligand catalyzed diboration of indene[166]

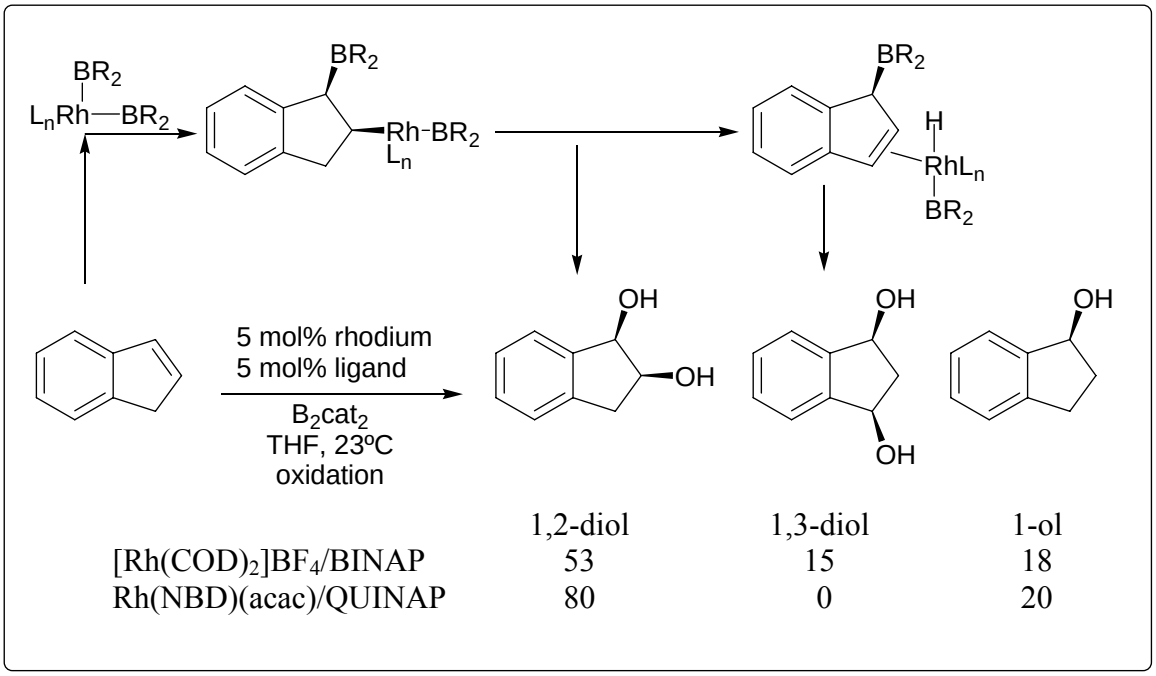

	1,2-diol	1,3-diol	1-ol
$[Rh(COD)_2]BF_4$/BINAP	53	15	18
Rh(NBD)(acac)/QUINAP	80	0	20

aqueous oxidative workup, regenerating indene[166]. This dissociation also produces a hydrido(boryl)rhodium intermediate that is an active hydroboration catalyst, leading to the formation of the 1-ol. The use of Rh (I)/QUINAP produces the 1,2-diol and the 1-ol in a 4:1 ratio with no production of 1,3-diol, suggesting that for this catalyst/ligand combination the β-hydride elimination pathway is hindered[166]. It is interesting to note that QUINAP again shows superior selectivity for the α-position giving the desired branched isomer in sterically demanding β-substituted alkenes[132, 167].

3.2 Deuterium Studies of Transition Metal Catalyzed Hydroborations

3.2.1 Background

Deuterium labeling is a critical part of many mechanistic studies. In organic chemistry, the challenge often lies in the placement of the label in the correct position of the molecule using known synthetic transformations. This often leads to changes in reactivity due to isotopic effects and differing bond strengths[168] and imposes limitations caused by the availability of sources of deuterium or deuterium containing reagents.

The one main advantage of deuterium labeling studies is that the observation of the fate of a given deuterium label can be readily monitored by ^{2}H NMR techniques. However, the observation of ^{2}H resonances at natural abundance cannot be achieved due to low receptivity and low natural abundance of ^{2}H[169]. This leads to ^{2}H NMR spectroscopy being less sensitive than ^{1}H NMR spectroscopy by a factor of 1.5×10^{-6}. A comparison of the isotopes ^{1}H and ^{2}H is given in **Table 3.1**.

Table 3.1: Properties of the two stable isotopes of hydrogen ^{1}H and ^{2}H[169]

property	^{1}H	^{2}H
natural abundance (%)	99.985	0.015
Nuclear spin	½	1
resonance frequency	100	15.351

The difference in nuclear spin of ^{2}H leads to efficient nuclear relaxation dominated by a quadrupolar mechanism that allows for nuclear Overhauser effects to be neglected[169]. This means that integration of ^{2}H NMR spectra can be treated as one would a ^{1}H NMR spectra, provided the nucleus that it is coupled to does not cause significant broadening. The property of resonance frequency is defined for a field ($B_o \sim 2.35$ T) in which the ^{1}H frequency is exactly 100 MHz. This allows for comparison with other nuclei to determine their frequency relative to ^{1}H. ^{2}H has a resonance frequency of 6.51

times lower than ^{1}H[169]. This decrease in sensitivity leads to broadening of signals, even at high field strength. To illustrate this, consider that for the ^{2}H NMR experiments described in this chapter were conducted on a 600 MHz field strength NMR spectrometer. While the ^{1}H NMR signal would be found near 600 MHz, the corresponding ^{2}H NMR signal would occur at approximately 92 MHz and have a resolution power analogous to that of ^{1}H NMR at 100 MHz.

This factor of 6.51 also reduces the observed scalar coupling of J(^{1}H, ^{2}H) similarly when compared to J(^{1}H,^{1}H). This does not affect the observed deuterium chemical shifts (ppm) and these are identical to the corresponding proton chemical shifts[169].

Deuterium labeling studies, all with DBcat, have been conducted prior to our work and are summarized in **Table 3.2**, with relevant solvents and substrate(s) noted.

Table 3.2: Summary of deuterium labeling studies with DBcat

	Catalyst	Solvent	Substrate(s)
Burgess[48]	$RhCl(PPh_3)_3$	THF	styrene, 1-decene
Evans[35]	$RhCl(PPh_3)_3$	THF	styrene, 1-decene
Baker, Marder, Burgess, Westcott[36]	$RhCl(PPh_3)_3$	THF	styrene
Brown[100]	$[RhCl(CH_2CH_2)_2]_2$	THF, toluene	styrene

From **Table 3.2**, the most important and relevant work to our studies have been conducted by Evans[35, 170] and Baker, Marder and Westcott[36]. The report of Burgess[48] is only useful for the fact that it highlights the issues faced to achieve reproducible, reliable results – high quality catalysts free of oxidative impurities, conducting the reactions under an anaerobic atmosphere and substrate purity. All of these issues have been addressed in the Evans and Westcott *et al.* studies, the results of which are described below.

3.2.2 Rhodium (I) Catalyzed Hydroboration Mechanistic Study of Evans

From the Evans' research group came the first mechanistic study of rhodium (I) catalyzed hydroborations[35, 170]. The study focused on the use of Wilkinson's catalyst applied to the hydroboration of various alkenes with DBcat. Evans also noted that cationic rhodium sources ([Rh(NBD)(DPPB)]BF_4) provided qualitatively similar results[170].

In this study, the two key substrates examined that are relevant to our own studies were styrene and 1-decene. In the case of styrene, Evans observed that the reaction of excess alkene with DBcat using $RhCl(PPh_3)_3$ afforded only one deuterium labeled product 1-phenyl-2-deuterioethanol (**Equation 3.4**).

Equation 3.4: Styrene deuterium labeling results of Evans[35, 170]

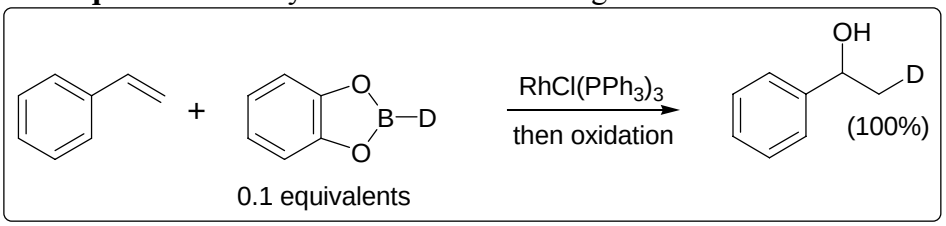

From this result, Evans concluded that no reversible alkene binding and hydride migration occurred for this substrate, but later added the caveat that the elementary steps of the hydroboration catalytic cycle could vary with substrate, with boron hydride and with catalyst[35].

In contrast with styrene, the hydroboration of excess 1-decene showed extensive deuterium incorporation in both the α and β positions of the alcohol and recovered alkene (**Equation 3.5**)[35, 170]. Evans took the presence of deuterium in the recovered alkene to demonstrate that migration, forming either a primary or secondary rhodium alkyl and alkene binding were reversible. The significant amounts of deuterium at the terminal carbons in both the alkene and alcohol was evidence that the migration of the deuteride to

the rhodium-bound alkene was non-selective and reversible, and it was the selective reductive elimination from the primary alkylrhodium species rather than the secondary alkylrhodium that controls the regioselectivity, giving the terminal alkylboronate[35, 170].

Equation 3.5: 1-Decene deuterium labeling results of Evans[35, 170]

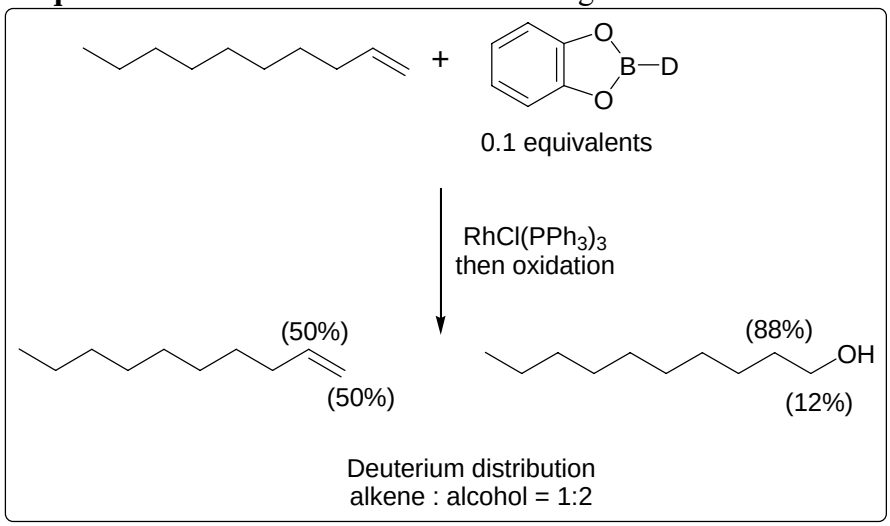

With the results of the deuterium studies in hand, Evans commented on the possibility that boron migration occurs before hydride to the bound alkene. Männig and Nöth had not addressed this issue, and on the basis of the extensive deuterium scrambling observed[35, 170], hydride migration observed in iridium catalyzed hydroboration of alkynes[60] and regioselectivity seen in directed hydroboration reactions[40, 171] Evans concluded that hydride migration was preferred and final product formation occurred from an irreversible reductive elimination of a rhodium-boryl species, as in Männig and Nöth's initial proposal.

3.2.3 Rhodium (I) Catalyzed Hydroboration Mechanistic Study of Burgess, Baker, Westcott and Marder

This seminal study[36] elucidated the complexity of the mechanistic pathway for rhodium (I) catalyzed hydroborations (Chapter 1.4), demonstrating that alkene insertion

into the rhodium-boron bond was a viable process in addition to insertion into the rhodium-hydride bond. If followed by β-hydride elimination, this led to the observation of vinylboronate esters and production of H_2 (DH or D_2) and the corresponding alkane. This in turn allows for the incorporation of deuterium into alkane and into the linear alkylboronate via hydrogenation of the respective alkene and vinylboronate ester[36].

Of interest with respect to our work were the results obtained by Baker, Westcott and Marder with styrene (**Equation 3.6**).

Equation 3.6: Styrene deuterium labeling results of Burgess, Baker, Westcott and Marder[36]

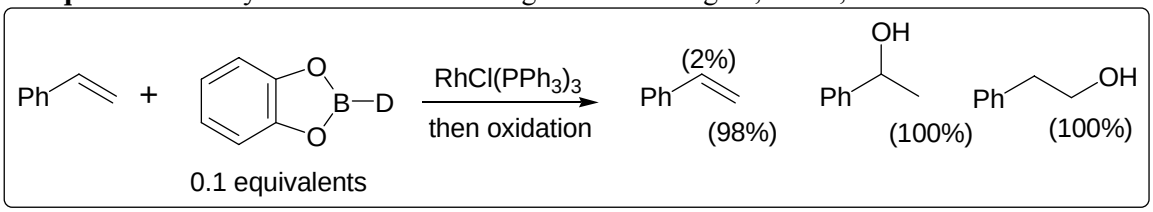

Their result with three deuterium-containing products was in sharp contrast to Evans' observation. Deuterium label was almost completely located at the terminal and β positions of alkene and alcohol products. Incorporation into starting alkene, suggested reversible alkene binding and hydride migration – Evans had only observed deuterium incorporation into the secondary alcohol. Additionally, hydroborations mediated by Wilkinson's catalyst handled and manipulated under aerobic conditions showed little tendency towards hydrogenation[36].

These studies shared two conclusions in common. The first was the profound influence of catalyst purity and composition on the observed deuterium label placement and product distributions. The second was the substrate influenced the product and label distribution, particularly for sterically hindered (slow reacting) alkenes[36].

The Baker, Westcott and Marder study revealed the complex nature of the combination of Wilkinson's catalyst and catecholborane, identifying multiple rhodium

species present and the associated degradation of catecholborane by the catalyst. It was stressed that due to the multiple pathways available during the catalytic cycle that deuterium labeling studies could only be reliable if product distributions were given to support the proposed mechanism(s) and any discussion of the reversibility of a step in the catalytic cycle. The observation of vinylboronate esters and contaminant hydrogenation were not observed by Evans and it was the production of these materials that provided the first evidence that insertion of alkenes into the rhodium-boron bond was a viable alternative to insertion into the rhodium-hydride bond.

3.3 Transition Metal Catalyzed Hydroborations with Deuterated Reagents

The following two sections on rhodium and iridium catalyzed hydroborations draw upon many of the issues related to the fate of the deuterium label detailed in the above sections.

There are several assumptions that are made with respect to the deuterium label to simply the analysis. They are as follows:

1) Once deuterium is incorporated into excess substrate or product, it remains there. Specifically, β-hydride elimination is preferred over β-deuteride elimination due to stronger C-D bond strengths.
2) Only one deuterium is incorporated at each site in each molecule. This applies to the deuterium label in the observed branched and linear boronate esters. This leads to simplified accounting of deuterium placement, yet may underestimate incorporation.

A screen of solvents was conducted to determine which was most suitable for our deuterium labeling study. The use of any solvent would require access to both the deuterated and non-deuterated versions for both ^{1}H and ^{2}H NMR studies. While THF has been used in all the past studies, d_8-THF has only been used in selected reactions due to its high cost. Toluene had been shown to be a poor solvent for the pre-catalysts (Chapter 2.4.2 Solvent Screen) and was therefore not tested. The results of the solvents screened are documented in **Table 3.3**.

Table 3.3: Metal catalyzed hydroboration of styrene with HBpin monitored by ^{1}H NMR

Catalyst	solvent	branched:linear	comments
$[Ir(COD)Cl_2]_2$/DPPB	d_4-1,2-dichloroethane	0:100	complete in 2 hrs
$[Rh(COD)_2]BF_4$/DPPB	d_4-1,2-dichloroethane	95:5	incomplete at 3.5 hrs
$[Ir(COD)Cl_2]_2$/DPPB	d_6-acetone	--:--	no reaction, precipitate forms
$[Rh(COD)_2]BF_4$/DPPB	d_6-acetone	95:5	incomplete at 3 hrs
$[Ir(COD)Cl_2]_2$/DPPB	$CDCl_3$	0:100	complete in 3 hrs
$[Rh(COD)_2]BF_4$/DPPB	$CDCl_3$	64:36	incomplete at 7.5 hrs

Chlorinated solvents (1,2-dichloroethane and chloroform) proved suitable for iridium catalyzed reactions which occurred at short reaction times in this solvent. Rhodium catalyzed reactions required substantially longer reaction times, between 20-24 hours to reach completion. The branched to linear selectivity also suffered significant erosion in $CDCl_3$. Acetone proved unsuitable for iridium catalysts and was not further explored.

With suitable reaction conditions determined and with quantities of DBpin in hand (Chapter 3.6.1), experiments to probe the mechanisms of rhodium and iridium catalyzed hydroborations were conducted.

3.3.1 Rhodium Metal Catalysis

Without question, rhodium has been the catalyst of choice in hydroborations due to its preference to generate the branched boronate product when conducted on vinylarenes, showing remarkable ligand dependance[37] and until recently, with HBcat as the hydroborating reagent. The reason for this regioselectivity in hydroborations was first proposed by Hayashi[64] and was attributed to the stabilizing effect of a π-benzyl interaction. Comparisons have been drawn to other rhodium catalyzed additions to carbon-carbon double bonds, such as hydrosilylation[100, 162] and hydroformylation[172, 173] by virtue of a similar pattern of reactivity and regioselectivity. Spencer[174] showed that substrate polarity was influential to the preferential addition of rhodium to the benzylic position of substituted styrenes in hydrogenation. Isolation and characterization of π-benzyl complexes of rhodium by Werner[175, 176], Fryzuk[177] and Stühler[178] have demonstrated their stability but no direct evidence of their involvement in the rhodium catalyzed hydroboration has been presented.

Rhodium catalyzed hydroborations with HBpin have been shown by our group and that of Fernandez to proceed with high branched selectivity[10] in the hydroboration of vinylarenes. It was hoped that deuterium labeling with DBpin would provide some insight into the mechanism and allow for comparison with HBcat/DBcat.

The hydroboration of one equivalent of styrene with one equivalent of DBpin catalyzed by cationic $[Rh(COD)_2]BF_4$/DPPB was monitored by ^2H NMR spectroscopy (d_4-1,2-dichloroethane internal standard, 3.8 ppm) and showed clean formation of the branched boronate ester along with HD (**Figure 3.3**) after 10 hours. The incorporation of deuterium into the methyl group is clean (**Figure 3.3**), with small signals for

hydrogenation present and a phase inverted signal for HD. Due to this phenomenon and its close proximity to the internal standard, proper integrations could not be obtained.

The reaction with cationic rhodium was typical, requiring 24 hours to reach completion. Further proof that the inverted signal shown in **Figure 3.3** is indeed HD was obtained by allowing the reaction to continue after the completion of hydroboration. The presence of rhodium catalysis effected H to D exchange of the alkene protons of styrene and reduction of the intensity of the HD signal and an increase in the alkane signals due to hydrogenation. Loss of intensity could also occur by escape of this small gaseous molecule from the NMR tube. No deuterium incorporation into styrene occurs during the course of the hydroboration. However, once the reaction is complete and left to continue stirring, deuterium signal is observed to appear in the alkene signals. Significant (33-35%) label is seen in the alkene when it is in large excess, suggesting the higher

Figure 3.3: Rhodium catalyzed hydroboration of styrene with DBpin

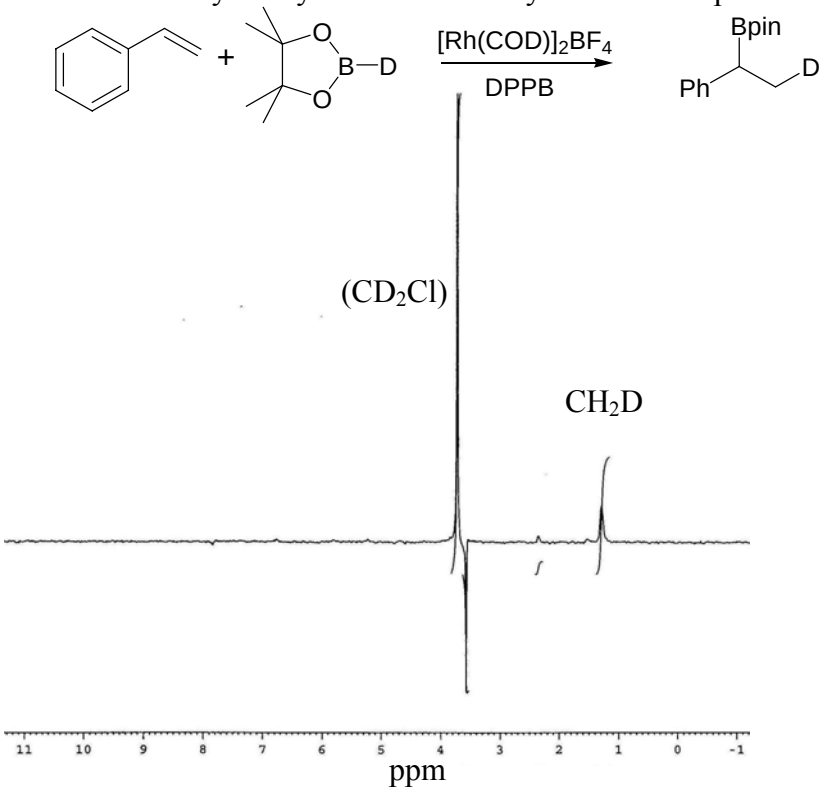

concentration of alkene favours rapid exchange by constant displacement of alkene from the metal center. **Table 3.4** illustrates the issue of deuterium balance for the reaction shown in **Figure 3.3**. The reaction requires 24 hours to reach completion, with the additional time to determine the fate of the HD peak. **Equation 3.7** shows the sites of deuterium incorporation.

Equation 3.7: Location of deuterium incorporation in the products

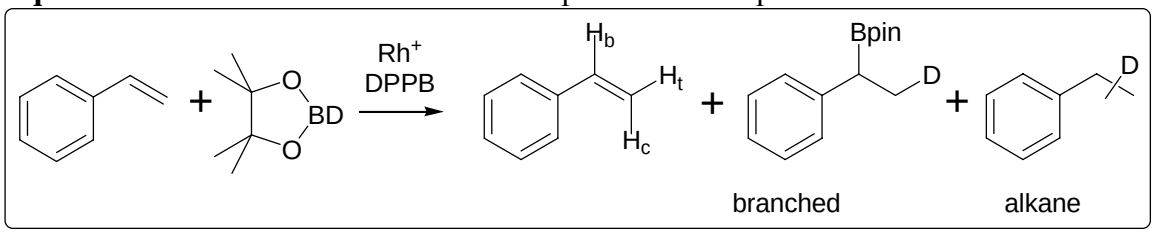

Table 3.4: Accounting for the observed deuterium distribution in rhodium catalyzed hydroboration

Time	% D incorporation					D mmol (0.42 DBpin added)					D	
hours	Alkene			Products		Alkene			Products		mmol	mmol (%)
	H_b	H_c	H_t	Alkane	Branch	H_b	H_c	H_t	Alkane	Branch		
6	-	-	-	-	92	-	-	-	-	0.376	0.376	90
12	-	-	-	10	90	-	-	-	0.026	0.250	0.276	66
18	-	-	-	6	47	-	-	-	0.032	0.257	0.289	69
24	-	-	-	13	80	-	-	-	0.036	0.220	0.256	61
48	1.75	1.4	1.6	11.4	78	0.009	0.007	0.008	0.059	0.407	0.466	111

Attempts to quantify the reversibility of the metal hydride addition were hampered by the poor deuterium balances seen when styrene and DBpin were used. With a range of 65 to 111% of the deuterium label found, this large variance within a single reaction makes the data gained difficult to interpret. During the course of these studies, the sensitivity of the reactions towards trace metals was noted, particularly on Telfon stirbars. To prevent the introduction of foreign metal that could lead to hydride or deuteride formation, a new stirbar was used for each deuterium labeling reaction. The DBpin utilized (Chapter 3.6.1)

was synthesized with iridium metals, but the isolated DBpin was distilled prior to use, greatly reducing the likelihood of metal contamination.

In order to solve this problem, we decided to examine the hydroboration using HBpin of d_3-styrenes, whose synthesis is described in Chapter 3.6.2. David Edwards conducted hydroborations with a limited amount of HBpin to yield incorporation of hydride into both the recovered styrene and product, indicating a reversible metal hydride insertion (**Equation 3.8**). The hydride of HBpin is incorporated to the P_β site of the product alcohol, with some benzylic placement (P_α). Recovered styrene shows nearly a third of the hydride label at position S_β. With the use of 5 equivalents of d_3-styrene, the reversible metal hydride insertion is operating at a comparable rate to hydroboration.

Equation 3.8: Rhodium catalyzed incorporation of hydride into d_3-styrenes

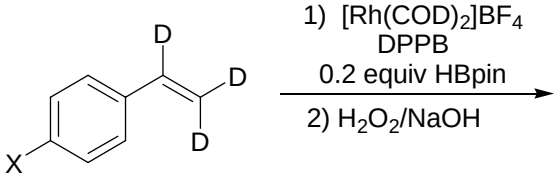

X	P_α	P_β	S_α	S_β
Cl	6	62	4	28
OCH_3	6	62	4	28

3.3.2 Iridium Metal Catalysis

The complimentary regioselectivity of iridium catalyzed hydroborations to rhodium catalysis, combined with few examples in the literature meant that mechanistic studies on a novel catalytic system could be undertaken. With only one product consistently observed in iridium catalyzed hydroborations, the expected result would be deuterium label at the benzylic (α) position and the boronate ester at the terminal (β) position, giving only linear boronate ester if this results from a direct hydroboration of styrene (**Equation 3.9**).

Equation 3.9: Expected fate of deuterium label

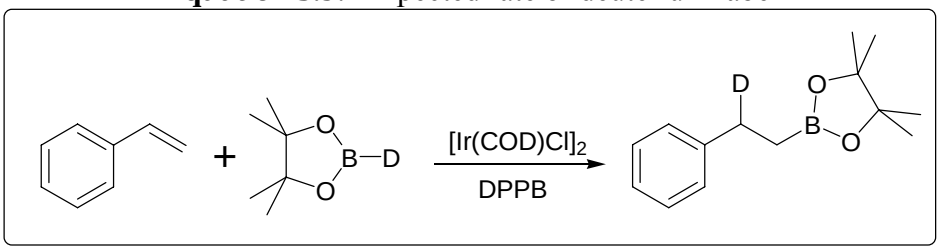

However, when styrene was treated with DBPin, deuterium incorporation into all available positions of both excess alkene and linear boronate ester was observed, but not at equal amounts. With nearly 90% of the introduced deuterium label being observed in the excess alkene, rapid hydride insertion is clearly reversible. Interestingly, the deuterium incorporation is also highly regiospecific as shown in (**Equation 3.10**). The mechanistic implications are discussed in more detail in Chapter 3.4, but the main conclusion is that a reversible hydride insertion causes the rapid incorporation of deuterium label into excess alkene and the preferential formation of a π-benzyl complex controls the regioselectivity of this process, even though the linear product is formed (**B_2** in **Figure 3.4** or **H_2** in **Figure 3.5**). However, the possibility that the metal hydride

Equation 3.10: Deuterium label in the presence of excess styrene

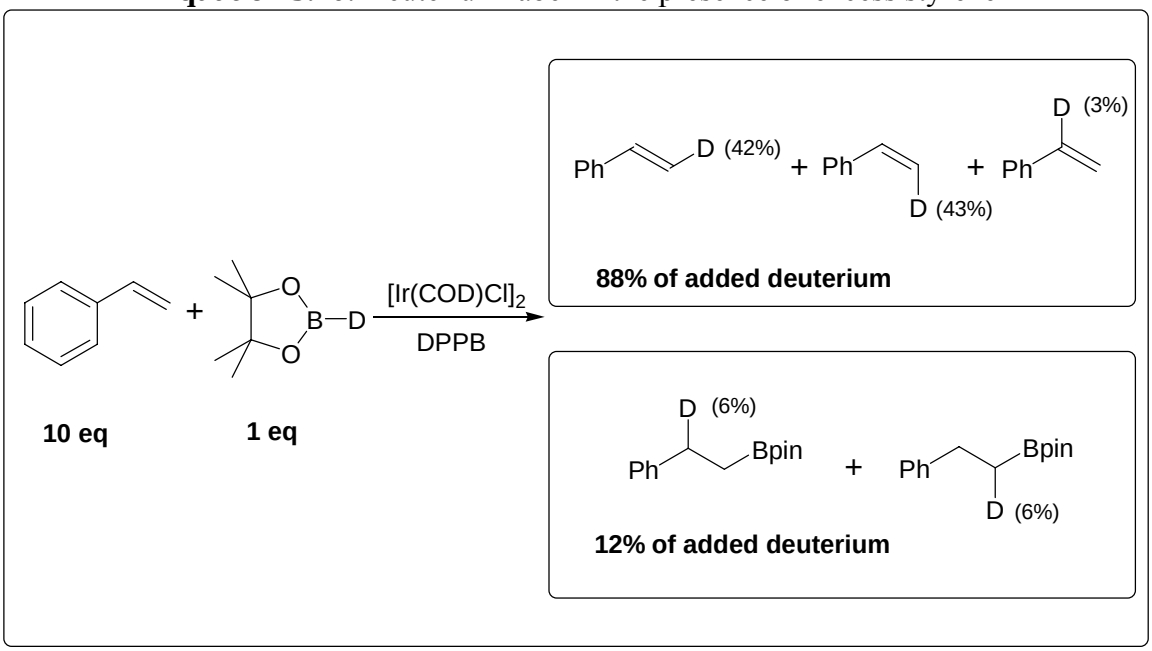

addition occurs tangentially to the actual reaction manifold and product is only generated by metal boryl insertion needs to be considered, and will be discussed in Chapter 3.4. As has been done in Chapter 3.3.1, a key experiment would be the hydroboration of d_3-styrene with HBpin in the presence of $[Ir(COD)Cl]_2$/DPPB and observe label – loss or lack of loss of deuterium at the benzylic site, plus at the terminal site where boron is incorporated, focusing on the rates of these exchanges.

Beyond the use of styrene, which is obviously a benchmark substrate, the scope of substrates used in metal catalyzed hydroborations, particularly that in which the mechanism is probed with deuterium labeling is quite limited. The early work of Burgess[48] is suspect due to the use of oxidized catalyst. This leaves only Evans work with 1-decene[35] in the presence of rhodium catalysts for comparison. Linear 1-alkenes are known to give terminal hydroboration products due to a combination of sterics from both the alkene and hydroboration reagent and the increased steric bulk of the alkylboronate intermediates. This is also attributed to a decreased rate of reductive

elimination compare to styrene systems[35]. With the lack of an adjacent phenyl group, no beneficial stabilization can be gained, as no π-benzyl intermediate can be formed.

The hydroboration of 1-octene with HBpin under iridium catalysis consistently gave high yields and linear boronate ester as the only product. Subjecting excess 1-octene to DBpin in the presence of iridium catalyst gave markedly different deuterium incorporation than that observed with styrene (**Equation 3.11**).

Equation 3.11: Deuterium label in the presence of excess 1-octene

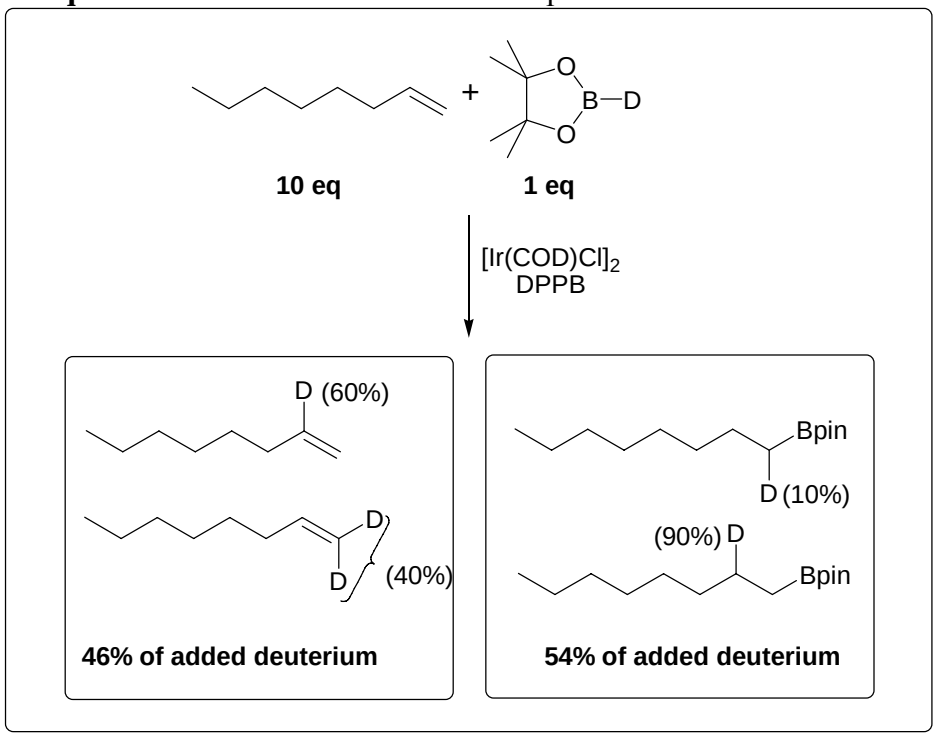

These results are quite similar to those observed by Evans[35] with 1-decene using Wilkinson's catalyst and DBcat, who observed more deuterium in the product than the starting material, equal incorporation at both sites in the starting material, and predominant incorporation at the internal carbon of the alcohol (**Equation 3.12**).

On the basis of the observed deuterium incorporation and placement of the deuterium label, it would appear that our reactions with iridium follow the same

Equation 3.12: Deuterium incorporation in 1-decene[35]

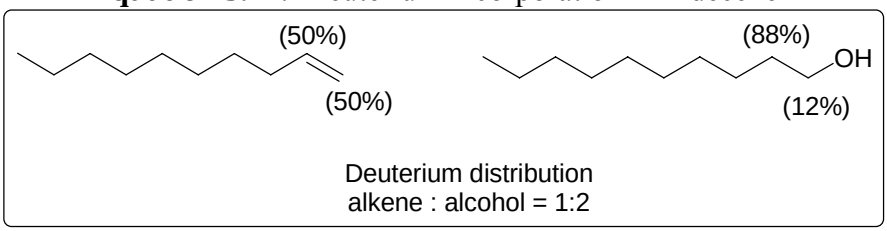

mechanism as observed by Evans[35], although the full mechanistic implications will be discussed in Chapter 3.4.

A similar study was also carried out in the hydroboration of β-methylstyrene, an internal alkene (**Equation 3.13**).

Equation 3.13: Deuterium label in the presence of excess β-methylstyrene

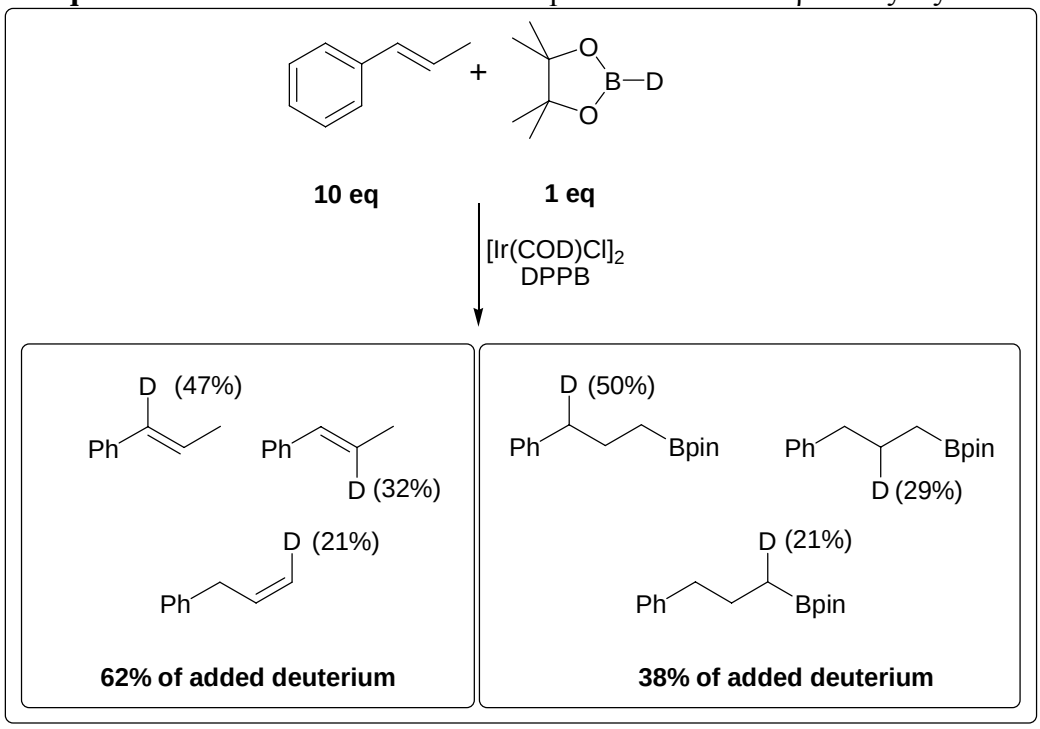

In this case, the only product observed resulted from isomerization and hydroboration to place the boron at the terminal (formerly methyl) carbon. Nearly two-thirds of the incorporated deuterium is found in the recovered alkene and the remaining third is retained in the product. Another striking feature is the similar deuterium content at both the α, β and γ positions in both the alkene and boronate product, with a slight

preference for placement at the benzylic position, suggesting that isomerization proceeds first, rapidly consuming the deuterium label from DBpin and leaving the elements of HBpin to complete the final hydroboration of the terminal alkene.

Isomerization during the course of uncatalyzed hydroboration reactions is not uncommon. H.C. Brown first reported the isomerization of internal trialkylboranes to the terminal trialkylborane upon heating the reaction mixture after rapid uncatalyzed hydroboration[179, 180]. It was also observed that trace amounts of free BH_3 acted as a catalyst increasing the rate of isomerization and lowering the required temperature.

Isomerizations involving catalytic systems have been seen by Morrill and Srebnik under different conditions. Morrill[79] used $RhCl_3/BH_3$ with both internal and terminal alkenes to give a rapid isomerization followed by hydroboration generating a wide variety of products, although considering that BH_3 is the hydroborating reagent in this case, it is unclear whether the isomerization involves the metal or not. Srebnik[17] observed the isomerization and hydroboration of *trans*-4-octene to the terminal alkylborane to occur with Wilkinson's catalysts while nickel and rhodium catalyst, $Rh(CO)Cl(PPh_3)_2$ lead only to hydroboration with no isomerization, although this work was also suspect due to the use of oxidized Wilkinson's catalyst[83]. This work was corrected and studied in more detail by our group, and employed in a one-carbon chain homologation of internal alkenes to the linear aldehydes[83]. It is well known that rhodium hydrides are extremely efficient catalysis for alkene isomerization[32, 33], especially when conducted in the presence of molecular oxygen[181]. With the use of iridium catalysts in hydroboration becoming more widespread, similar results involving isomerizations have been reported[182].

3.4 Proposed Mechanistic Cycle for Iridium (I) Catalyzed Hydroborations

The use of iridium (I) complexes as catalysts in hydroboration has been limited due to either slow catalytic turnover[60] or poor regioselectivity with alkynes for vinylboronate formation[61]. Some successful results were achieved using iridium precursors that required photolytic conditions to promote the loss of CO ligands[59].

Our research into iridium-catalyzed hydroborations with DPPB on styrene showed near perfect selectivity for the linear alkylboronate isomer[10] with the use of the neutral iridium complex $[Ir(COD)Cl]_2$. During the course of our research, Miyaura[11] also reported that the hydroboration of alkenes with pinacolborane gave high selectivity for the linear boronate under appropriate conditions ($[Ir(COD)Cl]_2$ in combination with bisphophines.

Equation 3.14: Results of pinacolborane hydroborations from Miyaura[11]

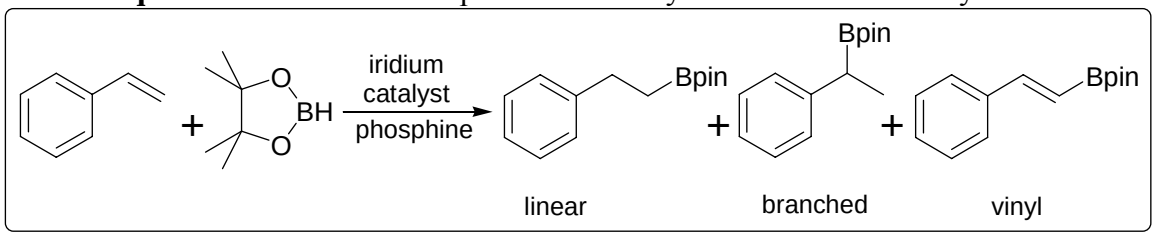

A comparison of our results with Miyaura's (**Equation 3.14**) is shown in **Table 3.5**. Both examples using neutral $[Ir(COD)Cl]_2$ (**Table 3.5** entries 2 and 5) are nearly identical, giving high linear selectivity. In our hands, cationic iridium catalysts gave high linear selectivity but moderate yields and therefore we settled on the use of $[Ir(COD)Cl]_2$. Under these conditions, linear boronate esters were obtained in perfect selectivity and high chemical yield in all cases, regardless of the electronic nature of the vinylarene employed[10] (Chapter 2.2.2, **Table 2.6**). In addition, Miyaura found that cationic iridium salts gave mixtures of products, including vinylboronates, which we did not observe.

Since different solvents were employed, this may have played a role; although the low yield we obtained in entry 3 (**Table 3.5**) indicates that the vinyl boronate may have been present as the data in **Table 3.5** represent isolated yields.

Table 3.5: Comparison of iridium catalyzed hydroboration studies

				product distribution		
Entry	Catalysts	Solvent	Yield	Linear	Branched	Vinyl
	From Crudden[10]					
1	5% $[Ir(COD)_2]BF_4$/5% DPPB	THF	68	100	0	0
2	2.5% $[Ir(COD)Cl]_2$/5% DPPB	THF	99	100	0	0
3	2.5% $[Ir(COD)Cl]_2$	THF	43	63	37	
	From Miyaura[11]					
4	1.5% $[Ir(COD)_2]PF_6$/1.5% DPPB	PhMe	25	67	12	21
5	1.5% $[Ir(COD)Cl]_2$/3% DPPB	PhMe	94	98	0	2
6	1.5% $[Ir(COD)Cl]_2$	PhMe	80	62	8	30

Miyaura's results with cationic iridium catalysts show low yields and considerable production of vinylboronate ester, which we had never observed during the course of our investigations. A possible explanation is the choice of solvent. In screening solvents to optimize hydroboration conditions (Chapter 2.4.2) it was noted that the catalysts and phosphines exhibited poor solubility in toluene, remaining a heterogeneous suspension. Not surprisingly, toluene is routinely used as solvent under conditions that promote vinylborane formation[65, 66]. Ethereal solvents (DME[64], THF[104, 127, 153]) are widely recognized as the solvent of choice in hydroboration chemistry due to catalyst solubility. Another explanation is catalyst loading, as we had noted issues of reproducibility at low catalysts loadings.

The mechanism put forth here is based the observed product distributions, thermodynamic studies by Hartwig[62], empirical studies on the behaviour of iridium complexes towards the reversible binding of hydrogen and alkenes by Vaska[54, 55] and our own deuterium labeling studies.

As mentioned in Chapter 1.3.2.3, Hartwig undertook calorimetric and computational methods to determine the bond dissociation energies (BDEs) of the Ir-H and Ir-B bonds at 66 and 60 kcal/mol respectively. The calculated ΔH values for the primary reactions reflect the favourable alkene insertion into the Ir-B bond (**Table 3.6**).

Table 3.6: Calclulated ΔH values based on BDEs[62] for iridium catalyzed hydroboration

reaction number	simplified primary reaction	ΔH (kcal/mol)*
1	[Ir] + H($BO_2C_6H_4$) → [Ir](H) ($BO_2C_6H_4$)	-15
2	[Ir](H) ($BO_2C_6H_4$) + CH_2CH_2 → [Ir](CH_2CH_3)($BO_2C_6H_4$)	2
3	[Ir](H) ($BO_2C_6H_4$) + CH_2CH_2 → [Ir](H)($CH_2CH_2BO_2C_6H_4$)	-6
4	[Ir](CH_2CH_3)($BO_2C_6H_4$) → [Ir] + CH_3CH_2($BO_2C_6H_4$)	-11
5	[Ir](H)($CH_2CH_2BO_2C_6H_4$) → [Ir] + CH_3CH_2($BO_2C_6H_4$)	-3
6	H($BO_2C_6H_4$) + CH_2CH_2 → CH_3CH_2($BO_2C_6H_4$)	-24

* based the following BDE data: C=C 163, C-C 88, C-H 98, H-($BO_2C_6H_4$) 111, C-($BO_2C_6H_4$) 113, H-[Ir] 60, C-[Ir] 35, B-[Ir] 66, [Ir] = *trans*-[$IrCl(CO)(PPh_3)_2$]

The mechanistic implications of alkene insertion into an Ir-H or Ir-B bond can be seen when these thermodynamic data are applied to the known reaction products and the intermediates that lead to them. The mechanistic consequences of both possibilities are shown below, beginning with boryl insertion.

Figure 3.4: Mechanistic consequences of alkene insertion into an Ir-B bond for the case of styrene.

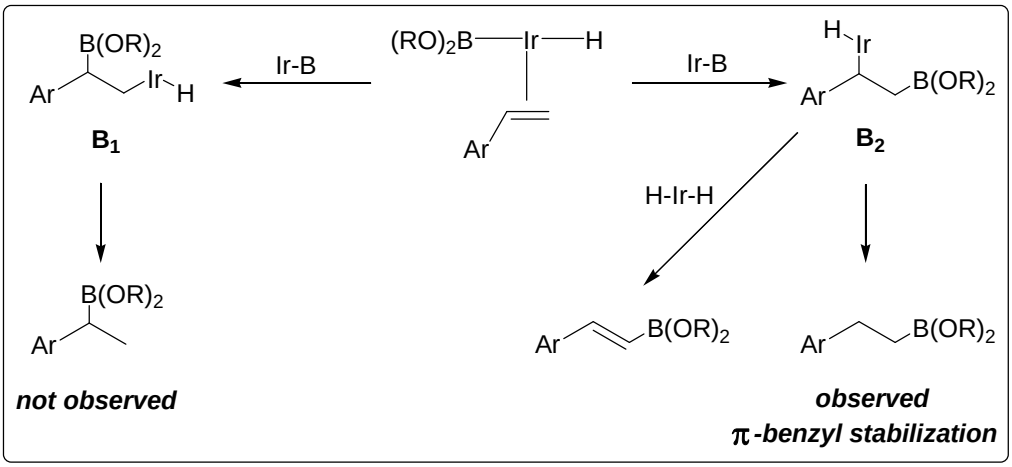

Alkene insertion into the Ir-B bond can occur in two ways (**Figure 3.4**). Insertion leading to placement of the boryl group on the benzylic position gives intermediate **B_1**

with the Ir-H bond on the terminal carbon. However, this does not reductively eliminate since the branched product is not observed. Alternatively, alkene insertion to place the boryl group on the terminal carbon gives intermediate **B_2**, which has the added benefit of π-benzyl stabilization and after reductive elimination, leads to the observed product. It should be noted that the pathway to **B_1** cannot be ruled out, due to the thermodynamic favourability of alkene insertion into Ir-B bonds[62] but is not observed under the experimental conditions of our mechanistic studies, yet may occur under other conditions where the branched isomer is observed (**Table 3.5**, entry 3). Interestingly those reaction conditions which generate the branched isomer as a minor product also generated the vinylboronate, implying that boryl insertion was occurring (**Table 3.5**, entries 4 and 6) It should be noted that several researchers[11, 59] have also observed vinylboronate formation during the course of their investigations.

Figure 3.5: Alkene insertion into Ir-H bond

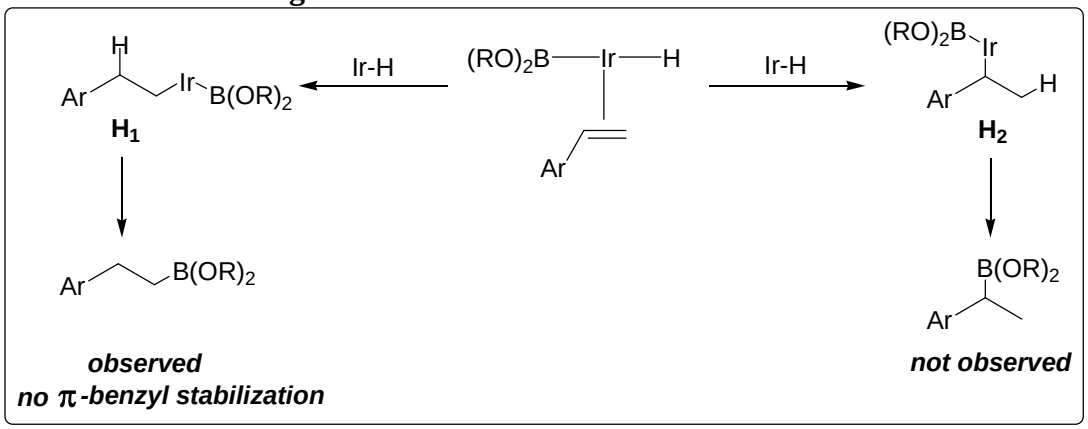

Alkene insertion into the Ir-H bond also presents two pathways (**Figure 3.5**). The formation of intermediate **H_1** placing the hydride in the benzylic position followed by reductive elimination leads to the observed product, however, this pathway does not benefit from any additional stability as no π-benzyl complex can occur. The pathway to intermediate **H_2** can generate a π-benzyl complex; however it does not lead to the

observed product. On the basis of deuterium studies both hydride pathways do occur and are reversible.

In the case of styrene, a reversible hydride insertion causes the rapid incorporation of deuterium label into excess alkene (88% of deuterium label) due to the preferential formation of a π-benzyl complex (**H_2**, **Figure 3.5**) this controls the regioselectivity of deuterium placement in this process, even though the linear product is formed. Metal hydride insertion from **H_2** must be reversible. With iridium at the branched secondary carbon position, β-hydride elimination is facile when compared to elimination from a primary carbon. On the basis of our results on only obtaining the linear isomer, the hydride insertion to **H_2** must be reversible and the boryl insertion to give **B_1** (**Figure 3.4**) cannot occur. If this pathway to **B_1** were active, the branched boronate ester would be observed, as the thermodynamics are favourable. Currently, there is no known precedent for reversible boryl migration, considered unlikely based on Ziegler's work[63].

For 1-octene, the thermodynamic preference for insertion of the alkene into the Ir-B bond this reaction manifold may contribute to the product distribution. The key intermediates resulting from alkene insertion into the Ir-D or Ir-B bond are shown in **Figure 3.6**.

The nearly equal percentages of deuterium at C_2 and C_1 of the recovered 1-octene suggest that when alkene insertion occurs into the Ir-D bond (intermediates **IrB_{C1}** and **IrB_{C2}**) that this process is at least somewhat reversible. This must be the case for **IrB_{C2}** as no secondary boronate product is obtained. **IrB_{C1}** could feasibly proceed to linear product, but is not thermodynamically favoured. Alkene insertion into the Ir-B bond gives two intermediates **IrD_{C2}** and **IrD_{C1}**. **IrD_{C1}** does not occur unless it is reversible

Figure 3.6: Iridium-boryl and iridium-deuterium intermediates of 1-octene

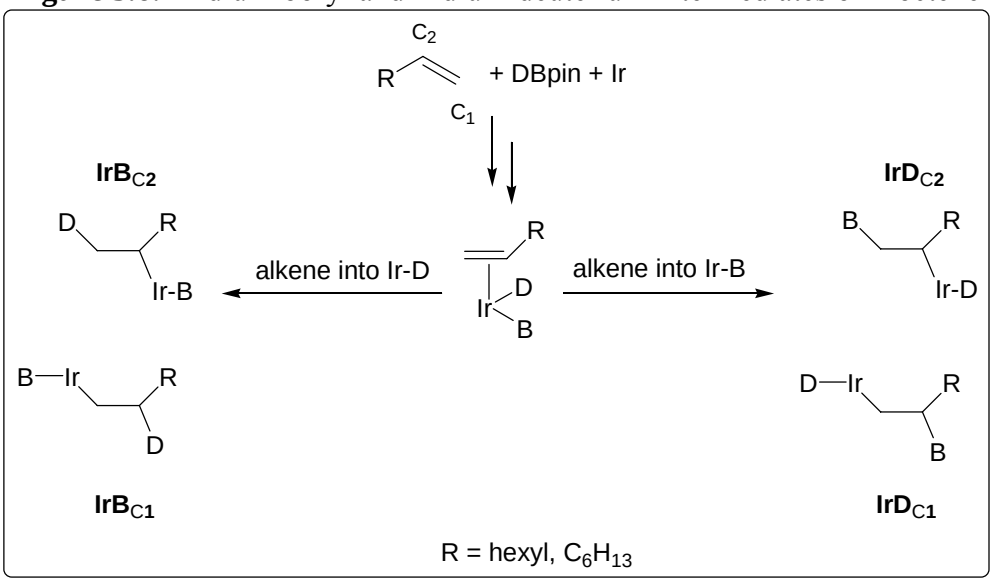

which is unlikely based on Ziegler's studies[63]. The formation of **IrD_{C2}** is favourable on thermodynamic grounds[62] and also explains the high percentage of D seen at C_2 in the product. Competition between the two pathways clearly occurs, although it seems likely that **IrD_{C2}** leads directly to the observed product and deuterium placement, while both **IrB_{C2}** and **IrB_{C1}** compete almost equally.

The proposed mechanism for iridium (I)-catalyzed hydroboration is shown in **Figure 3.7**.

The proposed mechanistic cycle is similar in many aspects to the mechanism of rhodium-catalyzed hydroboration. Formation of the active catalytic species **A** is generated by cracking the iridium chloro-bridged dimer with DPPB and displacement of the diene ligand COD, which then adds the dialkoxyborane to give **B**. Intermediates of this type have been isolated and characterized from reactions with catecholborane[59, 60]. Coordination of the alkene provides key intermediate **C** with 4 possible pathways available to it.

Figure 3.7: Proposed mechanism for iridium (I)-catalyzed hydroboration

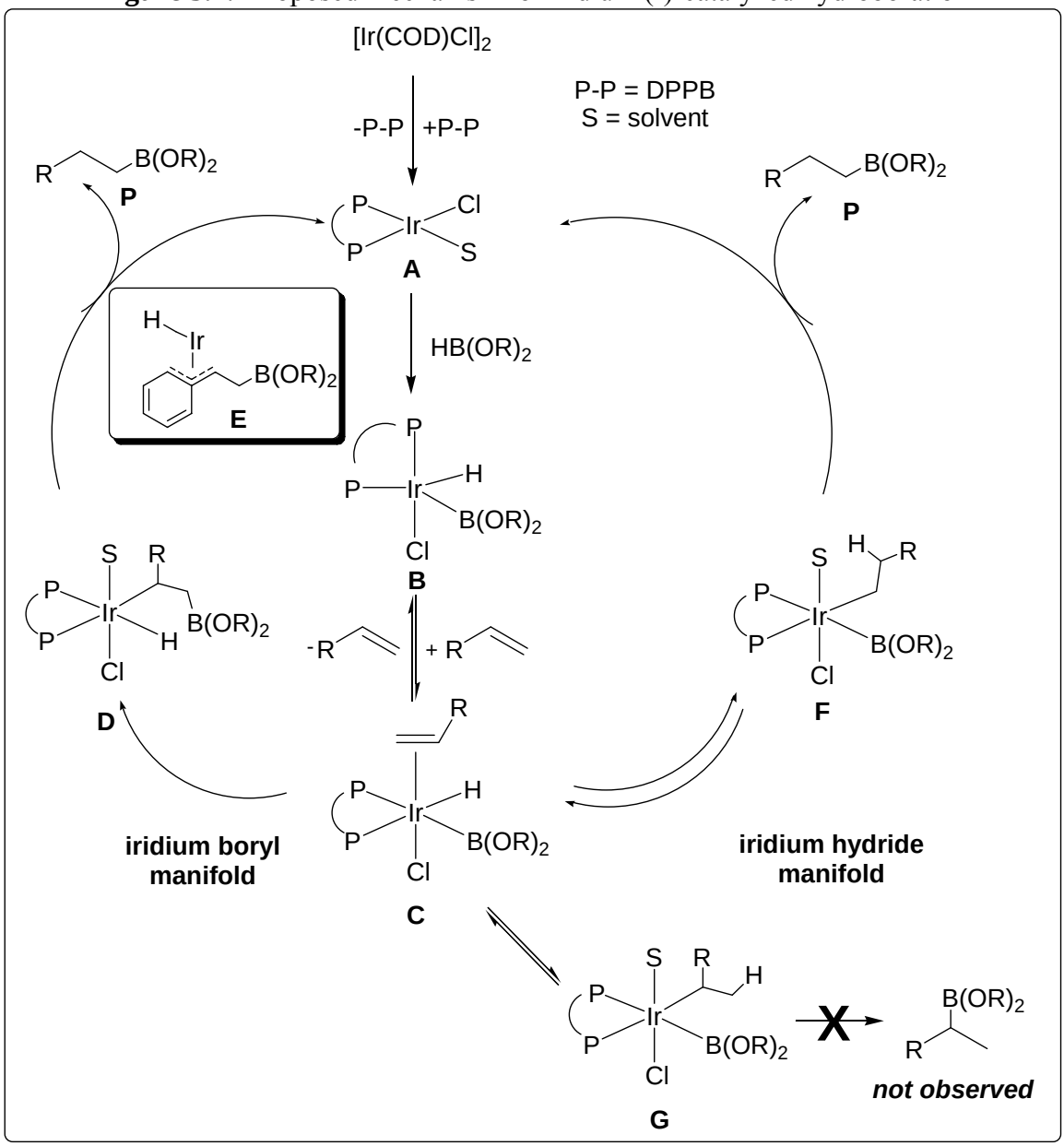

From key intermediate **C**, there are two possible manifolds, both of which lead to product **P**, the linear boronate ester. The first is an iridium boryl manifold (**C** – **D** – **A**). This route includes the insertion of the alkene into an Ir-B bond (**C** to **D**), which is known to be thermodynamically favoured[62]. The beneficial stability of a π-benzyl complex **E** is also attained via this route. Reductive elimination from **D** yields the observed product **P** and regenerates the active catalytic species **A**.

The alternative route is the iridium hydride manifold (**C** – **F** – **A**). The first step of this manifold (**C** – **F**) is reversible based on the observed incorporation of deuterium at the benzylic position of styrene. While intermediate **F** cannot form a π-benzyl complex it does still undergo reductive elimination to yield product **P** and regenerate **A**, completing the catalytic cycle. This is parallel to the formation of the linear boronate ester in rhodium-catalyzed hydroboration.

Immediate reversal of **C** to **B** can occur and would account for the incorporation of deuterium label when excess alkene substrate is used. Deuterium label is observed in all positions for styrene, with a majority occurring at the terminal position. This occurs via the pathway **C** – **G** – **C** – **B**. Note that when intermediate **G** is formed, this is a non-productive pathway as **G** itself does not lead to an observed product. The observation of deuterium label at the benzylic site is explained by pathway **C** – **F** – **C** – **B**. Since nearly 90% of the deuterium label was observed at the terminal position, pathway **C** – **G** – **C** – **B** is preferred. Intermediate **G** can form a π-benzyl complex whereas **F** cannot, and this obviously controls hydride (deuteride) incorporation, even if it does not control the product regiochemistry in this case.

The reader has no doubt noticed the striking difference in product outcome from intermediate **D** and its rhodium analog. With rhodium, in systems where alkene insertion is believed to occur into the rhodium-boryl bond[38], linear boronate ester and vinylboronate accompanied by contaminant hydrogenation of the olefin leading to alkane are observed. Under optimized conditions, iridium catalyzed hydroboration is remarkably clean and yields only the linear boronate ester in high isolated yield. Repeated monitoring of the reaction by ^{1}H NMR spectroscopy did not show any traces of

alkane or vinylboronate products. Miyaura's studies into iridium-catalyzed hydroboration[11] showed that the cationic iridium complex $[Ir(COD)_2]PF_6$ alone or in combination with bulky monodentate phosphine ligands and standard bidentate ligands (DPPP, DPPB) did yield vinylboronate, while the neutral iridium complex $[Ir(COD)Cl]_2$ gave uniformly high yields and near perfect linear selectivity. An explanation for this is the role of the halide as counterion. Bo and Fernández[117] found that the addition of ammonium halide salts RMe_3NX (X = Cl, Br, I) to cationic Rh-QUINAP catalysts lead to an increase in observed enantiomeric excess and concluded that the addition of the halide had a stabilizing effect by lowering the energy of the hexacoordinate rhodium-centered intermediate.

The stability of pinacolborane is also a contributing factor to the simplicity of the reaction. The lack of decomposition of pinacolborane (Chapter 2.3) avoids the formation of the disproportionation products H_2 and B_2pin_3 that would lead to complications such as hydrogenation of the substrate alkene.

While Miyaura[11] did report the observation of vinylboronate ester, no report is made of the formation of alkane from hydrogenation. It is possible that the iridium dihyride intermediate formed is a poor hydrogenation catalyst, as the stability of these complexes and their inability to catalyze hydrogenations is well known[57].

3.5 Fate of the Deuterium Label in Transition Metal Catalyzed Hydroborations

The hydroboration of excess styrene with DBpin under iridium catalysis lead to a deuterium distribution favouring incorporation into the product with interesting regiochemistry as previously discussed (**Equation 3.15**). When the total deuterium

incorporation was determined, taking into account relative amounts of deuterium label at each position in both the excess alkene and linear boronate ester, only 67% of the initially added deuterium could be accounted for with the $[Ir(COD)Cl]_2$ catalyst system. As mentioned before, the iridium catalyzed hydroborations are completed within a few hours, dependant on the solvent employed. This allows for the deuterium labeling experiment to be followed by multi-acquisition ^2H NMR spectroscopy, with the incorporated deuterium content monitored over time (**Figure 3.8**).

Equation 3.15: Location of deuterium label in the presence of excess styrene

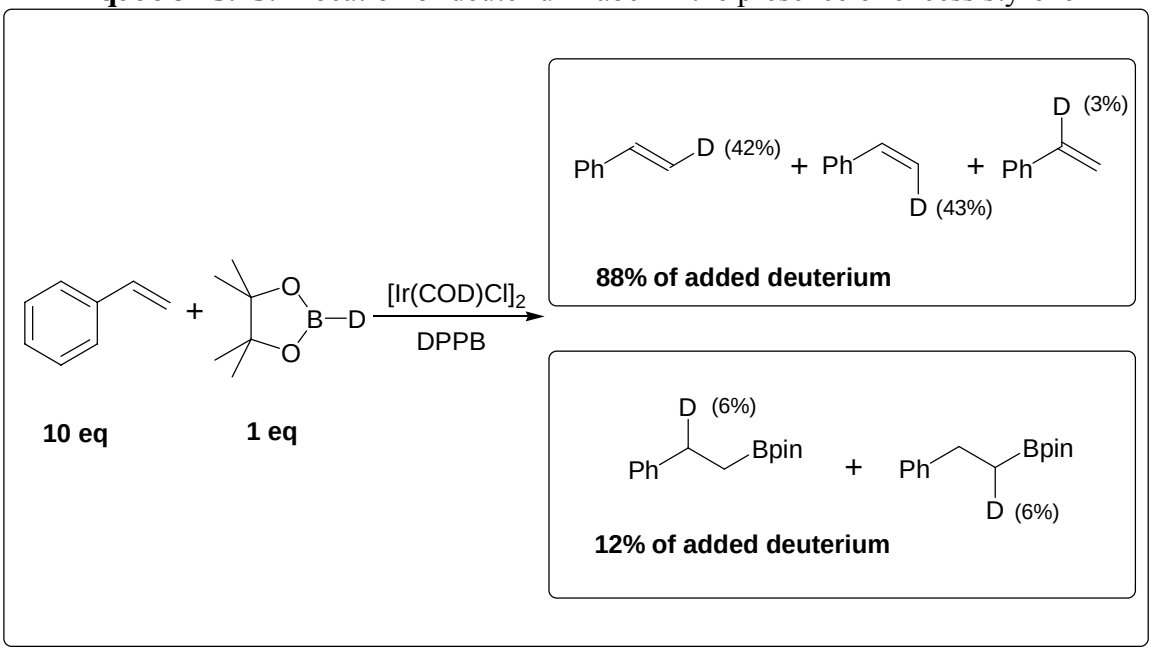

The reaction was monitored for a total of 160 minutes, and after 70 minutes, the deuterium content in the excess alkene and linear boronate product remains constant near 0.141 mmol. Of the initial 0.21 mmol of DBpin added, nearly a one-third cannot be accounted for. The explanation for the loss of deuterium label and quantification of deuterium content are constant challenges for those engaged in mechanistic research.

The general methods for quantification will be discussed first, with possible causes for the lost of the label dealt with on a case-by-case basis.

Figure 3.8: Deuterium content as a function of time, excess of styrene, iridium catalyst

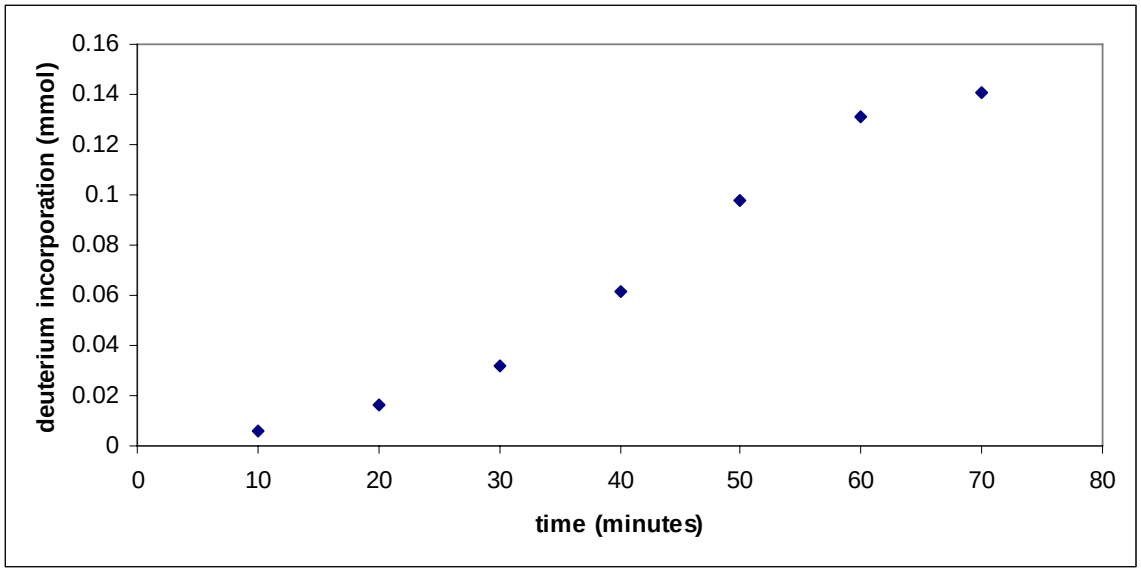

NMR and mass spectrometry can determine quantification of the deuterium label. For ^{1}H NMR spectroscopy, incorporation of deuterium is observed indirectly, through the loss of intensity of the known substrate or product resonances. The level of deuteration is calculated by dividing the integration of the compound of interest by the measured integration of an internal standard. The main limitation is that any reaction of the substrate, such as decomposition, would be perceived as deuteration. Control experiments can determine to what extent this may occur. The use of a reaction known to give clean conversion to known product(s) is also advantageous. Using these criteria, Bergman was able to reproduce the results of iridium catalyzed H/D exchange in D_2O within 5-10%[183]. The fact that the reaction in conducted in a deuterated solvent precludes the ability to make any quantitative analysis.

With ^{2}H NMR spectroscopy, conducted in a non-deuterated solvent, the incorporation can be monitored directly. The main disadvantage of this method is the broad nature of the resonances. Again, the use of a suitable deuterated internal standard and the known reaction stoichiometry are required. The analysis of deuterium incorporation by ^{2}H NMR spectroscopy has been conducted by researchers in **Table 3.2** and while the interpretation of the results is debated, all accept the method of analysis.

Bergman has discussed the use of mass spectrometry to determine levels of deuteration[183]. The main issue is the potential for underestimating the level of deuteration. Fragmentation of the molecule ion peak to more stable ions, particularly if the fragment lost is less than the mass due to hydrogens within the molecule, for example the loss of a proton or deuteron, leads to underestimation[183]. A further consideration is that deuteration may influence the molecular ion fragmentation by breaking C-H bonds over C-D bonds. This is due to the higher bond strengths of C-D bonds relative to C-H bonds[183]. In our own work, the use of mass spectrometry has been used only to confirm that certain deuterated species are present and proved unable to provide information on position and extent of deuteration.

In the context of mechanistic studies, the loss of one third of the deuterium label is troubling. Possible reactions and impurities that could facilitate the loss of label are covered below in detail.

The loss of substantial amounts of deuterium label was reported by Baldwin[41] in Wilkinson's catalyst promoted decarbonylations of deuterioaldehyes. The loss of label was highly dependant on the concentration of the deuterioaldehyde, with up to 86% of the label lost at 0.1M. Their initial suspicions centered on impurities in the rhodium

catalyst (Chapter 1.3.2). Regardless of the commercial source or the methods of its synthesis, all catalysts gave varying degrees of deuterium loss. Baldwin was also able to rule out *ortho*-metalation of the triphenylphosphines of the rhodium catalyst and subsequent deuterium incorporation, as label loss was observed when $RhCl(P(C_6D_5)_3)_3$ was used. The hydrogen source was traced to water retained in the Wilkinson's catalyst, which formed a mixture of rhodium-hydride/deuteride intermediates that readily exchanged. High preservation of the label could be restored by conducting decarbonylations in the presence of excess D_2O[41].

The presence of adventitious moisture during the course of catalysis is certainly a concern. Pinacolborane with its reactive B-H bond readily liberates H_2 gas on contact with water and forms mixed borates, chiefly the bis-O-borate, $(pinB)_2O$. Previous work on iridium catalyzed hydroboration was conducted in a glovebox which excludes atmospheric moisture. Isolated yields for these reactions are uniformly high (90-98%) and contain the linear boronate ester as the only observed product (section 2.2 Iridium catalyzed hydroborations). This brings up the presence of water retained in $[Ir(COD)Cl]_2$. Classical methods for its synthesis involve the use of aqueous ethanol[184] or aqueous 2-propanol[185] from the commercially available hydrated iridium (III) chloride. Iridium catalysts prepared by both of these methods has been suitable for iridium catalyzed hydroborations under glovebox conditions, while catalyst prepared from aqueous 2-propanol has been repeated used in both ^1H and ^2H NMR experiments and consistently shows clean production of linear boronate ester.

If one does consider a possible one-to-one coordination complex of iridium catalyst to water, at the loading of 2.5 mol% catalyst, this would allow for 2.5 mol%

water to be introduced. With two equivalents of acidic hydrogen (5 mol% or 8.9 x 10^{-3} mmol), the consumption of 5 mol % of hydroboration reagent is expected. This would result in the loss of only 1.9 x 10^{-3} mmol of hydroboration reagent (based on 0.21 mmol used). This is far from the observed loss of 33% and also does not correlate well with the isolated yields. Moisture could certainly be a contributing factor, present in solvent for example, but it is not the sole determinant.

As previously mentioned, the activation of the CH bonds *ortho* to phosphorus in phosphine ligands and hydrogen abstraction followed by deuterium exchange is another possibility. Iridium complexes, most notably the iridium analogue of Wilkinson's catalyst, $IrCl(PPh_3)_3$, are known to undergo this reaction on reflux in benzene solution[57]. These stable iridium hydrides are well characterized and undergo deuterium exchange on both Ir-H and C-H bonds on exposure to deuterium gas[57] (**Equation 3.16**).

Equation 3.16: C-H activation of $IrCl(PPh_3)_3$[57]

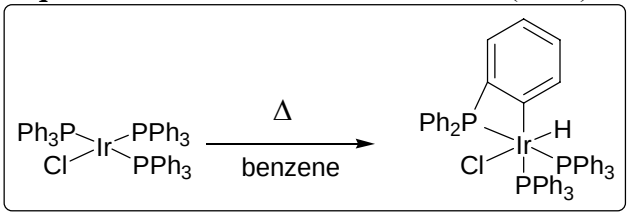

While our catalytic system employs $[Ir(COD)Cl]_2$ with 2 equivalents DPPB, similar activation should occur after cracking of the iridium dimer and displacement of COD (**Figure 3.7**). This would provide 8 possible C-H bonds to act as sites for H to D exchange to occur. With 5 mol% DPPB (generating 8 C-H equivalents) used, this could theoretically consume 40 mol% of the D introduced from DBpin, resulting in a loss of 0.084 mmol of hydroboration reagent of a total of 0.21 mmol. Unfortunately, no

deuterium signal is observed in the aromatic region and recovery of the DPPB ligand[186] and analysis by ^{2}H NMR spectroscopy shows no deuterium incorporation.

$[Ir(COD)Cl]_2$ as a catalyst precursor has several properties itself that have the potential to add to the mystery of the loss of deuterium label. This complex is used as a key intermediate for the *in situ* generation of active catalytic species[31] and we have shown it gives near perfect linear selectivity in hydroborations (Chapter 2.2). $[Ir(COD)Cl]_2$ is known to undergo direct oxidative addition of two equivalents of HX (X = Cl, Br, I)[187, 188] to give the isolatable Ir(III) dimer. This Ir (III) dimer has been shown to undergo ring deuteration when treated with DCl in EtOD[188] (**Equation 3.17**).

Equation 3.17: Ring deuteration of coordinated 1,5-cyclooctadiene[188]

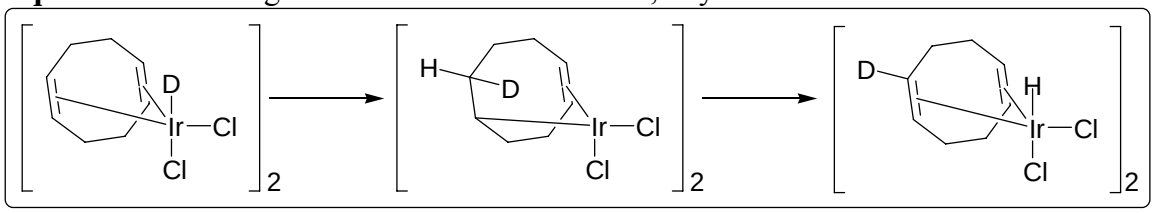

This result opens up several routes for deuterium loss through exchange into the coordinated COD ligand and its displacement from the metal center. Direct displacement by phosphine ligands is a common method for *in situ* active catalysis formation. In a stoichiometric reaction HBcat has been shown to add to $[Ir(COD)Cl]_2$ in the absence of alkene[59] to give an iridium-boryl species and B_2cat_3 and a complicated mixture of iridium-hydride resonances. By comparison, the reaction of HBcat with $[Ir(COE)_2Cl]_2$ generates a similiar boron species with many well defined iridium-hydride signals. This suggests that the loss of the alkene COE ligand is easier to achieve than loss of the diene COD ligand. Westcott has similiarly used $[Ir(COE)_2Cl]_2$ reacted with four equivalents of P^iPr_3, then treated with HBcat to give well characterized $Ir(H)(Cl)(P^iPr_3)_2(BCat)$[59].

The reaction of $[Ir(COD)Cl]_2$ with DBpin has two possible pathways that could lead to the loss of deuterium label (**Equation 3.18**). The first is the ring deuteration discussed above by Shaw[188]. The coordinated diene shows the vinyl proton resonance at 4.22 ppm[185, 189], with the free diene having the vinyl proton resonance at 5.57 ppm. No signal for deuterated coordinated diene is observed, which is not surprising when one takes into account that it is only used in catalytic amounts. The vinyl proton resonance at 5.57 ppm is not seen as this occurs at the same position as the proton *cis* to the phenyl ring in styrene.

Equation 3.18: Modes of deuterium loss, reaction of $[Ir(COD)Cl]_2$ with DBpin

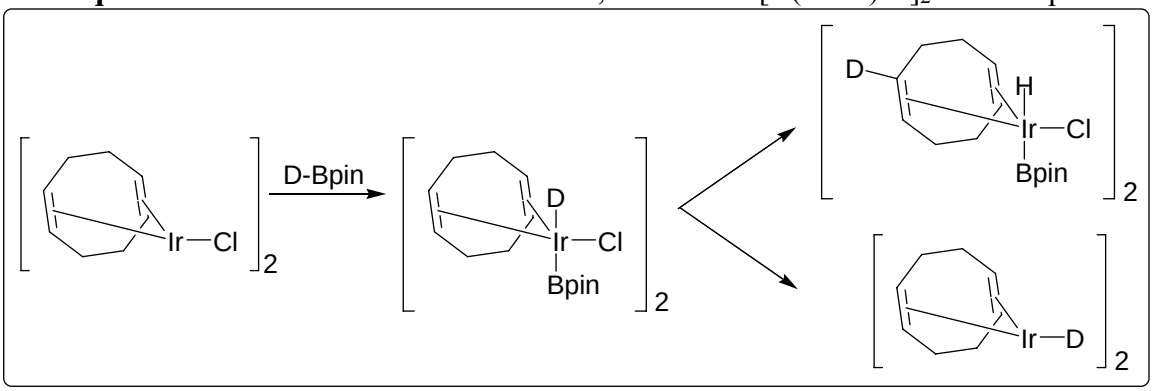

Another possible pathway is the formation of a bridging hydride iridium dimer that occurs from the loss of Cl-Bpin to form an active catalytic species. The hydride region spanning -7 to -20 ppm is known to show many iridium-hydride species[59]. Iridium-hydride formation has not been examined so far in this study and represents a gap in our understanding of the mechanistic process. The resolution of the signals will certainly be less for an Ir-D species, but could be feasibly studied with HBpin to monitor the formation of Ir-H species.

Further means of deuterium loss and removal of the COD ligand, if not displaced by the diphosphine DPPB, include hydroboration or worse, hydrogenation, are shown in

Equation 3.19 and **Equation 3.20**. With 2.5 mol% $[Ir(COD)Cl]_2$ (0.011 mmol, generating 4 C=C per equivalent of catalyst) is 10 % of the introduced DBpin that this potential reaction could consume.

Equation 3.19: Loss of COD ligand by hydroboration

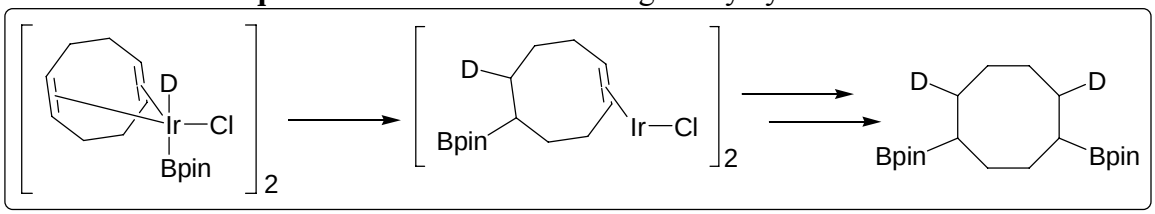

It appears unlikely that hydroboration is responsible for the loss of COD from the metal center. ^{11}B NMR spectroscopy of the reaction mixtures consistently shows only the signal for the linear boronate ester derived from the hydroboration of styrene. Displacement by phosphine is favoured by the fact that $[Ir(COD)Cl]_2$ is premixed with DPPB for several minutes prior to the addition of the hydroboration reagent. The high isolated yields of the desired linear boronate esters do not suggest such a loss of hydroboration reagent either.

Equation 3.20: Loss of COD ligand by hydrogenation

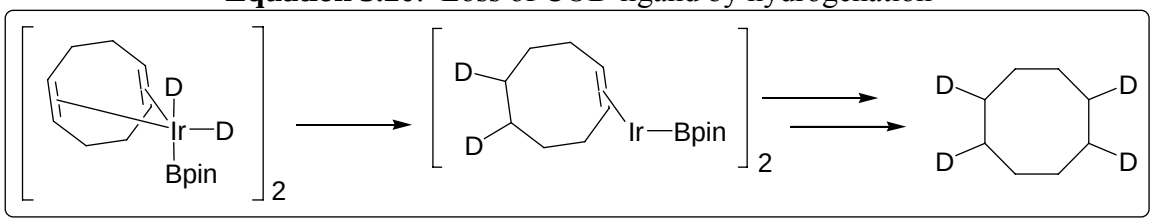

The spectre of hydrogenation as a means of loss of deuterium label as well as by sacrificial hydrogenation of substrate is an unwarranted fear. No signals corresponding to free cyclooctane (1.5 ppm) were observed. Reactions of iridium catalyzed hydroborations, monitored by ^{1}H NMR spectroscopy with either an excess or one equivalent of styrene do not show signals for phenylethane, the result of hydrogenation of substrate. As discussed above, it is more likely that displacement of COD by phosphine

has occurred prior to the formation of hydroboration reagent and iridium dihydride complexes of this type $Ir(H)_2Cl(P)_3$ known to be poor hydrogenation catalysts[57]. However, the formation of an iridium-dihydride cannot be discounted yet due to the observations below.

During the course of our investigations two separate signals in the ^2H NMR spectra that could not be identified appeared under both rhodium and iridium catalysis. Iridium catalysis showed a signal at approximately 2 ppm with all other signals readily identified as the internal standard, the signals from the substrate styrene and the signals of the linear boronate ester. Similarly for rhodium catalysis, an unknown signal appeared at 3.4 ppm. The analysis for the case of iridium catalysis will be presented first. The reader should bear in mind that both the iridium and rhodium cases were under investigation simultaneously.

Figure 3.9: ^2H NMR spectrum of iridium catalyzed hydroboration with DBpin and excess styrene

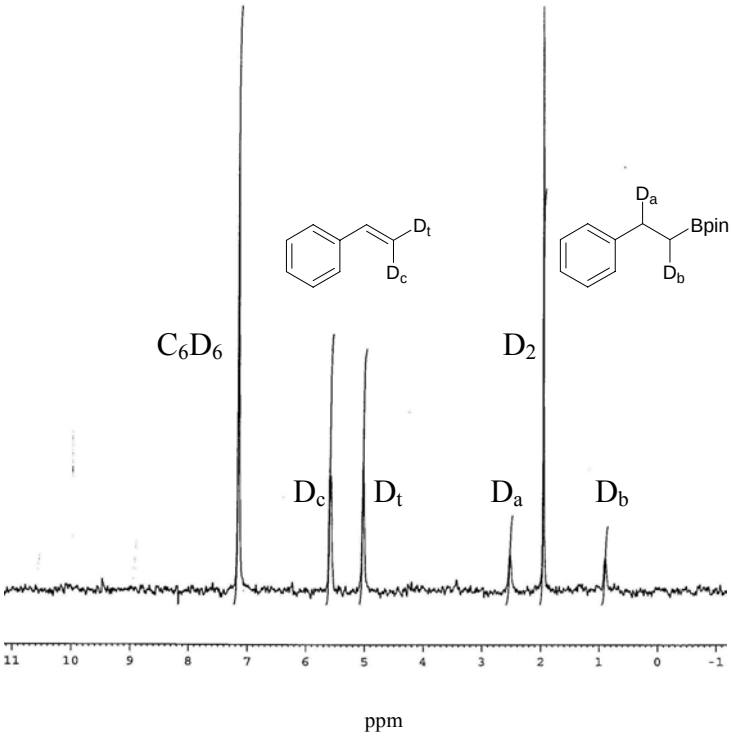

Figure 3.9 shows a typical spectrum for iridium catalyzed hydroboration conducted with an excess of styrene relative to hydroborating reagent DBpin. All signals are identified for the substrate styrene, the linear boronate ester product with integrations relative to the internal standard C_6D_6. The unknown signal appears at 2 ppm. The linear product with deuterium label at the benzylic positions is shown, resulting from expected hydroboration through intermediate **B_2** (**Figure 3.4**). The production of linear boronate ester with deuterium label in the β-position occurs by the hydroboration of terminally deuterium labeled styrene, with the HBpin generated by β-hydride elimination during deuterium exchange into the starting olefin (**Equation 3.21**). Statistically, the C-H bond is favoured, aided by an isotope effect favouring retention of the C-D bond over the C-H bond which leads to preferential H instead of D elimination[190].

Equation 3.21: Production of β-position labeled linear boronate

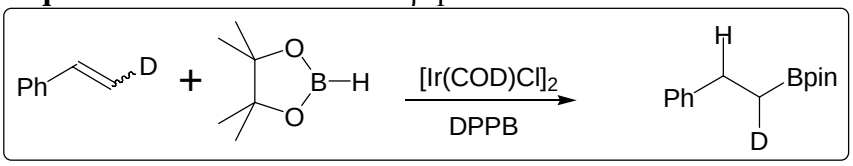

Our work has shown that iridium catalyzed hydroborations can exhibit nearly perfect regioselectivity and high isolated yields with no observable side products. This is not to say that there are no side reactions occurring with the catalyst that ultimately are not detrimental to the reaction. Westcott[59] did report the observation of up to 10% of alkane caused by the consumption of alkene by hydrogenation for iridium catalyzed hydroboration with HBcat, although this is likely dependent on the exact nature of the catalyst. This indicates that at some point during the catalytic cycle, an iridium dihydride must evolve either from β-hydride elimination of an intermediate such as **B_2** (**Figure 3.4**), with concurrent vinylboronate production, or via the reaction of a pre-existing iridium

hydride reacting with another molecule of hydroboration reagent. In our case, NMR monitoring has never revealed the presence of vinylboronate during the course of the iridium catalyzed reaction. If an iridium dihydride intermediate was produced, then it would be reasonable to expect the formation of hydrogen gas from reductive elimination. The possibility of β-hydride elimination with vinylboronate product by rhodium catalysts is well known[36, 38, 39] and this influenced the next course of action.

The production of H_2 (or D_2 or HD) could be responsible for the poor deuterium balance and explain the observed unknown peaks. The ^{1}H NMR signal of H_2 occurs at the same δ value in a variety of solvents: 4.6 ppm ($CDCl_3$), 4.6 ppm (C_6D_6)[191] and 4.6 ppm (CH_3OH)[192]. The signal occurs at 4.6 ppm in both the liquid phase and gas phase ^{1}H NMR spectra in methanol, but is broader in the gas phase[192].

Transition metals are well known to catalyze H/D exchange with mixtures of H_2 and D_2 gas through the formation of metal hydride complexes. Iridium in the form of Vaska's complex readily catalyzes this exchange[193], as does ruthenium[194] and rhodium[195-197]. Since the signal for H_2 did not agree with the unidentified signals and with deuterium exchange occurring with the substrate, the production of HD from exchange or D_2 from direct elimination from a metal dideuteride was considered.

The ^{2}H NMR spectrum obtained by bubbling D_2 in THF, referenced to C_6D_6 is shown in **Figure 3.10**. The signal for D_2 occurs at 2.0 ppm, matching perfectly with the unidentified signal observed during the course of iridium catalysis. However, this tentative identification of the unknown signal had to be confirmed by its interaction with the iridium catalyst, substrate and hydroboration reagent.

Figure 3.10: ^{2}H NMR spectrum of D_2 in THF, C_6D_6 internal standard

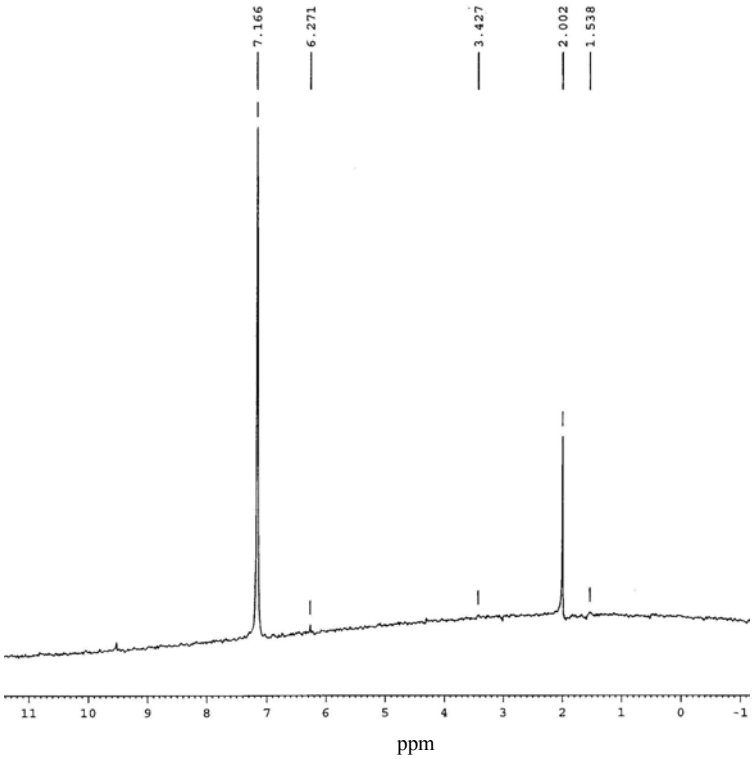

The following series of spectra (**Figure 3.11**) show an iridium catalyzed hydroboration with DBpin with excess styrene conducted with D_2 gas in solution present from the start of the reaction. Initial mixing of $[Ir(COD)Cl]_2$ and DPPB shows no reaction but leads to phase inversion of the D_2 signal. Addition of DBpin gives a broad ^{2}H signal that remains constant for 30 minutes, with a new signal appearing at 1.2 ppm. Upon styrene addition, the DBpin signal has almost completely vanished and the signals for the known product and terminal alkene deuteration appear. Approximately 58 minutes later, the D_2 gas signal remains, and a near statistical 1:1:1 ratio of deuterium is observed in the excess styrene with the two deuterated signals for the linear boronate ester also seen. Poor phase resolution of the D_2 signal prevented its integration, yet the deuterium incorporation in the product and excess styrene is 81% of the initially added DBpin.

Figure 3.11A: ^{2}H NMR spectrum of $[Ir(COD)Cl]_2$/DPPB with D_2 and DBpin after 30 minutes

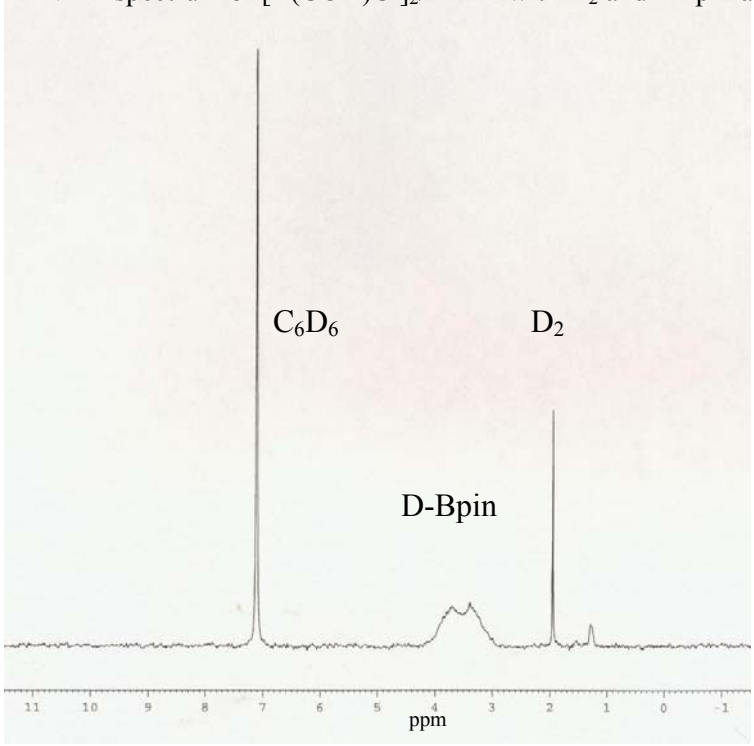

Figure 3.11B: ^{2}H NMR spectrum of $[Ir(COD)Cl]_2$/DPPB with D_2/DBpin after addition of styrene

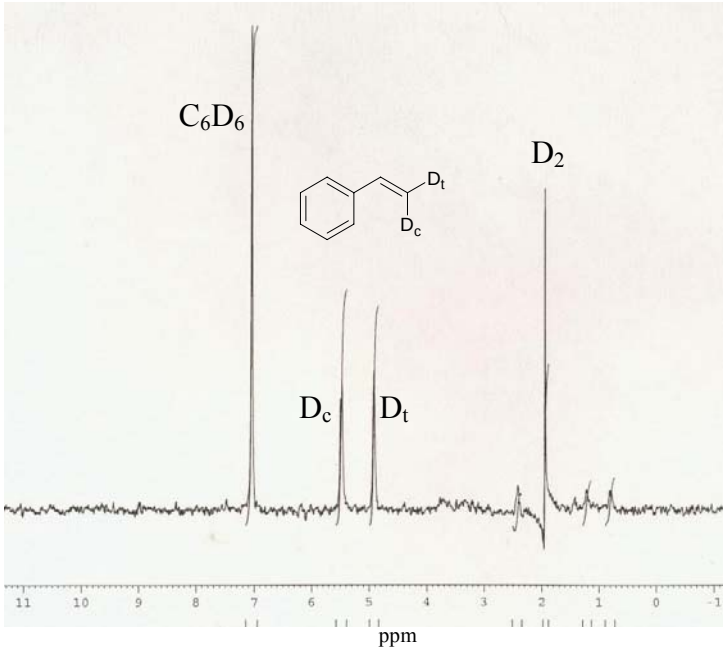

Most noteworthy is the lack of hydrogenation in the presence of D_2. Iridium complexes such as *trans*-$IrCl(CO)(PPh_3)_2$ and $IrCl(PPh_3)_3$ are known to be ineffective

hydrogenation catalysts [57, 193] due to lack of dissociation of ligands and the strength of the Ir-H bond. The formation of the active catalytic species from $[Ir(COD)Cl]_2$/DPPB must also share this property. Supporting this is the high yields of boronate ester with no observed hydrogenation. With no vinylboronate ester seen during the course of the reaction means that the iridium-deuteride intermediate does not undergo any β-hydride elimination to form a mixed Ir-(H)-(D) species as HD is not observed.

Another interesting feature is the slow reaction of the catalyst with DBpin which is uncommon. Iridium complexes are known to give degradation products with HBcat and isolated iridium boryl compounds are ineffective catalyst precursors for hydroborations[59]. Two additional factors at work here may explain these observations: the increased strength of the B-D bond undergoing slow oxidative addition to the iridium center and the increased stability of pinacolborane towards degradation and disproportionation. One may also consider the large excess of styrene and its effect on the displacement of ligands about the metal center leading to an active catalytic species.

A troubling outcome of this experiment is that H_2 production has never been observed in any ^1H NMR monitoring of the reaction under the same iridium catalyzed conditions with excess styrene. While the identity of the unknown signal can be tentatively assigned as D_2 in the iridium case from these experiments, the production of D_2 can only feasibly be occurring through an iridium-dideuteride (**Equation 3.18**) as a means to create an active catalytic species. Rhodium dimers with bridging hydrides are proposed by Brown[100] and the formation of iridium-deuterides in this manner may account for the loss of some of the deuterium label.

Another outcome of this work was the lack of HD observed from any of the types of exchange noted above. While it does not appear to arise from exchange processes, it would rapidly be generated in the presence of any moisture, yet it is not seen for iridium catalysis.

Smooth generation of HD gas was achieved independently by treating a suspension of NaH in THF with D_2O and bubbling the resulting gas though THF, with C_6D_6 internal standard, in a screw cap NMR tube. ^2H NMR analysis of the solution (**Figure 3.12**) showed the internal standard (7.16 ppm) and a strong signal for HD (3.3 ppm). The HD signal also underwent phase inversion. The position of HD coincides with the appearance of the unknown signal at 3.4 ppm (**Figure 3.33** for confirmation) observed in rhodium catalyzed hydro orations. It is interesting to note that the average of the two known signals of H_2 (4.6 ppm) and D_2 (2.0 ppm), occurs at 3.3 ppm, where HD is observed, however this type of comparison here is tenuous at best when dealing with two different molecules.

H to D exchange by rhodium complexes is well documented. Wilkinson[195] reported exchange with $Rh(D)(CO)(PPh_3)_3$ with 1-alkenes to occur with a half-life of 20 seconds. Using $Rh(H)(CO)(PPh_3)_3$, Brown[172] found that the isomerization of *cis*-dideuterated styrene was rapid, within 180 seconds, and showed a distinct preference for isomerization at the terminal carbon and little or no loss of deuterium label at the benzylic carbon. Using $[RhCl(CH_2CH_2)_2]_2$ in hydroborations, Brown[100] observed similar label distributions and isomerizations.

Since the mechanism of rhodium catalyzed hydroborations has many pathways that may provide the observed products including direct hydroboration, dehydrogenative

hydroboration, hydrogenation of vinyl borane and direct hydrogenation of the starting material, complex ^{2}H NMR spectra might be anticipated. In nearly all

Figure 3.12: ^{2}H NMR of HD in THF, C_6D_6 internal standard

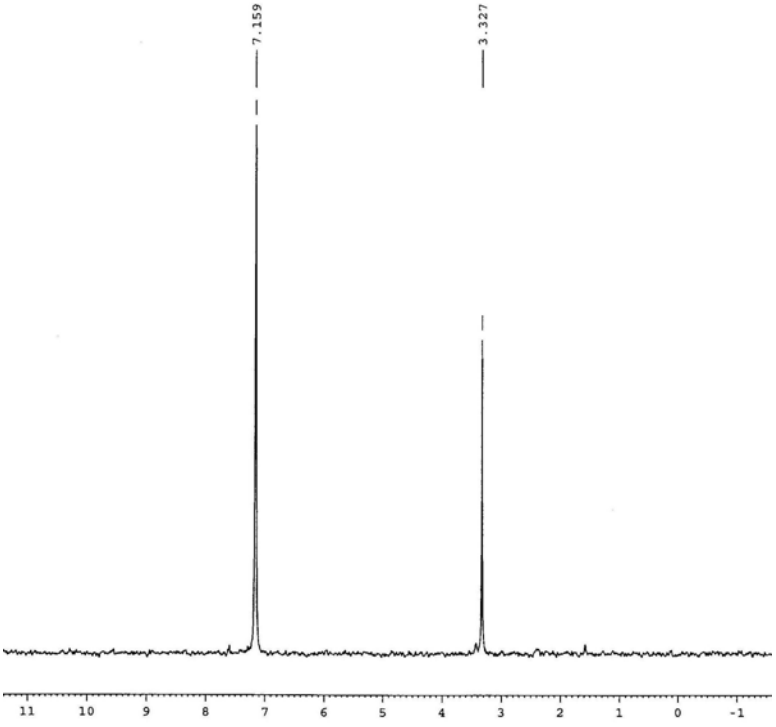

cases, deuterium label was observed in all alkene C-H positions and the branched boronate ester was the major observed product. However, since β-hydride elimination and hydrogenation do not require the involvement of deuterium label, it is not surprising that they were not seen by ^{2}H NMR spectroscopy, yet they are also never observed in ^{1}H NMR spectra, nor is the signal at 3.3 ppm for HD.

Additionally, reactions of HBpin with rhodium are considerably slower compared to iridium, requiring 20-24 hours for completion. A split test reaction was conducted, with half left under inert atmosphere in a glovebox, while the other half was sealed in a screw cap NMR tube as in the monitoring experiments. The distributions are shown in **Figure 3.13**, but again suffer from wide ranges in total deuterium incorporation, with material outside of the glovebox ranging from 13% (at 3 hours) to 119% (at 24 hours)

and material maintained in the glovebox maintaing a moderate deuterium percentage (64% after 24hours).

Figure 3.13: Distribution ratios of deuterium label into excess styrene

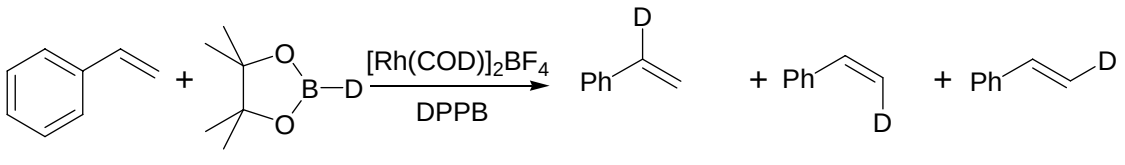

inert	2	1	1
oxygenated	1	2	2

Differences in deuterium label distributions due to the presence of oxygen using Wilkinson's catalyst were the cause of confusion and debate in the early mechanistic studies of rhodium catalyzed hydroborations with DBcat[48, 170]. It was Evans[35] and Baker, Westcott and Marder[36, 37] who later determined that exposure of the rhodium catalyst (Wilkinson's) to oxygen, lead to catalyst oxidation, decreased regioselectivity for the branched boronate ester and the discrepancies in the deuterium labeling.

The results of the catalyst system obtained using $[Rh(COD)_2]BF_4$/DPPB exposed to oxygen shows no decrease in regioselectivity as both inert and oxygenated samples show only branched boronate ester by ^2H NMR spectroscopy. However different results are obtained for deuterium labeling, where oxygenation increases the exchange at the terminal positions of styrene, suggesting that a π-benzyl rhodium intermediate is still operative.

In both aerobic and anerobic cases, HD is evolved. Doping of the oxygenated rhodium sample with HD by bubbling gas through the solution gave immediate hydrogenation of styrene and continued monitoring by ^2H NMR spectroscopy showed the

presence of α- and β-deuteriophenylethane. This hydrogenation reaction is not usually seen during the course of the reaction, despite its known occurance[38, 39] and could be a function of HD gas concentration under these experimental conditions.

Brief notes on two other suspected culprits for erratic results in the deuterium labeling experiments were investigated: moisture and trace metals.

As mentioned before, the presence of moisture with an active boron hydride will immediately generate H_2 and boric acid. If moisture were responsible for the generation of HD gas, then silylation of any glassware, especially the NMR tube would reduce or prevent this. Protection of the glassware was affected with a 5% solution of $SiCl_2Me_2$ in CH_2Cl_2, rinsed in CH_2Cl_2, treated with anhydrous CH_3OH, and warmed under vacuum prior to admission into the glovebox for use. The results obtained from such rigourous exclusion of moisture were the same as those seen before when conducted in an inert atmosphere, as seen in **Figure 3.14**. This confirms that moisture is not responsible for any major losses of deuterium label, nor does it have deleterious effects when normal glovebox techniques are followed.

When checking the results of the background reaction, styrene with DBpin with no catalyst at room temperature, deuterium label incorporation was observed. Co-workers in the lab on other transition metal catalyzed projects suggested the presence of trace metals mediating this reaction. Indeed, careful repetition of this vital experiment with the same reagents, but with a brand new stirbar showed no deuterium incorporation. This shows the sensitivity of the reaction to contamination by extraneous metals. Once this source of metal was identified and eliminated, all further deuterium labeling experiments, and all the results previously presented were carried out with a new stir bar.

Figure 3.14: ^{2}H NMR spectrum of Rh catalyzed hydroboration conducted with silylated glassware

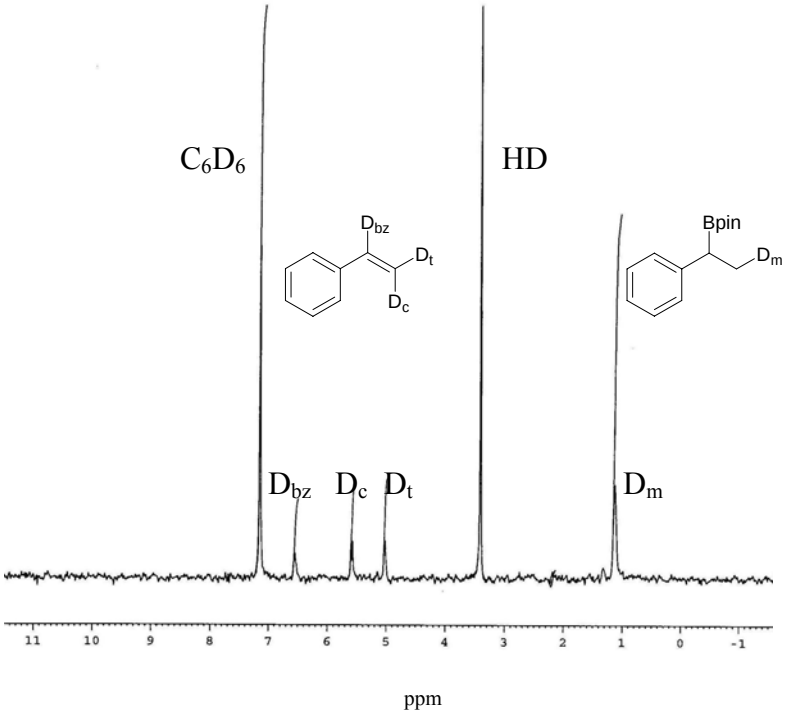

The controlling factor in the production of the gaseous by-products of HD with rhodium catalysts and D_2 with iridium catalysts is the characteristics of the metals themselves. Rhodium is well known to catalyze H to D exchange[195, 196] and in rhodium catalyzed hydroborations, the side reactions of hydrogenation and β-hydride elimination are common aspects of rhodium chemistry. The degradation of catecholborane by Wilkinson's catalyst[36] generates H_2 gas, both hydrides derived from the reagent. It is then plausible to envisage a rhodium center reacting with a deuterated hydroboration reagent, exchanging the deuteride into substrate and then have the newly formed rhodium-hydride react with another molecule of deuterated reagent to produce HD.

The formation of D_2 with iridium is more difficult to explain. As iridium species such as $IrCl(PPh_3)_3$ are known to be poor hydrogenation catalysts[57], that form stable dihydrides, the loss of D_2 is puzzling. Iridium catalysts are known to degrade catecholborane in a manner similar to rhodium[59], allowing for the process described

above to occur. It is possible the active catalyst in iridium catalyzed hydroborations behaves fundamentally different than $IrCl(PPh_3)_3$ – the combination of $[Ir(COD)Cl]_2$ and PPh_3 dissolved in neat pinacolborane and reacted under a D_2 atmosphere is our method of synthesis of DBpin.

3.6 Synthesis of Deuterated Substrates and Reagents

The targets for use in deuterium labeling experiments were deuterated pinacolborane (DBpin) and the d_3-styrenes 4-chlorostyrene and 4-methoxystryene. These vinylarenes were chosen for comparison to the mechanistic work by David Edwards and for exploration of electronic properties and influences.

3.6.1 Deuterated Pinacolborane, DBpin

Deuterated hydroborating reagents have been synthesized for use in deuterium studies, but the methods of synthesis suffer from a number of drawbacks. Deuterated catecholborane, DBcat is known and widely used[35, 36, 48, 100], being synthesized from BD_3 gas generated *in situ* from $NaBD_4$ or a solution of BD_3•THF and reacted with a solution of catechol in ethereal solvent, commonly THF. This then requires the removal of solvent under reduced pressure by slow addition of the solution of hydroboration reagent. This can lead to ring cleavage in the case of THF to give butylboronate species that contaminate the desired reagent. The cost of deuterated hydride reagents, specifically BD_3•THF, is also a drawback.

Deuterated pinacolborane is known in the literature via a route involving $RuH_2(H_2)_2(PCy_3)_2$ and D_2 to exchange H for D in pinacolborane[198]. Unfortunately this catalyst is obtained from Ru(COT)(COD), an organometallic complex that is difficult to

handle due to its limited stability to air and laborious low yielding synthesis[199-201]. Alternate routes explored involved the use of the diboron reagent B_2pin_2 with catalysts that are known to activate the B-B bond such at Pd[89, 202] and Rh[165, 166, 203]. These routes were tried, but none led to the desired DBpin.

An attractive route appeared from the report of Brown to synthesize HBcat from the bridged catecholate B_2cat_3[78]. The use of B_2pin_3 in combination with BD_3 could lead to a successful large scale synthesis, if BD_3 was readily available at low cost. At the time of these experiments, it was not, but has recently become available from Aldrich in the form of BD_3•THF, however this still has the drawbacks outlined above.

The report of synthesis of DBpin by ruthenium catalyzed exchange with D_2 gas held the promise that other metals would be able to achieve this transformation. A survey of the literature revealed work by Hawthorne on the preparation of deuterated carboranes and metallocarboranes[204, 205]. The most active metal catalyst was '$[(PPh_3)_2IrCl]$' prepared *in situ* from $[Ir(COD)Cl]_2$ and PPh_3 which gave complete exchange at low temperature

Equation 3.22: Synthesis of deuterated pinacolborane

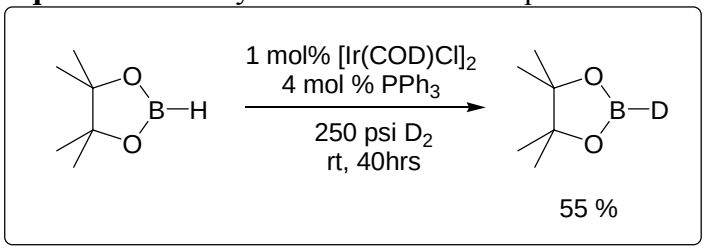

and short reaction time. When applied to the synthesis of DBpin, a further advantage realized was that the reaction could be conducted in neat liquid HBpin under D_2 pressure and direct distillation of the reaction mixture furnished spectroscopically pure deuterated pinacolborane, DBpin (**Equation 3.22**). With quantities of DBpin in hand, this material was utilized in iridium and rhodium catalyzed deuterioborations.

3.6.2 Synthesis of 4-substituted-d_3-styrenes

The next challenge lay in the synthesis of the desired *para*-substituted-d_3-styrenes. The synthesis of alkenes is a huge area of organic synthesis, and the synthesis of substituted styrenes has been widely studied[206]. The additional challenge of the incorporation of 3 deuterium atoms in olefinic positions and the possible construction of a carbon-carbon double bond rapidly limits the synthetic methodology available.

The most elegant route to d_3-styrene involved vinylic H/D exchange in alkenes using Milstein's $[Rh(COE)_2(P^tBu_2(CH_2Ph))]BF_4$ in deuterated solvent (CD_3OD) as the source of deuterium[207]. The phosphine $P^tBu_2(CH_2Ph)$ proved to be air-sensitive, but this was circumvented by use of the phosphonium hydrobromide salt[208]. However, prolonged reaction in a vast excess of CD_3OD solvent at elevated temperature showed minimal H/D exchange into the alkene C-H position of styrene by ^1H and ^2H NMR spectroscopy.

With the lack of success of the initial attempt, a synthetic route to the desired styrenes was devised. Introduction of deuterium was envisioned to occur in three ways. H to D exchange, either by deprotonation by strong base or equilibration in a deuterated solvent would be useful if acidic/exchangable protons were present in a molecule. Addition across a double or triple bond would allow for the incorporation of 2 atoms of deuterium in a known geometry and position. Carbon-carbon bond formation or olefination of a carbonyl group with a deuterated reagent achieves the third method. As with any synthetic route, any starting material should be a readily available material that would allow for bulk synthesis.

The initial synthetic route was based on the retrosynthetic analysis in **Scheme 3.1**.

Scheme 3.1: Retrosynthetic analysis to 4-substituted-d_3-styrenes

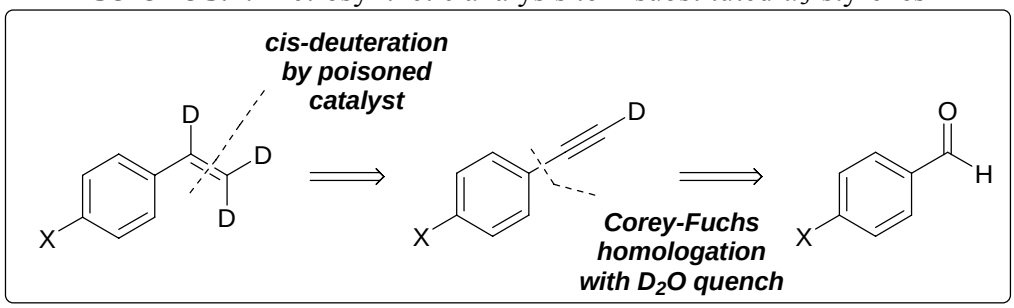

Available 4-substituted benzaldehydes would be subjected to Corey-Fuchs homologation[209, 210] with a D_2O quench to install the terminal deuterium label. *Cis*-deuteration of the triple bond to a double bond with a poisoned catalyst ($Pd/BaSO_4$, quinoline, D_2)[211] would then yield the desired d_3-alkene.

In practice, this route suffered from several drawbacks. The Corey-Fuchs homolgation generated significant waste triphenylphosphine oxide and was not atom-economical to install the C_1 fragment from CBr_4. The amounts of PPh_3 and CBr_4 on scale up were considerable, as they were required in 4 and 2 equivalents respectively. Scaling up was also a problem as the semi-hydrogenation (deuteration) was slow when tested on a 5 mmol scale and a proper hydrogenation set-up was unavailable. Combined with the cost of D_2 gas and the possible loss of a desired substitutent (X = Cl) due to hydrogenolysis led to the search for an alterative route.

These problems led to the next retrosynthetic proposal, detailed in **Scheme 3.2**. It was decided that the starting material would have all carbons in place and that manipulation of atoms would focus on the key feature of H to D exchange and D incorporation. This would then leave simplistic steps of leaving group activation and then elimination after the desired D atoms were in place. Additionally, no problems with the desired X groups (X = Cl, OMe) were anticipated.

Scheme 3.2: Second retrosynthetic analysis to 4-substituted d_3-styrenes

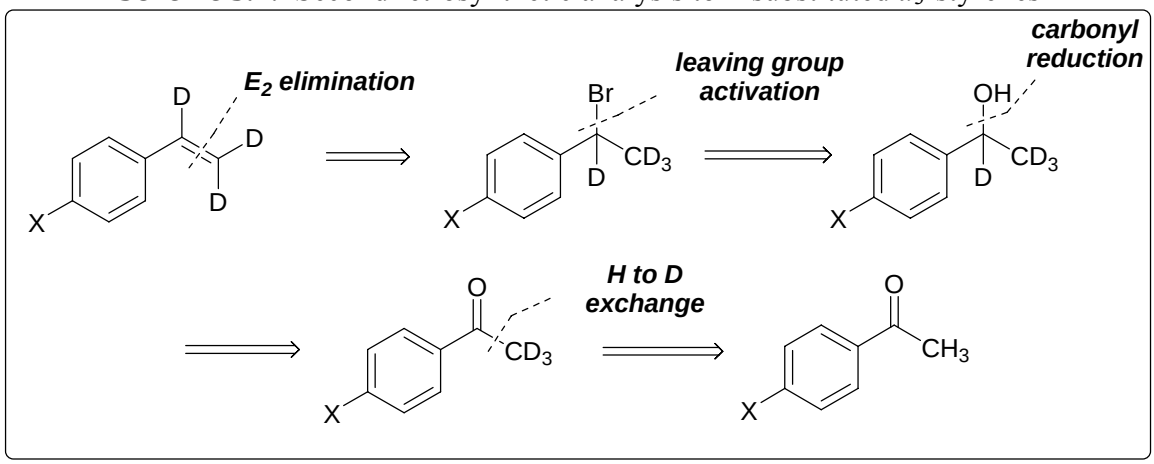

The 4-substituted acetophenones provided an inexpensive starting material that could easily be scaled up to a 60 mmol scale. Clean H to D exchange[212] was obtained in > 95% for X = Cl and > 99% for X = OMe by catalytic NaOD in D_2O. Reduction using $LiAlD_4$[213] proceeded smoothly to give the d_4-benzylic alcohol. However, only when X = Cl did the leaving group activation and E_2 elimination proceed smoothly. In both cases (X = Cl, OMe) the d_4-benzylic bromide[214] was sensitive to light and trace acid and could not be stored, requiring immediate use in the next step. E_2 elimination achieved by a bulky base under refluxing conditions was the only successful protocol to give the desired styrene (for X = Cl) (**Equation 3.23**). The use of DBU[215] and Ag_2O[216] were unsuccessful. When this was applied to X = OMe, the yield of the desired d_3-styrene was less then 5% with impurities visible by ^2H NMR spectroscopy.

Equation 3.23: Synthesis of d_3-4-chlorostyrene

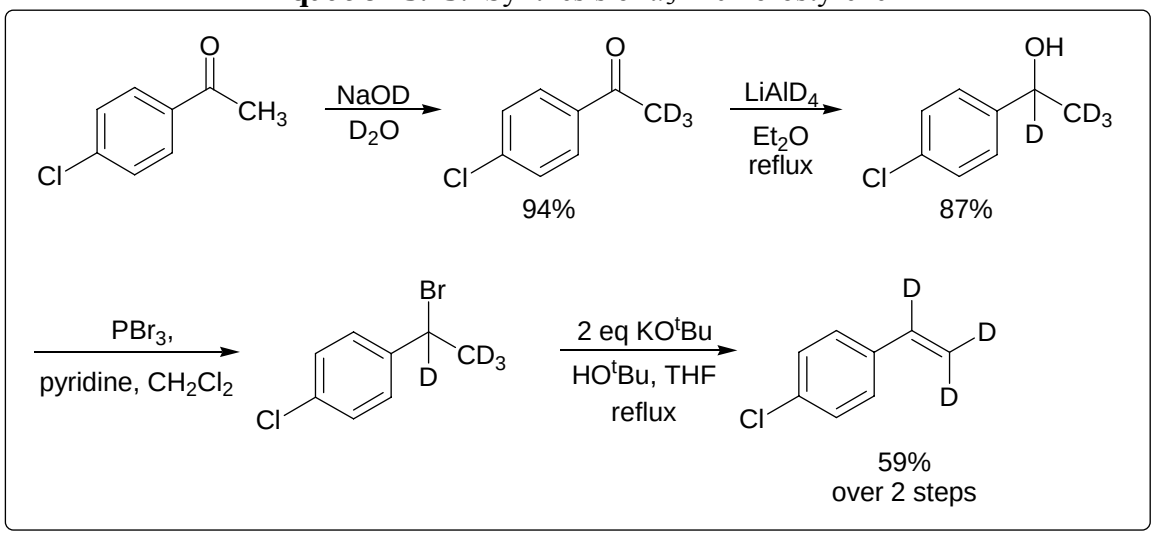

A literature search revealed that one of the target styrenes, 4-methoxystyrene, was a challenging target to synthesize in reasonable yields, as olefination methods using phosphorus ylides (Wittig reagents) consistently gave low yields[217]. Routes like the one employed above were only useful for electron withdrawing targets. One promising report by Simoni[218] used strong bicylic guanidine bases to superior yields (70%) of the desired target by Wittig chemistry.

Unfortunately, this again required modifying the route, with the substituted benzaldehyde as the requisite starting material. The retrosynthetic analysis is presented in **Scheme 3.3**.

Scheme 3.3: Retrosynthetic analysis for d_3-4-methoxystyrene

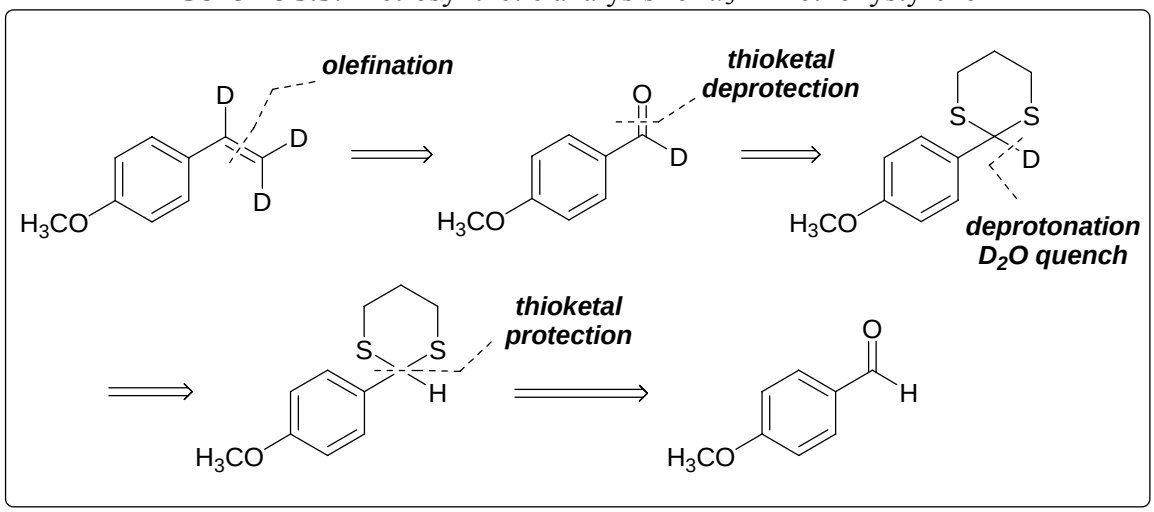

Equation 3.24: Synthetic route to d_1-4'-methoxybenzaldehyde

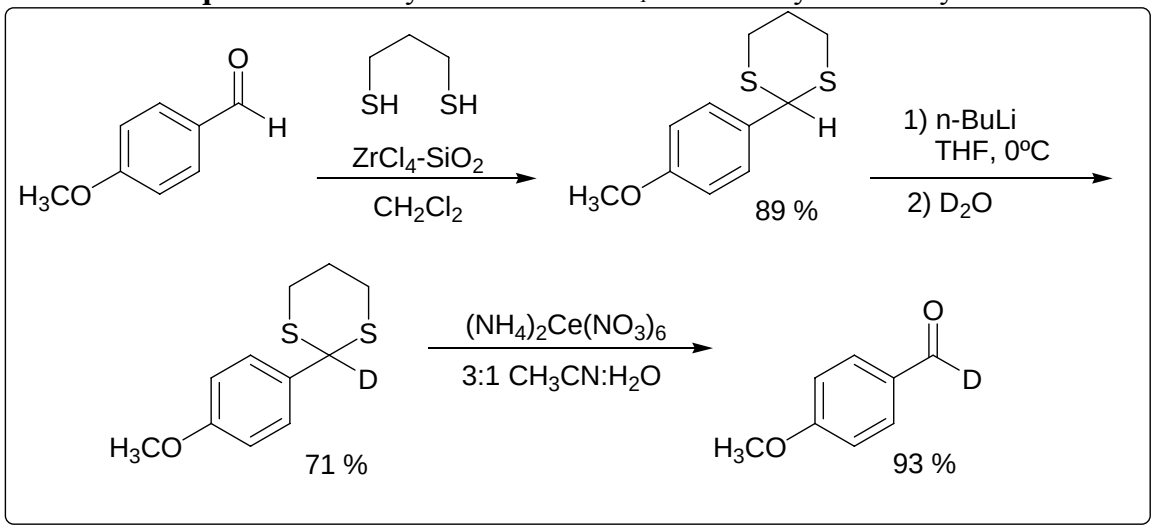

The synthesis of the d_1-aldehyde was straightforward as seen in **Equation 3.24**. Protection of the aldehyde carbonyl as the 1,3-dithiane ring[219] followed by treatment with strong base (*n*-BuLi) and D_2O quench provided the d_1-1,3-dithiane by umpolung methodology. Rapid oxidative removal of the sulfur groups[220] gave the desired d_1-aldehyde. The two advantages were realized from this route: all products could be obtained by recrystallization or distillation, on a large scale to provide multigram amounts of d_1-aldehyde.

The final step of the synthesis by Wittig olefination (**Equation 3.25**) was ultimately disappointing. Classical methods using strong base (*n*-BuLi) gave poor yields, incomplete reaction and loss of deuterium label from the phosphorus ylide. The bicyclic guanidine base TBD gave greatly increased yield[218] but also suffered from incomplete deuterium label incorporation (**Equation 3.25**). Recently Mioskowski[221] has reported the use of TBD for deuterium exchange and a deuterated version of TBD is known[222] that would overcome the incomplete deuterium exchange, introduced from the amine hydrogen.

Equation 3.25: Wittig olefination with incomplete deuterium incorporation

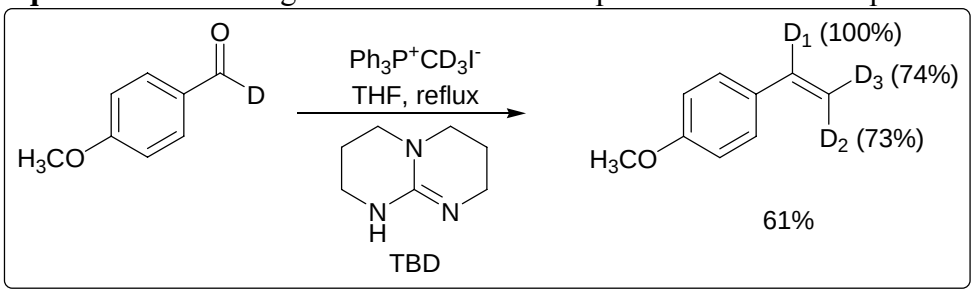

To salvage this route, a final olefination method was tested using a deuterated one carbon unit that did not require deprotonation or would not be as sensitive as the phosphorus ylide. Application of $Cp_2ZrCl_2/CD_2Br_2/Zn$[223] successfully provided the target styrene, with full deuterium label, although in low isolated yield (**Equation 3.26**).

Equation 3.26: Successful synthesis of *d_3*-4-methoxystyrene

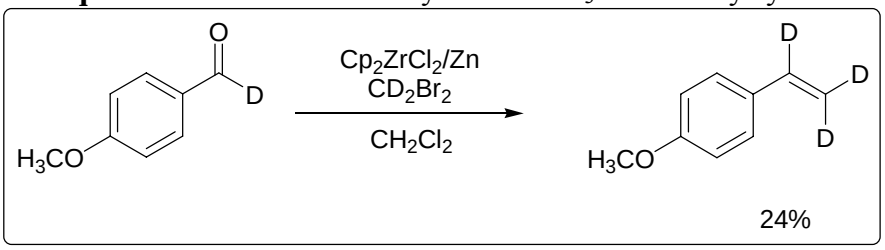

3.7 Conclusions

This chapter has put forth a proposed mechanism for iridium catalyzed hydroborations with HBpin that involves a reversible iridium-hydride insertion, with the product forming step being the insertion of the alkene into the iridium-boryl bond, followed by reductive elimination of the iridium-hydride to furnish product. This proposed mechanism is supported by thermodynamic data, known reactivity of iridium complexes and deuterium labeling studies.

During the course of the deuterium labeling experiments, low deuterium balances were found, due to the formation of HD from rhodium catalyzed exchange. D_2 was seen in iridium catalysis from generation of the active iridium-hydride catalyst.

Deuterium studies also required the use of deuterated hydroboration reagent and substrates. A direct synthesis of deuterated pinacolborane (DBpin) has been disclosed, free of the complications of other methods. Routes to d_3-styrenes are also outlined.

Chapter 4

Future Work

4.1 Future Work

The work presented here adds increased scope and mechanistic understanding to the fundamentals that are known for transition metal catalyzed hydroborations. A key feature of this work is the use of pinacolborane (HBpin) in both rhodium and iridium catalyzed hydroborations of vinyl arenes. The next step is to further expand the range of substrates for hydroboration with this reagent, with the most promising being cyclic alkenes such as indene that possess both an aromatic ring to aid with π-benzyl stabilization and a β-substituent on the carbon-carbon double bond. How this will influence the regioselectivity of the reaction, especially considering increased steric bulk of pinacolborane is of considerable interest.

Mechanistic issues are on the forefront of hydroboration chemistry. The invoking of rhodium and iridium π-benzyl intermediates, while helpful in explaining the observed regioselectivity, has little experimental support. The synthesis of rhodium and iridium π-benzyl complexes is known and the reaction of these complexes with a hydroboration reagent (HBcat or HBpin) would give invaluable insight into the validity of their proposed roles.

The lack of a model to adequately explain the observed enantioselectivity in rhodium catalyzed hydroborations is another area that deserves study. The study of the combination and variation of chiral ligands, deuterated hydroborating reagents and/or deuterated substrates, could provide evidence into the reversibility of hydride/deuteride migration and key product determining steps, which would help delineate which is the enantiodetermining step.

With respect to iridium catalyzed hydroborations, full characterization and identification of the active catalytic species is required to complete the understanding of this highly regioselective hydroboration reaction. This information can then be utilized to apply this catalytic system to other alkene substrates taking into account its ability to act as both isomerization and hydroboration catalysis.

Chapter 5

Experimental Procedures

5.1: Experimental Procedures for Chapter 2

5.1.1 General Experimental Procedures

Unless otherwise noted, all manipulations were carried out under an inert atmosphere (nitrogen) with dried glassware. NMR spectra were recorded as follows: ^{1}H at 400 MHz, ^{13}C at 100 MHz, ^{11}B at 128 MHz, in $CDCl_3$ unless otherwise noted. Gas chromatography (He carrier, 10 psi of head pressure) was performed with FID detection using a split/splitless injector (split ratio 50) and hexanes solution. Retention times are given in minutes. All analyses were performed using a Supelco BETA DEX™ 225 fused silica capillary column (2,3-di-*O*-acetyl-6-*O*-*tert*-butyldimethylsilyl-β-cyclodextrin column, 30 m, 0.25 mm diameter, 0.25 μm thickness). Chiral HPLC separations were achieved on a ChiralCel OD chiral column using a Waters 486 HPLC solvent delivery systems and detector at 256 nm. Thin-layer chromatography was done on aluminum backed silica gel plates with an F-254 indicator (Silicycle, 250 μm thickness) and visualization achieved with UV light and phosphomolybdic acid. Flash column chromatography was carried out with flash grade silica gel (230-400 mesh, Silicycle), with A.C.S. reagent grade solvents, according to Still's method[224]. Internal reaction temperatures were monitored with a digital thermometer and a Teflon-coated probe.

5.1.2 Experimental Procedures for Chapter 2

5.1.2.1 Materials

All reaction solvents were dried according to literature procedures[225] prior to use, and for those required in the glovebox, were purged of oxygen using a minimum of three freeze-pump-thaw cycles and stored under nitrogen. All vinyl arenes and other reagents

were from a commercial source (Aldrich Chemical Co.) and were distilled, stored cold under nitrogen, and percolated through a plug of basic alumina immediately before use. 2-methoxy-6-vinylnaphthalene was prepared according to Nugent[160]. Neat pinacolborane (Aldrich, 97%) was distilled under vacuum (bp 42-44ºC at 69 mmHg) and stored under nitrogen. Catalyst precursors $[M(COD)_2]BF_4$, M=Rh, Ir were prepared using a literature procedure[111] and stored cold under nitrogen. Phosphines (DPPB, DPPP, DPPE, PPh_3) were recrystallized from hot alcoholic solutions (2-propanol for DPPB, DPPP, DPPE; absolute ethanol for PPh_3). (*S*)-(*R*)- and (*R*)-(*S*)-JOSIPHOS were obtained from Strem Chemicals. The actual concentrations of all organolithium bases used were determined by titration with *N*-benzylbenzamide.

5.1.2.2 Representative Pinacolborane Hydroboration with cationic Rhodium

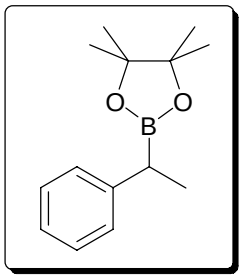

Synthesis of pinacol(1-phenylethyl)boronate

In an N_2-filled glovebox (H_2O less than 1 ppm, O_2 1 ppm) a 10 mL rbf and stirbar, previously oven-dried and introduced to the glovebox antechamber while hot, was charged with $[Rh(COD)_2]BF_4$ (5 mol %, 17.87 mg, 0.044 mmol, stored cold under N_2) and DPPB (5 mol%, 18.77 mg, 0.044 mmol). The solids were then dissolved in THF (2 mL) and stirred for 10 minutes to give a clear orange solution. To this solution was then added styrene (0.10 mL, 0.88 mmol) and stirring continued for another 10 minutes. Pinacolborane (0.15 mL, 1.03 mmol) was added, the flask capped with a septum and the reaction mixture left to stir for 24 hours. After this time, the reaction mixture was removed from the glovebox, concentrated in vacuo and the dark residue was subjected to flash chromatography (silica gel, 20:1 hexanes:ethyl acetate) to yield the desired boronate ester as a clear oil (0.147 g, 72%).

This material corresponded with known spectra[103] and ^{1}H NMR analysis showed a branched to linear ratio of 98:2.

5.1.2.3 Representative Pinacolborane Hydroboration with neutral Iridium

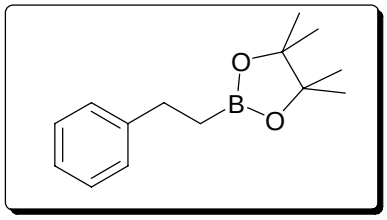

Synthesis of pinacol(2-phenylethyl)boronate

The reaction was set-up as described above, except that $[Ir(COD)Cl]_2$ (2.5 mol%, 14.78 mg, 0.022 mmol) was used as catalyst with DPPB to generate a clear yellow solution in THF. Isolation by flash chromatography (silica gel, 20:1 hexanes:ethyl acetate) yielded a white crystalline solid (0.2046 g, quantitative yield) with a branched to linear ratio of 0:100, determined by ^{1}H NMR spectroscopy.

^{1}H NMR (400 MHz, $CDCl_3$), δ:

7.30 (m, 3H), 7.24 (m, 2H), 2.79 (t, *J* = 8.1 Hz, 2H), 1.25 (s, 12H), 1.19 (t, *J* = 8.1 Hz, 2H)

^{13}C NMR (100 MHz, $CDCl_3$), δ:

144.7, 129.3, 127.8, 126.6, 83.4, 30.3, 25.7, 24.6

^{11}B NMR (128 MHz, $CDCl_3$), δ:

33.8

IR (NaCl, neat), cm^{-1}:

2979 (s), 2930 (s), 1454 (s), 1372 (s) (B-O), 1322 (s), 1146 (s), 699 (s)

HRMS (TOF MS EI+):

calculated for $C_{14}H_{21}BO_2$ 232.1635, found 232.1637

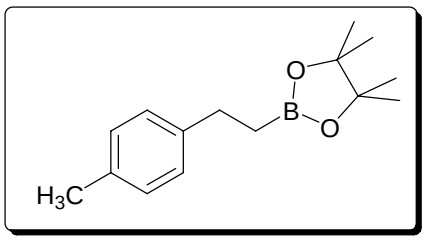

Synthesis of pinacol(2-(4-methylphenyl)ethyl)boronate

Prepared as described above, as a pale yellow solid (0.2047 g, 95%).

^{1}H NMR (400 MHz, $CDCl_3$), δ:

7.15 (d, *J* = 8.0 Hz, 2H), 7.11 (d, *J* = 8.0 Hz, 2H), 2.76 (t, *J* = 8.1 Hz, 2H), 1.27 (s, 12H), 1.17 (t, *J* = 8.1 Hz, 2H)

^{13}C NMR (100 MHz, $CDCl_3$), δ:

141.7, 135.2, 129.0, 128.4, 83.4, 29.9, 25.7, 24.6, 21.9

^{11}B NMR (128 MHz, $CDCl_3$), δ:

33.9

IR (NaCl, neat), cm^{-1}:

2979 (s), 2927 (s), 1515 (s), 1371 (s) (B-O), 1320 (s), 1146 (s)

HRMS (TOF MS EI+):

calculated for $C_{15}H_{23}BO_2$ 246.1791, found 246.1787

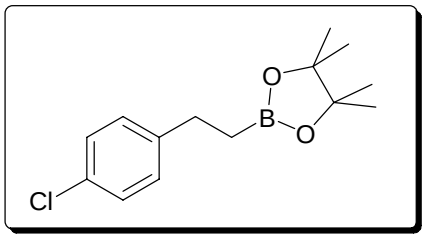

Synthesis of Pinacol(2-(4-chlorophenyl)ethyl)boronate

Prepared as described above, as a white solid (0.2322 g, 99%).

^{1}H NMR (400 MHz, $CDCl_3$), δ:

7.22 (d, *J* = 8.4 Hz, 2H), 7.13 (d, *J* = 8.4 Hz, 2H), 2.71 (t, *J* = 8.1 Hz, 2H), 1.21 (s, 12H), 1.10 (t, *J* = 8.1 Hz, 2H)

^{13}C NMR (100 MHz, $CDCl_3$), δ:

143.1, 130.4, 129.4, 129.3, 83.4, 29.6, 26.9, 25.7

^{11}B NMR (128 MHz, $CDCl_3$), δ:

33.6

IR (NaCl, neat), cm^{-1}:

2979 (s), 2930 (s), 1492 (s), 1372 (s) (B-O), 1319 (s), 1145 (s)

HRMS (TOF MS EI+):

calculated for $C_{14}H_{20}BClO_2$ 266.1245, found 266.1245

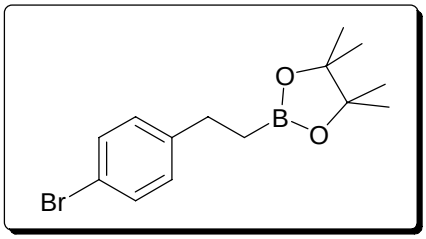

Synthesis of pinacol(2-(4-bromophenyl)ethyl)boronate

Prepared as described above, as a white solid (0.2543 g, 90%).

^{1}H NMR (400 MHz, $CDCl_3$), δ:

7.36 (d, *J* = 8.3 Hz, 2H), 7.08 (d, *J* = 8.3 Hz, 2H), 2.69 (t, *J* = 8.1 Hz, 2H), 1.22 (s, 12H), 1.11 (t, *J* = 8.1 Hz, 2H)

^{13}C NMR (100 MHz, $CDCl_3$), δ:

143.7, 132.3, 130.9, 129.4, 83.5, 29.7, 28.5, 27.0

^{11}B NMR (128 MHz, $CDCl_3$), δ:

33.6

IR (NaCl, neat), cm^{-1}:

2978 (s), 2930 (s), 1488 (s), 1372 (s) (B-O), 1319 (s), 1145 (s)

HRMS (TOF MS EI+):

calculated for $C_{14}H_{20}BBrO_2$ 310.0740, found 310.0725

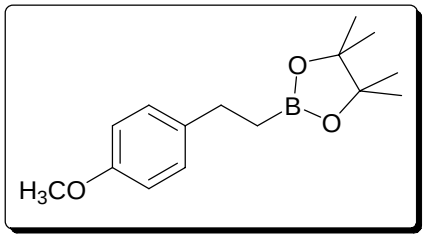

Synthesis of pinacol(2-(4-methoxyphenyl)ethyl)boronate

Prepared as described above, as a clear oil (0.2267 g, 98%).

^{1}H NMR (400 MHz, $CDCl_3$), δ:

7.14 (d, *J* = 8.4 Hz, 2H), 6.82 (d, *J* = 8.4 Hz, 2H), 3.77 (s, 3H), 2.72 (t, *J* = 8.0 Hz, 2H), 1.23 (s, 12H), 1.14 (t, *J* = 8.0 Hz, 2H)

^{13}C NMR (100 MHz, $CDCl_3$), δ:

157.9, 136.8, 130.0, 128.4, 83.3, 54.7, 29.4, 25.9, 25.7

^{11}B NMR (128 MHz, $CDCl_3$), δ:

33.8

IR (NaCl, neat), cm^{-1}:

2978 (s), 2934 (s), 1612 (s), 1513 (s), 1372 (s) (B-O), 1321 (br), 1245 (br), 1145 (s)

HRMS (TOF MS EI+):

calculated for $C_{15}H_{23}BO_3$ 262.1740, found 262.1736

5.1.2.4 Representative Hydroboration with cationic Rhodium and chiral Phosphine

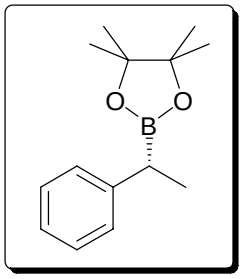

Synthesis of (R)-Pinacol(1-phenylethyl)boronate

In an N_2-filled glovebox (H_2O less than 1 ppm, O_2 1 ppm) a 10 mL rbf and stirbar, previously oven-dried and introduced to the glovebox

antechamber while hot, was charged with $[Rh(COD)_2]BF_4$ (5 mol %, 17.87 mg, 0.044 mmol, stored cold under N_2) and (*S*)-(*R*)-JOSIPHOS (6.5 mol%, 34.01 mg, 0.057 mmol). The solids were then dissolved in $ClCH_2CH_2Cl$ (2 mL) to immediately give a clear orange solution that was stirred for 10 minutes. To this solution was then added styrene (0.10 mL, 0.88 mmol) and stirring continued for another 10 minutes. Pinacolborane (0.15 mL, 1.03 mmol) was added, the flask capped with a septum and the reaction mixture left to stir for 24 hours. After this time, the reaction mixture was removed from the glovebox, concentrated and the dark residue was subjected to flash chromatography (silica gel, 20:1 hexanes:ethyl acetate) to yield (*R*)-boronate ester as a clear oil (0.156 g, 77%), consistent with published spectra[103]. ^1H NMR analysis showed a branched to linear ratio of 84:16.

5.1.2.5 Representative Determination of Enantiomeric Excess of Hydroboration

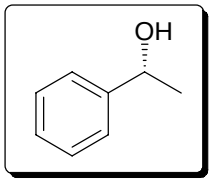

Oxidation of (R)-pinacol(1-phenylethyl)boronate to (R)-1-phenylethanol

To a 25 mL rbf was added (*R*)-boronate ester (39.13 mg, 0.17 mmol) under N_2 and dissolved in ether (10 mL). The solution was cooled to 0ºC with an ice-water bath and NaOH (1 mL of a 2 M aqueous solution) was added followed by H_2O_2 (1 mL of a 30% aqueous solution). After stirring at 0ºC for 1 hour, then at rt for 1 hour, the reaction mixture was diluted with ether and distilled water. The organic layer was separated and the aqueous layer extracted with ether (2 x 10 mL). Organics were combined, washed with brine, dried with Na_2SO_4, filtered and concentrated to give a sweet-smelling oil. A sample was prepared in hexanes (10 mL) for analysis by chiral GC, with the enantiomeric ratio determined to be 90:10 (temperature protocol, 70ºC for 5

minutes, then increased by 1ºC per minute to 150ºC for 30 minutes; retention time (R) = 45.7 minutes, (S) = 47.7 minutes, linear (2-phenylethanol) = 51.7 minutes). The branched to linear ratio was confirmed as 84:16, in agreement with ^{1}H NMR analysis.

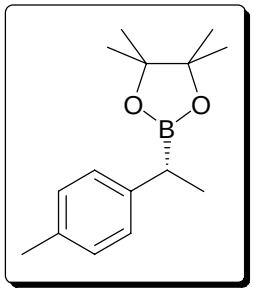

(R)-Pinacol(1-(4-methylphenyl)ethyl)boronate

Prepared as described above for (*R*)-pinacol(1-phenylethyl)boronate, following the same hydroboration procedure, with a reaction time of 72 hours to give a 50% yield of the boronate ester in a 81:19 branched to linear ratio, consistent with published spectra[103].

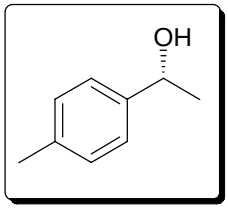

(R)-1-(4-methylphenyl)ethanol

The boronate ester was oxidized as described above to furnish the alcohol, consistent with published spectra[103], with an e.r. of 91:9 determined by chiral GC (temperature protocol 100ºC for 3 minutes, then 1ºC/minute to 150ºC for 10 minutes; retention times (*R*) = 28.4 minutes, (*S*) = 30.1 minutes, linear (2-(4-methylphenyl) ethanol) = 32.2 minutes).

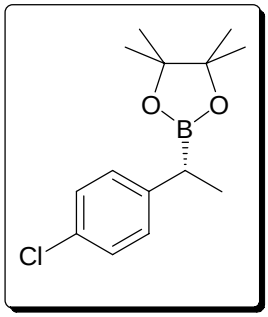

(R)-Pinacol(1-(4-chlorophenyl)ethyl)boronate

Prepared as described above for (*R*)-pinacol(1-phenylethyl)boronate, following the same hydroboration procedure to give a 91% yield of the boronate ester in a 83:17 branched to linear ratio, consistent with published spectra[103].

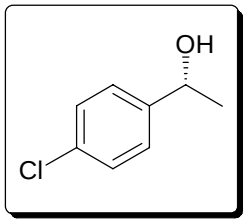

(R)-1-(4-chlorophenyl)ethanol

The boronate ester was oxidized as described above to furnish the alcohol, consistent with published spectra[103] with an e.r. of 88:12 determined by chiral GC (temperature protocol 100ºC for 3 minutes, then 1ºC/minute to 160ºC for 15 minutes; retention times (*R*) = 45.8 minutes, (*S*) = 47.0 minutes, linear (2-(4-chlorophenyl)ethanol) = 53.0 minutes).

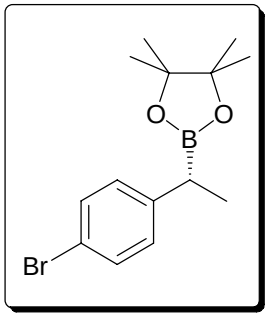

(R)-Pinacol(1-(4-bromophenyl)ethyl)boronate

Prepared as described above for(*R*)-pinacol(1-phenylethyl)boronate, following the same hydroboration procedure to give a 50% yield of the boronate ester in a 86:14 branched to linear ratio, consistent with published spectra[136].

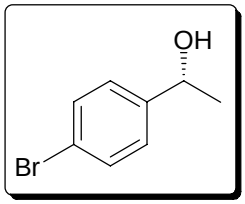

(R)-1-(4-bromophenyl)ethanol

The boronate ester was oxidized as described above to furnish the alcohol, consistent with published spectra[136], with an e.r. of 88:12 determined by chiral GC (temperature protocol 100ºC for 3 minutes, then 1ºC/minute to 190ºC for 15 minutes; retention times (*R*) = 55.5 minutes, (*S*) = 56.5 minutes, linear (2-(4-bromophenyl)ethanol) = 62.9 minutes).

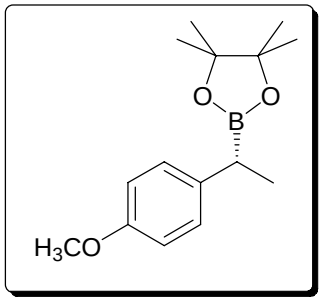

(R)-Pinacol(1-(4-methoxyphenyl)ethyl)boronate

Prepared as described above for(*R*)-pinacol(1-phenylethyl)boronate, following the same hydroboration

procedure to give a 85% yield of the boronate ester in a 85:15 branched to linear ratio, consistent with published spectra[37].

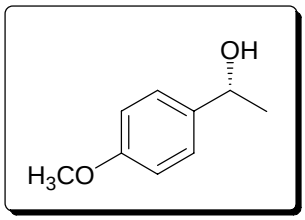

(R)-1-(4-methoxyphenyl)ethanol

The boronate ester was oxidized as described above to furnish the alcohol, consistent with published spectra[37], with an e.r. of 88:12 determined by chiral GC (temperature protocol 100ºC for 3 minutes, then 1ºC/minute to 160ºC for 15 minutes; retention times (*R*) = 46.4 minutes, (*S*) = 48.1 minutes, linear (2-(4-methoxyphenyl) ethanol) = 52.2 minutes).

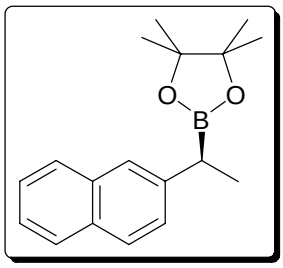

(S)-Pinacol 1-(6-naphthylethyl)boronate

In an N_2-filled glovebox (H_2O less than 1 ppm, O_2 1 ppm) a 10 mL rbf and stirbar, previously oven-dried and introduced to the glovebox antechamber while hot, was charged with $[Rh(COD)_2]BF_4$ (5 mol %, 17.87 mg, 0.044 mmol, stored cold under N_2) and (*R*)-(*S*)-JOSIPHOS (6.5 mol%, 34.01 mg, 0.057 mmol). The solids were then dissolved in $ClCH_2CH_2Cl$ (2 mL) to immediately give a clear orange solution that was stirred for 10 minutes. To this solution was then added 2-vinylnaphthalene (135 mg , 0.88 mmol) and stirring continued for another 10 minutes. Pinacolborane (0.15 mL, 1.03 mmol) was added, the flask capped with a septum and the reaction mixture left to stir for 24 hours. After this time, the reaction mixture was removed from the glovebox, concentrated and the dark residue was subjected to flash chromatography (silica gel, 20:1 hexanes:ethyl acetate) to yield the (*S*)-enantiomer as a white solid (0.1658 g, 67% yield). ^1H NMR analysis showed a branched to linear ratio of 95:5.

^{1}H NMR (400 MHz, $CDCl_3$), δ:

7.80 (m, 3H), 7.49 (s, 1H), 7.45 (m, 3H), 2.67 (q, *J* = 7.4 Hz, 1H), 1.49 (d, *J* = 7.4 Hz, 3H), 1.26 (s, 6H), 1.24 (s, 6H)

^{13}C NMR (100 MHz, $CDCl_3$), δ:

142.9, 134.2, 132.1, 128.7 127.2, 126.8, 126.3 125.9, 125.2, 124.4, 83.7, 25.5, 24.4, 16.7

^{11}B NMR (128 MHz, $CDCl_3$), δ:

33.6

IR (NaCl, neat), cm^{-1}:

2976 (s), 2729 (w), 1914 (s), 1322 (s, br) (B-O), 1143 (s, br), 1070 (s), 982 (s), 857 (s), 817 (s), 748 (s)

HRMS (TOF MS EI+):

calculated for $C_{18}H_{23}BO_2$ 282.1791, found 282.1790

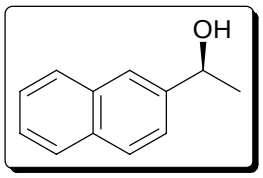

Oxidation of (S)-Pinacol 1-(6-naphthylethyl)boronate to (S)-1-naphthylethanol

To a 25 mL rbf was added (*S*)-boronate ester (59.22 mg, 0.21 mmol) under N_2 and dissolved in ether (10 mL). The solution was cooled to 0ºC with an ice-water bath and NaOH (1 mL of a 2 M aqueous solution) was added followed by H_2O_2 (1 mL of a 30% aqueous solution). After stirring at 0ºC for 1 hour, then at rt for 1 hour, the reaction mixture was diluted with ether and distilled water. The organic layer was separated and the aqueous layer extracted with ether (2 x 10 mL). Organics were combined, washed with brine, dried with Na_2SO_4, filtered and concentrated to give a

white solid. The crude material was subjected to flash chromatography (silica gel, 7:1 hexanes: ethyl acetate) to give the pure branched alcohol (R*f* 0.42) in 86% yield (31.1 mg) free of the linear achiral alcohol (R*f* 0.29). Analysis of the branched alcohol by chiral SFC (ChiralCel OD-H column, 10% CH_3OH carrier, flow rate 1 mL/minute; retention times (*S*) = 7.50 minutes, (*R*) = 8.44 minutes) showed an e.r. of 93:7.

^{1}H NMR (400 MHz, $CDCl_3$), δ:

7.84 (m, 3H), 7.80 (s, 1H), 7.50 (m, 3H), 5.05 (q, *J* = 6.4 Hz, 1H), 1.58 (d, *J* = 6.4 Hz, 3H)

^{13}C NMR (100 MHz, $CDCl_3$), δ:

143.6, 133.7, 133.2, 129.4, 127.8, 127.4, 127.2, 126.9, 125.7, 123.4, 71.5, 24.9

IR (NaCl, thin film CH_2Cl_2), cm^{-1}:

3317 (br) (O-H), 2970 (w), 2921 (w), 1364 (w), 1075 (w), 902(s), 861(s), 822 (s), 742 (s)

HRMS (TOF MS EI+):

calculated for $C_{12}H_{12}O$ 172.0888, found 172.0888

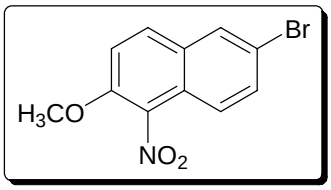

1-nitro-2- methoxy-6-bromonaphthalene

2-methoxy-6-bromonaphthalene was nitrated[226] to give the title compound in 63% yield.

^{1}H NMR (400 MHz, $CDCl_3$), δ:

8.01 (s, 1H), 7.88 (d, *J* = 9.2 Hz, 2H), 7.67 (d, *J* = 9.2 Hz, 2H), 7.56 (d, *J* = 9.2 Hz, 2H), 7.37 (d, *J* = 9.2 Hz, 2H), 4.04 (s, 3H)

^{13}C NMR (100 MHz, $CDCl_3$), δ:

149.2, 136.2, 131.9, 129.4, 124.6, 123.3, 121.8, 119.3, 115.3, 113.7, 57.6

IR (NaCl, thin film CH_2Cl_2), cm^{-1}:

1636 (m), 1592 (m), 1519 (s) (N-O sym), 1501 (s) (N-O asym), 1356 (m) (Ar-NO_2), 1279 (s) (C-O-C), 1256 (m) (C-O-C), 1081 (m), 875 (m), 800 (m)

HRMS (TOF MS EI+):

calculated for $C_{11}H_8BrNO_3$ 280.9688, found 280.9691

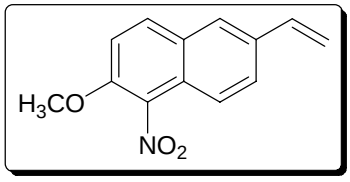

1-nitro-2-methoxy-6-vinylnaphthalene

1-nitro-2-methoxy-6-bromonaphthalene was subjected to a Heck reaction under ethene gas pressure[227] to give the title alkene in 72% yield after flash chromatography (10:1 hexanes: ethyl acetate).

^{1}H NMR (400 MHz, $CDCl_3$), δ:

7.88 (d, *J* = 9.1 Hz, 1H), 7.73 (d, *J* = 8.9 Hz, 1H), 7.70 (s, 1H), 7.62 (d, J = 8.9 Hz, 1H), 7.28 (d, *J* = 9.1 Hz, 1H), 6.82 (dd, *J* = 17.6 Hz, *J'* = 10.8 Hz, 1H), 5.86 (d, *J* = 17.6 Hz, 1H), 5.37 (d, *J'* = 10.8 Hz, 1H), 4.01 (s, 3H)

^{13}C NMR (100 MHz, $CDCl_3$), δ:

148.9, 137.0, 135.5, 132.0, 131.7, 127.1, 126.3, 125.4, 121.8, 120.3, 114.4, 112.9, 57.5

IR (NaCl, thin film CH_2Cl_2), cm^{-1}:

2987 (w), 2949 (w), 2850 (w), 1634 (m), 1602 (m), 1521 (s) (N-O sym), 1489 (m) (N-O asym), 1365 (m), 1348 (m), 1282 (s) (C-O-C), 1172 (m), 1079 (m), 1014 (w), 990 (s), 892 (s), 824(m), 806 (s)

HRMS (TOF MS EI+):

calculated for $C_{13}H_{11}NO_3$ 229.0739, found 229.0731

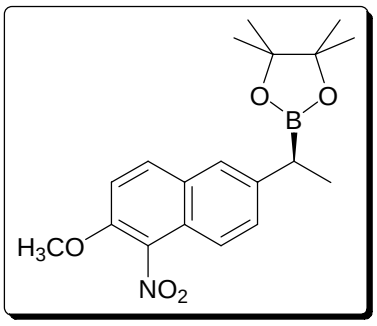

(S)-Pinacol(1-(1-nitro-2-methoxy-6-naphthylethyl)boronate

In an N_2-filled glovebox (H_2O less than 1 ppm, O_2 1 ppm) a 10 mL rbf and stirbar, previously oven-dried and introduced to the glovebox antechamber while hot, was charged with $[Rh(COD)_2]BF_4$ (5 mol %, 17.87 mg, 0.044 mmol, stored cold under N_2) and (R)-(S)-Josiphos (6.5 mol%, 34.01 mg, 0.057 mmol). The solids were then dissolved in $ClCH_2CH_2Cl$ (2 mL) to immediately give a clear orange solution that was stirred for 10 minutes. To this solution was then added 1-nitro-2-methoxy-6-vinylnaphthalene (201 mg, 0.88 mmol) and stirring continued for another 10 minutes. Pinacolborane (0.15 mL, 1.03 mmol) was added, the flask capped with a septum and the reaction mixture left to stir for 24 hours. After this time, the reaction mixture was removed from the glovebox, concentrated and the dark residue was subjected to flash chromatography (silica gel, 20:1 hexanes:ethyl acetate) to yield the (*S*)-enantiomer as a red solid (0.1604g, 51% yield). ^{1}H NMR analysis showed a branched to linear ratio of 91:9.

^{1}H NMR (400 MHz, $CDCl_3$), δ:

7.87 (d, *J* = 9.2 Hz, 1H), 7.60 (m, 2H), 7.50 (m, 1H), 7.28 (m, 1H), 4.00 (s, 3H), 2.60 (q, *J* = 7.4 Hz, 1H), 1.14 (d, *J* = 7.4 Hz, 3H), 1.21 (s, 6H), 1.20 (s, 6H)

^{13}C NMR (100 MHz, $CDCl_3$), δ:

148.2, 142.4, 136.3, 132.0, 130.9, 129.1, 125.6, 124.1, 120.6, 113.2, 83.9, 57.4, 25.1, 24.9, 16.8

^{11}B NMR (128 MHz, $CDCl_3$), δ:

33.4

IR (NaCl, neat), cm^{-1}:

2920 (br), 1635 (m) (NO_2 asy), 1568 (NO_2 sym), 1505 (m), 1447 (m), 1393 (m) (B-O), 1075 (m), 926 (m), 869 (m)

HRMS (TOF MS EI+):

calculated for $C_{19}H_{24}BNO_3$ 357.1748, found 357.1758

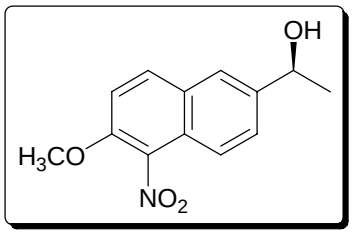

Oxidation of (S)-Pinacol 1-(1-nitro-2-methoxy-6-naphthylethyl)boronate to (S)-1-(1-nitro-2-methoxy-6-naphthyl)ethanol.

To a 25 mL rbf was added (*S*) boronate ester (27.75 mg, 0.077 mmol) under N_2 and dissolved in ether (10 mL). The solution was cooled to 0ºC with an ice-water bath and NaOH (1 mL of a 2 M aqueous solution) was added followed by H_2O_2 (1 mL of a 30% aqueous solution). After stirring at 0ºC for 1 hour, then at rt for 1 hour, the reaction mixture was diluted with ether and distilled water. The organic layer was separated and the aqueous layer extracted with ether (2 x 10 mL). Organics were combined, washed with brine, dried with Na_2SO_4, filtered and concentrated to give a yellow solid. The crude material was subjected to flash chromatography (silica gel, 2:1 hexanes: ethyl acetate) to give the pure branched alcohol in 77% yield (14.7 mg). Analysis of the branched alcohol by chiral SFC (ChiralCel OD-H column, 10% CH_3OH carrier, flow rate 1 mL/minute; retention times (*S*) = 11.4 minutes, (*R*) = 11.9 minutes showed an e.r. of 92:8.

^{1}H NMR (400 MHz, $CDCl_3$), δ:

7.97 (d, *J* = 9.2 Hz, 1H), 7.84 (s, 1H), 7.68 (d, *J* = 8.8 Hz, 1H), 7.63 (d, J = 8.8 Hz, 1H), 7.36 (d, *J* = 9.2 Hz, 1H), 5.08 (q, *J* = 6.4 Hz, 1H), 4.05 (s, 3H), 1.58 (d, *J* = 6.4 Hz, 3H)

^{13}C NMR (100 MHz, $CDCl_3$), δ:

152.6, 148.6, 142.7, 132.2, 128.2, 127.3, 125.1, 123.8, 120.9, 113.4, 69.9, 57.0, 25.2

IR (NaCl, thin film), cm^{-1}:

3401 (br), 1638 (m) (NO_2 asy), 1525 (NO_2 sym), 1076 (m), 806 (m)

HRMS (TOF MS EI+):

calculated for $C_{13}H_{13}NO_4$ 247.0845, found 247.0845

5.1.2.6 Asymmetric Hydroboration en route to Naproxen™

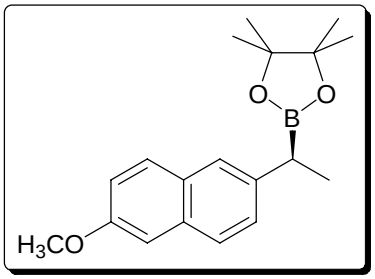

Hydroboration with cationic Rhodium and chiral Phosphine : (S)-Pinacol(1-(2-methoxy-6-naphthylethyl)boronate

In an N_2-filled glovebox (H_2O less than 1 ppm, O_2 1 ppm) a 25 mL rbf and stirbar, previously oven-dried and introduced to the glovebox antechamber while hot, was charged with $[Rh(COD)_2]BF_4$ (1 mol %, 16.24 mg, 0.04 mmol, stored cold under N_2) and (*R*)-(*S*)-JOSIPHOS (2 mol%, 47.57 mg, 0.08 mmol). The solids were then dissolved in $ClCH_2CH_2Cl$ (4 mL) to immediately give a clear orange solution that was stirred for 10 minutes. To this solution was then added 2-methoxy-6-vinylnaphthalene[160] (738 mg, 4.0 mmol in 5 mL $ClCH_2CH_2Cl$) and stirring continued for another 5 minutes. Pinacolborane (0.68 mL, 4.68 mmol) was added, the

flask capped with a septum. The reaction mixture was allowed to stir for 24 hours. After this time, the reaction mixture was removed from the glovebox, concentrated, and a sample of the dark orange residue taken for ^{1}H NMR analysis ($CDCl_3$, branched to linear ratio 95:5). Flash chromatography (silica gel, 20:1 hexanes:ethyl acetate) yielded the ester as a white solid (1.039 g, 83% yield). ^{1}H NMR analysis of the purified material showed a branched to linear ratio of 95:5. If desired, the boronate ester can be obtained as the pure branched isomer by another chromatography treatment on a Cyclograph™ centrifugal chromatography system (Analtech Inc), however, with a decrease in overall yield to 51% (0.638 g).

^{1}H NMR (400 MHz, $CDCl_3$), δ:

7.68 (m, 2H), 7.60 (m, 1H), 7.38 (m, 1H), 7.13 (m, 2H), 3.92 (s, 3H), 2.60 (broad q, *J* = 4.8 Hz, 1H), 1.44 (d, J = 4.8 Hz, 3H), 1.23 (s, 6H), 1.21 (s, 6H)

^{13}C NMR (100 MHz, $CDCl_3$), δ:

156.9, 140.2, 132.6, 129.4, 129.0, 127.7, 126.6, 125.2, 118.4, 105.6, 83.3, 55.3, 24.8, 24.6, 16.9

^{11}B NMR (128 MHz, $CDCl_3$), δ:

33.5

IR (NaCl, neat), cm^{-1}:

2976 (s, br), 2840 (s), 1910 (m), 1505 (s), 1484 (s), 1373 (s, br) (B-O), 1264 (s), 1034 (s), 968 (s), 922 (s), 810 (s)

HRMS (TOF MS EI+):

calculated for $C_{19}H_{25}BO_3$ 312.1897, found 312.1903

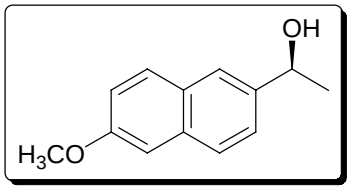

Determination of Enantiomeric Excess of Hydroboration: Oxidation of (S)-Pinacol(1-(2-methoxy-6-naphthylethyl)boronate to (S)-1-(2-methoxy-6-naphthyl)ethanol

To a 25 mL rbf was added the pinacolboronate ester (97.48 mg, 0.313mmol) under N_2 and ether (20 mL). The solution was cooled to 0ºC with an ice-water bath and NaOH (1 mL of a 2 M aqueous solution), followed by H_2O_2 (1 mL of a 30% aqueous solution) was added. After stirring at 0ºC for 1 hour, then at rt for 1 hour, the reaction mixture was diluted with ether and distilled water. The organic layer was separated and the aqueous layer extracted with ether (2 x 10 mL). The organics were combined, washed with brine, dried with Na_2SO_4, filtered and concentrated to give a white solid. The crude material was subjected to flash chromatography (silica gel, 7:1 hexanes: ethyl acetate) to give the pure branched alcohol (R*f* 0.36) in 83% yield (52.9 mg) free of the linear achiral alcohol (R*f* 0.26). Analysis of the branched alcohol by chiral HPLC (ChiralCel OD column, 9:1 hexanes: 2-propanol, flow rate 1 mL/minute; retention times (*S*) = 12.3 minutes, (*R*) = 17.0 minutes) showed an e.r. of 94:6.

^{1}H NMR (400 MHz, $CDCl_3$), δ:

7.75 (m, 3H), 7.50 (m, 1H), 7.18 (m, 2H), 5.07 (q, *J* = 6.4 Hz, 1H), 3.95 (s, 3H), 1.76 (broad s, 1H), 1.59 (d, *J* = 6.4 Hz, 3H)

^{13}C NMR (100 MHz, $CDCl_3$), δ:

157.7, 140.9, 134.1, 129.4, 128.8, 127.2, 124.4, 123.8, 119.0, 105.7, 70.5, 55.3, 25.1

IR (NaCl, thin film CH_2Cl_2), cm^{-1}:

3327 (br), 2964 (w), 1634 (w), 1606 (m), 1267 (m), 1162 (m), 1077 (m), 1028 (m), 890 (w), 853 (m), 813 (w)

HRMS (TOF MS EI+):

calculated for $C_{13}H_{14}O_2$ 202.0994, found 202.0984

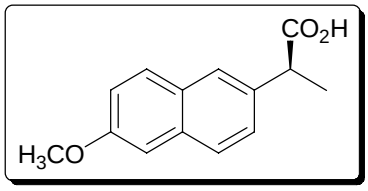

Homologation/Lindgren Oxidation: (S)-(+)-6-methoxy-α-methyl-2-naphthalene acetic acid (Naproxen™)

Homologation

A 25 mL rbf and stirbar were flame-dried under N_2 purge, cooled to rt and charged with the boronate ester (145.45 mg, 0.465 mmol). Ester was dissolved in THF (8 mL) and CH_2Cl_2 (0.95 mL, 30 equivalents, 14.4 mmol) and cooled to –105ºC using an anhydrous EtOH/liquid N_2 bath under N_2. *n*-BuLi (0.65 mL, 3.3 equivalents, 1.58 mmol of a 2.5 M solution in hexanes, Aldrich) was added down the side of the flask to ensure addition of the cooled reagent to the ester solution (this leads to very stable temperature control, with the temperature remaining constant at –105ºC during addition). On completion of addition, a white solid is suspended in the clear solution (the homologating reagent $LiCHCl_2$). The reaction was left to warm to rt overnight. After this time, the reaction mixture was concentrated, and the thick brown residue was taken up in Et_2O, and then quenched with saturated aqueous NH_4Cl solution. Separation of the organic layer and extraction with Et_2O (5 x 10 mL), followed by combination of the Et_2O extracts, washing with brine (1 x 25 mL), drying with $MgSO_4$, filtration and concentration yielded

a viscous brown oil (0.2051g). NMR analysis indicated conversion (89%) and this material was taken directly to the next step.

Lindgren oxidation

A 250 mL rbf with a stirbar, containing the crude α-chloroboronate ester (0.2051 g, 0.569 mmol) was flushed under N_2, and taken up in a 1:1 mixture of amylene : *t*–BuOH (12.5 mL). $NaClO_2$ (0.6483 g, 10 equivalents, 7.11 mmol of 80% purity) and KH_2PO_4 (0.9316 g, 12 equivalents, 6.83 mmol) in distilled water (25 mL) was added dropwise to give a biphasic mixture which was left to stir at ambient temperature for 24 hours. At 24 hours and 48 hours a second and third batch of aqueous $NaClO_2$- KH_2PO_4 solution was added and the reaction mixture left to stir for another 48 hours, for a total reaction time of 90 hours. The volatile components were then removed under reduced pressure at room temperature to give a milky aqueous suspension that was then extracted with Et_2O (2 x 40 mL) and EtOAc (4 x 40 mL). The combined pale yellow organics were then extracted with distilled water (1 x 20 mL) and saturated aqueous $NaHCO_3$ (5 x 40 mL). The combined basic aqueous extracts were cooled in an ice bath to below 10ºC and carefully acidified to pH ~1 using concentrated HCl with vigorous stirring, keeping the internal temperature between 4 to 9ºC. The frothy, milky suspension of acidified aqueous extract was then extracted with EtOAc (200 mL initally, 6 x 40 mL), the pale yellow EtOAc extracts combined, quickly washed with brine (1 x 50 mL) and dried with $MgSO_4$. Filtration and concentration yielded a deep yellow oil.

Dissolving the oil in hexanes and passing it through a plug of basic alumina purified this material. After elution of coloured contaminants with hexanes, the plug was

eluted with EtOAc and then CF_3CO_2H. Concentration of these fractions yielded 79.8 mg (66%) of the pure Naproxen™, in agreeance with published spectra[160].

A portion of this material was subjected to the reduction described below to determine the enantiomeric excess.

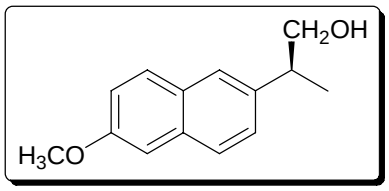

Determination of Enantiomeric Excess of Hydrocarboxylation: Reduction of (S)-(+)-6-methoxy-α-methyl-2-naphthalene acetic acid (Naproxen ™) to (S)-2-(6-methoxynaphthalene)propanol

A 100 mL flame-dried rbf equipped with a stirbar was charged with Naproxen (15.8 mg, 0.069 mmol) and Et_2O (10 mL) under N_2. The solution was then cooled to 0ºC and the borane-dimethyl sulfide complex (0.10 mL, 1.05 mmol, excess) was added dropwise. The mixture was allowed to stir at 0ºC for 0.5 hours, and allowed to warm to room temperature for 0.5 hours. Then the reaction mixture was cooled again, and quenched with CH_3OH, then distilled water, followed by dilution with ether and distilled water. Separation of ether layer and extraction of the aqueous layer with ether (2 x 10 mL) was followed by washing of the combined ether extracts with brine and drying with Na_2SO_4. Filtration and concentration gave a white solid. Purification by flash chromatography (silica gel, 7:1 hexanes : ethyl acetate) gave 9.1 mg (61%) of a white solid, Rf = 0.33 (2:1 hexanes : ethyl acetate) as one spot. HPLC analysis (ChiralCel OD column, 98:2 hexanes : isopropanol, flow rate 1mL/minute; retention times (*S*) = 20.0 minutes, (*R*) = 21.5 minutes) found the e.r. to be 94:6. The enantiomeric composition was authenticated by

comparison to the alcohol obtained from the reduction of commercial (*S*)-Naproxen™ (Aldrich, 98%) which had an e.r. of 100:0 and retention time of 20.1 minutes.

^{1}H NMR (400 MHz, $CDCl_3$), δ:

7.73 (m, 2H), 7.63 (m, 1H), 7.37 (m, 1H), 7.17 (m, 2H), 3.94 (s, 3H), 3.80 (d, J = 6.8 Hz, 2H), 3.13 (m, 1H), 1.44 (broad s, 1H), 1.38 (d, J = 4.8 Hz, 3H)

^{13}C NMR (100 MHz, $CDCl_3$), δ:

157.5, 138.7, 133.6, 129.1, 129.0, 127.2, 126.3, 125.9, 118.9, 105.6, 68.6, 55.3, 42.4, 17.6

IR (NaCl, thin film CH_2Cl_2), cm^{-1}:

3276 (br), 2960 (w), 2936 (w), 1605 (w), 1463(w), 1391 (w), 1263 (w), 1212 (w), 1164 (w), 1028 (w), 854 (w), 814 (m)

HRMS (TOF MS EI+):

calculated for $C_{14}H_{16}O_2$ 216.2756, found 216.1155

Chapter 5.2: Experimental Procedures for Chapter 3

5.2.1 General Experimental Procedures and Materials

All reaction solvents were dried according to literature procedures[225] prior to use. Solvents required in the glovebox, were purged of oxygen using a minimum of three freeze-pump-thaw cycles and stored under nitrogen. All glassware was flame-dried and cooled under an inert atmosphere of N_2 and the reactions conducted under N_2. All vinyl arenes and other reagents were from a commercial source (Aldrich Chemical Co.) and were distilled, stored cold under nitrogen, and percolated through a plug of basic alumina immediately before use. Neat pinacolborane (Aldrich, 97%) was distilled under vacuum

(bp 42-44ºC at 69 mmHg) and stored under nitrogen. Catalyst precursors $[Rh(COD)_2]BF_4$ and $[Ir(COD)Cl]_2$ were prepared using a literature procedure[112] and stored cold under nitrogen. Phosphines (DPPB, DPPP, DPPE, PPh_3) were recrystallized from hot alcoholic solutions (2-propanol for DPPB, DPPP, DPPE; absolute ethanol for PPh_3). 4-methoxybenzaldehyde was purified by bulb-to-bulb distillation (157-160ºC/22 mmHg) and stored cold. Lithium aluminum deuteride (Aldrich 98% atom D, 90% CP), and phosphorous tribromide (Aldrich, 99%) were used as received.

5.2.2 Deuterated Pinacolborane

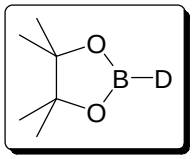

Synthesis of 2-deutero-4,4,5,5-tetramethyl-1,3,2-dioxaborolane, deuteropinacolborane, DBpin

A specialized 14 joint glass vessel, to enable direct distillation from the reaction mixture, was charged with $[Ir(COD)Cl]_2$ (134.34 mg, 0.2 mmol, 1 mol%) and PPh_3 (210 mg, 0.8 mmol, 4 mol %) and suspended in neat HBpin (3.0 mL, 20 mmol). This vessel was sealed in a stainless steel autoclave, the line and vessel flushed once with D_2 gas, then pressurized to 260 psi. After 16 hours at rt, it was vented and repressurized to 260 psi. Further stirring at rt for 24 hours, then vented and the contents analyzed by ^{11}B NMR spectroscopy to show the broad triplet for the product. Distillation (65-66ºC/184 mmHg) gave the desired borane as a clear liquid (1.46 g, 55%) consistent with published spectra[198].

Synthesis of $[Ir(COD)Cl]_2$[185]

To a 25 mL rbf with stirbar was added distilled water (3.0 mL), *i*PrOH (1.05 mL) and COD (0.67 mL, 5.44 mmol) and the emulsion vigourously stirred with N_2 bubbling through the solution. Addition of $IrCl_3 \cdot 3H_2O$ (600 mg, 1.70 mmol) gave a yellow-black

suspension that was heated to reflux for 18 hours. Cooling to rt provided red crystalline material that was collected by vacuum filtration, washed with distilled water (1 x 5 mL) and *i*PrOH (2 x 2 mL), and dried overnight under vacuum (515 mg, 89%).

5.2.3 Transition Metal Catalyzed Hydroborations with Deutrated Pinacolborane

Typical procedure for Rhodium-catalyzed hydroboration with DBpin

In the glovebox, a 5 mL screw cap vial was charged with $[Rh(COD)_2]BF_4$ (3.6 mg, 5 mol %, 0.0089 mmol) and DPPB (4.5 mg, 6 mol %, 0.0107 mmol) and stirred in THF (0.8 mL) to give an orange suspension. C_6D_6 internal standard (4 μL) and styrene (205 μL, 1.78 mmol) added and the reaction mixture stirred, then DBpin (60 μL, 0.42 mmol) added. After stirring for 24 hours in the glovebox, the reaction mixture was transferred to a J-Young NMR tube and analyzed by ^2H NMR spectroscopy to determine the extent of deuterioboration/hydroboration and deuterium incorporation into the excess styrene.

Typical procedure for Iridium-catalyzed hydroboration with DBpin

In the glovebox, a 5 mL screw cap vial was charged with $[Ir(COD)Cl]_2$ (3.0 mg, 2.5 mol %, 0.0045 mmol) and DPPB (3.8 mg, 5 mol %, 0.0090 mmol) and stirred in THF (0.8 mL) to give a yellow solution. C_6D_6 internal standard (4 μL) and styrene (205 μL, 1.78 mmol) added and the reaction mixture stirred, then DBpin (60 μL, 0.42 mmol) added. After stirring for 24 hours in the glovebox, the reaction mixture was transferred to a J-Young NMR tube and analyzed by ^2H NMR spectroscopy to determine the extent of deuterioboration/hydroboration and deuterium incorporation into the excess styrene.

Typical procedure for Rhodium-catalyzed hydroboration of d_3-styrenes with HBpin

In the glovebox, a 25 mL rbf was charged with $[Rh(COD)_2]BF_4$ (3.6 mg, 5 mol %, 0.0089 mmol) and DPPB (4.5 mg, 6 mol %, 0.0107 mmol) and stirred in THF (0.8 mL) to give an orange suspension. The *para*-substituted d_3-styrene (205 μL, 1.78 mmol) added and the reaction mixture stirred, then HBpin (60 μL, 0.42 mmol) added. After stirring for 24 hours in the glovebox, the reaction mixture was removed from the glovebox, diluted with Et_2O (10 mL) and oxidized with 2M NaOH (1 mL) and H_2O_2 (30% aqueous, 1 mL) at 0ºC for 1 hour and at rt for 1 hour. Extraction with Et_2O and drying of the extracts with Na_2SO_4, followed by concentration gave an oil that was subjected to flash chromatography on silica gel with hexanes eluant to isolate the unreacted styrene then 7:1 hexanes:EtOAc to give the alcohol. These were then analyzed by ^2H NMR spectroscopy to determine the extent of deuterioboration/hydroboration and deuterium incorporation into the excess styrene.

Typical procedure for Iridium-catalyzed hydroborations monitored by NMR

In the glovebox, a screw cap NMR tube was charged with stock $[Ir(COD)Cl]_2$ and DPPB solutions in $CDCl_3$, diluted with $CDCl_3$, internal standard of $ClCH_2CH_2Cl$ added followed by styrene. In all trials a constant volume of 1276 μL was maintained. The sealed tube was placed in 600 MHz NMR, and then locked and shimmed at temperature of 298.0 K. A multi-collection experiment was set (re 1 d1 72s, ns 1; re 2 ds 2) and data collected every 3 minutes, 49 seconds over a period of 1 hour and 15 minutes (20 experiments). After integration of the ^1H NMR spectra, the data was analyzed using PRISM® graphical software.

5.2.4 Synthesis of *para*-substituted-d_3-styrenes

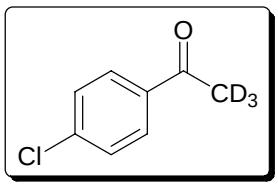

Synthesis of 4-chloro-α,α,α-trideutero-acetophenone[212]

An adapted procdure from Horino[212] was used as follows. A 250 mL rbf with stirbar was charged with Na metal (113 mg, 5 mmol). D_2O (5 mL) was added slowly dropwise with vigourous gas evolution and the resulting clear solution was further diluted with D_2O (40 mL, 2 mol). Neat 4-chloroacetophenone (9.28g, 7.8 mL, 60 mmol) was added to the NaOD/D_2O solution to give a milky white emulsion. After stirring for 24 hours at rt a sample was analyzed by ^{1}H NMR spectroscopy in D_2O and indicated >95% D incorporation. The reaction mixture was then diluted with Et_2O (50 mL), the organic separated and the aqueous layer was extracted with Et_2O (2 x 50 mL). The combined organics were dried with $MgSO_4$, filtered and concentrated to give a pale yellow liquid that was further purified by bulb-to-bulb distillation (155ºC/34 mmHg) to give a clear colourless liquid (8.885 g, 94%).

^{1}H NMR (600 MHz, $CDCl_3$), δ:

7.86 (d, *J* = 8.4 Hz, 2H), 7.40 (d, *J* = 8.4 Hz, 2H)

^{2}H NMR (92 MHz, $CDCl_3$), δ:

2.41 (s, 3D)

^{13}C NMR (150 MHz, $CDCl_3$), δ:

196.9, 139.5, 135.4, 129.7, 128.9, 25.8 (multiplet)

IR (NaCl, neat), cm^{-1}:

3090 (w), 3064 (w), 2255 (w) (C-D), 1683 (s) (C=O), 1591 (s), 1487 (s), 1399 (s), 1261 (s), 1177 (m), 1107 (m), 1089 (m), 1014 (m), 984 (s), 812 (s), 751 (s)

HRMS (TOF MS EI+):

calculated for $C_8H_4D_3ClO$ 157.0371, found 157.0318

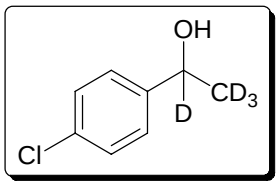

Synthesis of 1-deuterio-1-(4'-chlorophenyl)-2,2,2-trideuterioethanol[213]

The procedure of Buchwald[213] was followed as described here. A 250 mL rbf with stirbar equipped with a pressure-equalizing dropping funnel was charged with $LiAlD_4$ (0.325 eq, 771 mg, 16.5 mmol) and suspended in Et_2O (50 mL). The funnel was charged with a solution of 4-chloro-α,α,α-trideutero-acetophenone (8.00 g, 6.8 mL 50 mmol) in Et_2O (20 mL). The $LiAlD_4$ slurry was brought to reflux and the ketone solution added dropwise over 10 minutes. At the end of the addition, the funnel was rinsed with additional Et_2O (15 mL). The reaction mixture was left to stir at reflux overnight, allowed to cool back to rt, and then quenched slowly by the addition of 1 M H_2SO_4 (10 mL). The resulting emulsion was poured into a separatory funnel, the Et_2O layer separated and the aqueous slurry of $Al(OH)_x$ was broken up by the addition of 1 M HCl (~30 mL). Further extracted with Et_2O (2 x 50 mL) and the combined Et_2O extracts were dried with $MgSO_4$, filtered and concentrated to give a thick clear oil. Purification by flash chromatography (silica gel 7:1 hexanes:ethyl acetate) gave a clear sweet smelling oil (7.13 g, 88%).

^{1}H NMR (600 MHz,$CDCl_3$), δ:

7.30 (d, *J* =8.4 Hz, 2H), 7.27 (d, *J* = 8.4 Hz, 2H)

^{2}H NMR (92 MHz, $CHCl_3$), δ:

4.68 (s, 1D), 1.26 (s, 3D)

^{13}C NMR (150 MHz, $CDCl_3$), δ:

144.2, 133.1, 128.6, 126.8 (deuterated benzylic and methyl carbons not observed)

IR (NaCl, neat), cm^{-1}:

3350 (br), 2230 (s) (C-D), 2152 (s) (C-D), 1902 (br), 1599 (s), 1492 (s), 1400 (s), 1228 (m), 1145 (m), 1091 (m), 1073 (m), 1048 (m), 1012 (m), 928 (s), 843 (m), 805 (m)

HRMS (TOF MS EI+):

calculated for $C_8H_5D_4ClO$ 160.0589, found 160.0547

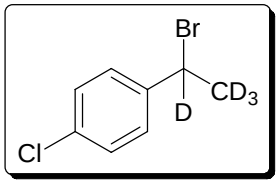

Synthesis of 1-deuterio-1-(4'-chlorophenyl)-2,2,2-trideuterio-1-bromoethane[214]

The procedure of Fu[214] was adapted for this substrate as outlined. A 250 mL rbf with stirbar, equipped with a pressure-equalizing dropping funnel was charged with the *d*$_4$-*para*-chlorobenzylic alcohol (6.19 g, 39 mmol) and pyridine (0.8 mL), then dissolved in CH_2Cl_2 (160 mL). The reaction mixture was cooled to ~ -10ºC with an ice-methanol bath and the funnel charged with CH_2Cl_2 (80 mL) and PBr_3 (3.7 mL, 1 equiv., 39 mmol) and this solution added dropwise over 10 minutes to give a milky solution with a purple-pink colouration. The funnel was rinsed with additional CH_2Cl_2 (10 mL) and then left to stir overnight. The now clear, colourless reaction mixture was quenched with saturated aqueous $NaHCO_3$ (100 mL), with gas evolution. The CH_2Cl_2 layer was separated, and the aqueous layer extracted with CH_2Cl_2 (3 x 50 mL). Combined organics were dried with $MgSO_4$, and this dried suspension was then filtered through a bed of basic alumina slurried in CH_2Cl_2 to provide a clear, colourless solution that was concentrated to yield clear oil (10.34 g). This material decomposes in the presence of light and traces of acid and was used immediately in the next step.

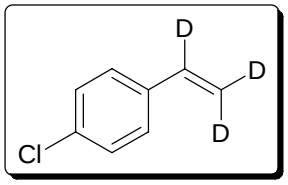

Synthesis of d_3-4-chlorostyrene

A 4-necked rbf with stirbar, equipped with a pressure-equalizing dropping funnel and reflux condenser was charged with *tert*-butyl alcohol (^{t}BuOH, 47.44 g, 640 mmmol, 8 equiv to K), placed in a warm water bath and pieces of K metal (3.34 g, 80 mmol, 2 equiv to alkyl halide) added under N_2 purge. The mixture is then brought to reflux to allow K metal to fully react and after 2 hours[228], the solution of KO^{t}Bu in ^{t}BuOH is diluted with THF (85 mL). The crude isolated d_4-4-chlorobenzylic bromide dissolved in THF (40 mL) was charged into the dropping funnel and added dropwise to the refluxing base solution to immediately give a milky orange reaction mixture. After 20 hours of reflux, the reaction mixture was diluted with distilled water (75 mL) and the organic layer separated, washed with distilled water (75 mL), brine (75 mL), dried with $MgSO_4$, then filtered and concentrated to give a golden orange liquid. This was subjected to flash chromatography (silica gel, pet ether bp 36-60ºC) to remove remaining ^{t}BuOH to give a clear liquid (4.27 g), that was then further purified by bulb-to-bulb distillation (110ºC/48 mm Hg) to give the desired styrene (3.24 g, 22.9 mmol, 59 % over 2 steps).

^{1}H NMR (600 MHz, $CDCl_3$), δ:

7.33 (d, J = 9 Hz, 2H), 7.28 (d, J = 9 Hz, 2H)

^{2}H NMR (92 MHz, $CHCl_3$), δ:

6.71 (s, 1D), 5.71 (s, 1D), 5.26 (s, 1D)

^{13}C NMR (150 MHz, $CDCl_3$), δ:

135.6, 133.1 128.8, 127.0 (alkene carbons not seen)

IR (NaCl, thin film), cm^{-1}:

2959 (m), 2928 (m), 2872 (w), 2056 (w), 1897 (w), 1589 (w), 1488 (m), 1465 (w), 1379 (w), 1092 (m), 1031 (m), 835 (m)

HRMS (TOF MS EI+):

calculated for $C_8H_4D_3Cl$ 141.6124, found 141.0423

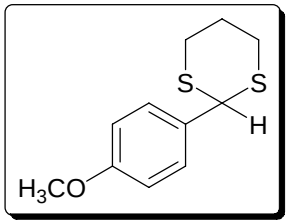

Synthesis of 2-(4'-methoxyphenyl)-1,3-dithiane[219]

The procedure of Patney[219] was followed with changes to the method of isolation. A 500 mL rbf with stirbar, was charged with 4-methoxybenzaldehyde (13.6 g, 100 mmol) and dissolved in CH_2Cl_2 (250 mL). 1,3-propanedithiol (12 mL, 1.2 equiv, 120 mmol) was added with vigourous stirring to give a clear colourless solution. Addition of $ZrCl_4$-SiO_2 powder (10 g, 1 g/10 mmol aldehyde) created a milky pale yellow suspension that was stirred for 20 hours at rt. The reaction mixture was then quenched with 2M NaOH (20 mL) and solid Na_2SO_4 (10 g). The congealed solids were filtered off and washed with CH_2Cl_2. The CH_2Cl_2 filtrates were extracted with 2M NaOH (2 x 150 mL), distilled water (1 x 150 mL), brine (1 x 150 mL) and dried with Na_2SO_4, filtered and concentrated to give a white crystalline solid (23.76 g). Recrystallization from boiling hexanes (800 mL) gave white needles that were collected by suction filtration, washed with cold hexanes and dried under vacuum to give the desired thioketal (20.11g, 89%).

^{1}H NMR (600 MHz, $CDCl_3$), δ:

7.38 (d, *J* = 8.4 Hz, 2H), 6.85 (d, *J* = 8.4 Hz, 2H), 5.12 (s, 1H), 3.78 (s, 3H), 3.04 (t, *J* = 14.4 Hz, 2H), 2.89 (m, 2H), 2.15 (m, 1H), 1.91 (m, 1H)

^{13}C NMR (150 MHz, $CDCl_3$), δ:

159.6, 131.3, 129.0, 114.1, 55.3, 50.7, 32.2, 25.1

IR (NaCl, thin film), cm^{-1}:

2937 (m), 2903 (m), 2836 (m), 1608 (s), 1581 (s), 1508 (s), 1463 (m), 1441 (m), 1415 (m), 1315 (m), 1302 (m), 1249 (m), 1180 (s), 1110 (m), 1030 (m) (1,3-dithiane ring), 847 (w), 817 (w)

HRMS (TOF MS EI+):

calculated for $C_{11}H_{14}OS_2$ 226.0486, found 226.0481

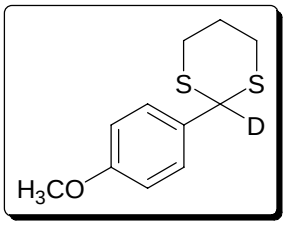

Synthesis of 2-deutero-2-(4'-methoxyphenyl)-1,3-dithiane

A 1000 mL rbf and stirbar, equipped with a pressure-equalizing dropping funnel was charged with dithiane (13.59 g, 60 mmol) and dissolved in THF (240 mL) and the milky solution cooled to 0ºC. The funnel was charged with n-BuLi (1.25 M in hexanes, 1.1 equiv, 66 mmol, 55 mL) and slowly added dropwise over 30 minutes to the cooled solution to give a bright orange reaction mixture. Further stirred for 30 minutes at 0ºC then a solution of D_2O (4 mL, 198 mmol) in THF (25 mL) added over 5 minutes. The now yellow reaction mixture was stirred at 0ºC for 30 minutes, and warmed to rt over 90 minutes. The reaction mixture was then concentrated to ¼ volume and partitioned between CH_2Cl_2 (200 mL) and water (150 mL). The CH_2Cl_2 layer was separated, dried with $MgSO_4$, filtered and concentrated to give a thick yellow oil that solidified on standing (16.60 g). This material was recrystallized from boiling hexanes (800 mL) to give yellow cubic crystals that were

collected by vacuum filtration, washed with cold hexanes and dried under vacuum to give the desired deuterated dithiane (9.70 g, 71%).

^{1}H NMR (600 MHz, $CDCl_3$), δ:

7.38 (d, *J* = 9 Hz, 2H, 6.85 (d, *J* = 9 Hz, 2H), 3.78 (s, 3H), 3.04 (t, *J* = 12.6 Hz, 2H), 2.88 (m, 2H), 2.15 (m, 1H), 1.92 (m, 1H)

^{2}H NMR (92 MHz, $CHCl_3$), δ:

5.19 (s, D)

^{13}C NMR (150 MHz, $CDCl_3$), δ:

159.8, 131.5, 129.1, 114.4, 55.6, 55.4, 32.4, 25.3

IR (NaCl, thin film), cm^{-1}:

2932 (m), 2891 (m), 2838 (w), 1610 (s), 1581 (m), 1512 (s), 1461 (m), 1442 (m), 1415 (m), 1301 (s), 1252 (s), 1178 (s), 1112 (s), 1030 (s) (1,3-dithiane ring), 906 (w), 892 (m), 834 (s), 817 (m)

HRMS (TOF MS EI+):

calculated for $C_{11}H_{13}DOS_2$ 227.0548, found 227.0546

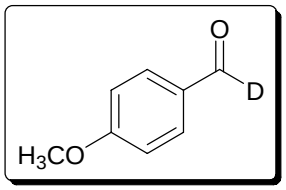

Synthesis of d_1-4'methoxybenzaldehyde[229]

Deprotection according to Chavan[229] required extended heating at reflux as described below. A 1000 mL rbf with stirbar was charged with deuterated dithiane (7.96 g, 35 mmol) and $FeCl_3$ (5.78 g, 35 mmol) and suspended in CH_3OH with heat evolution. To this stirred suspension was added KI (5.85 g, 35 mmol) to give a red-brown suspension, which was heated to reflux for 40 hours. After this time, the resulting clear orange solution was concentrated to give a brown

slurry that was taken up in Et_2O (200 mL) and distilled water (200 mL). The red organic layer was separated and the aqueous layer extracted with Et_2O (2 x 100 mL). Combined organics were dried with $MgSO_4$, filtered and concentrated to give a dark yellow liquid. Bulb-to-bulb distillation (180ºC/50 mm Hg) gave the title aldehyde as a yellow low-melting solid (4.45g, 93%).

^{1}H NMR (600 MHz, $CDCl_3$), δ:

7.77 (d, *J* = 9 Hz, 2H), 6.94 (d, *J* = 9 Hz, 2H), 3.89 (s, 3H)

^{2}H NMR (92 MHz,$CHCl_3$), δ:

9.78 (s, D)

^{13}C NMR (150 MHz, $CDCl_3$), δ:

190.4 (t), 164.6, 131.9, 129.9, 114.4, 55.6

IR (NaCl, thin film), cm^{-1}:

1674 (s) (C=O), 1600 (s), 1578 (m), 1511 (m), 1261 (s), 1163 (s), 1024 (m)

HRMS (TOF MS EI+):

calculated for $C_8H_7DO_2$ 137.0586, found 137.0590

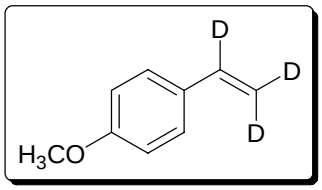

Synthesis of d_3-4-methoxystyrene[223]

The procedure of Tour[223] was applied using a deuterated aldehyde and C_1 fragment. A 100 mL rbf with stirbar was charged with *d_1*-4-methoxybenzaldehyde (3.46 g, 25 mmol) and suspended in THF (30 mL). Addition of zinc metal powder (5.23 g, 80 mmol, 8 equiv) and Cp_2ZrCl_2 (3.54 g, 12 mmol, 1.2 equiv) to gave a grey slurry. CD_2Br_2 was added dropwise and then left to stir under N_2 for 24 hours. A sample taken at this time was checked by ^{2}H NMR

and showed no aldehyde signal (9.78 ppm). The reaction mixture was quenched with H_2O (30 mL, violent reaction) and filtered through Celite to remove excess zinc. The yellow filtrate was diluted with and then extracted with CH_2Cl_2 and combined organics washed with 2M HCl (2 x 200 mL), H_2O (1 x 200 mL) and brine (1 x 200 mL). Dried with $MgSO_4$ and filtered to give a yellow solution that was concentrated to give a yellow liquid. Purification by flash chromatography (silica gel, hexanes) gave the desired styrene (0.326 g, 24 %).

^{1}H NMR (600 MHz, $CDCl_3$), δ:

7.35 (d, *J* = 9 Hz, 2H), 6.86 (d, *J* = 9 Hz, 2H), 3.82 (s, 3H)

^{2}H NMR (92 MHz,$CHCl_3$), δ:

6.68 (s, 1D), 5.62 (s, 1D), 5.14 (s, 1D)

^{13}C NMR (150 MHz, $CDCl_3$), δ:

159.4, 135.7 (t), 130.4, 127.3, 113.9, 110.7 (m), 55.2

IR (NaCl, thin film), cm^{-1}:

3002 (w), 2955 (m), 2836 (s), 2207 (w), 2051 (w), 1610 (s), 1583 (s), 1507 (s), 1465 (m), 1442 (m), 1299 (s), 1250 (s), 1177 (s), 1114 (m), 1033 (s), 837 (s)

HRMS (TOF MS EI+):

calculated for $C_9H_7D_3O$ 137.1933, found 137.0839

References

(1) Brown, H.C., *Hydroboration*. **1962**, New York: W. A. Benjamin Inc. 290.
(2) Brown, H.C., *Boranes in Organic Chemistry*. **1972**, Ithica: Cornell University Press. 462.
(3) Brown, H.C., *Organic Syntheses via Boranes*. **1975**, Toronto: John Wiley & Sons. 283.
(4) Brown, H.C. and Zweifel, G. *J. Am. Chem. Soc.* **1960**, *82*, 4708-4712.
(5) Pelter, A.;Smith, K., and Brown, H.C., *Borane Reagents*. Best Synthetic Methods, ed. A.R. Katritzky, O. Meth-Cohn, and C.W. Rees. **1988**, San Deigo: Academic Press Limited. 503.
(6) Brown, H.C. and Sharp, R.L. *J. Am. Chem. Soc.* **1966**, *88*, 5851-5854.
(7) Männig, D. and Nöth, H. *Angew. Chem. Int. Ed. Eng.* **1985**, *24*, 878-879.
(8) Wilczynski, R. and Sneddon, L.G. *Inorg. Chem.* **1981**, *20*, 3955-3962.
(9) Wilczynski, R. and Sneddon, L.G. *Inorg. Chem.* **1982**, *21*, 506-514.
(10) Crudden, C.M.;Hleba, Y.B., and Chen, A.C. *J. Am. Chem. Soc.* **2004**, *123*, 9200-9201.
(11) Miyaura, N.;Yamamoto, Y.;Fujikawa, R., and Umemoto, T. *Tetrahedron* **2004**, *60*, 10695-10700.
(12) He, X. and Hartwig, J.F. *J. Am. Chem. Soc.* **1996**, *118*, 1696-1702.
(13) Pender, M.J.;Carroll, P.J., and Sneddon, L.G. *J. Am. Chem. Soc.* **2001**, *123*, 12222-12231.
(14) Burgess, K. and van der Donk, W.A. *J. Am. Chem. Soc.* **1994**, *116*, 6561-6569.
(15) Srebnik, M. and Pereira, S. *Organometallics* **1995**, *14*, 3127-3128.
(16) Srebnik, M. and Pereira, S. *Tetrahedron Lett.* **1996**, *37*, 3283-3286.
(17) Srebnik, M. and Pereira, S. *J. Am. Chem. Soc.* **1996**, *118*, 909-910.
(18) Sneddon, L.G. and Wilczynski, R. *J. Am. Chem. Soc.* **1980**, *102*, 2857-2858.
(19) Zaidlewicz, M. and Meller, J. *Tetrahedron Lett.* **1997**, *38*, 7279-7282.
(20) Zaidlewicz, M. and Meller, J. *Main Group Met. Chem.* **2000**, *23*, 765-772.
(21) Zaidlewicz, M. and Meller, J. *Collect. Czech. Chem. Commun.* **1999**, *64*, 1049-1056.
(22) Kabalka, G.W.;Narayana, C., and Reddy, N.K. *Synth. Commun.* **1994**, *24*, 1019-1023.
(23) Gridnev, I.D.;Miyaura, N., and Suzuki, A. *Organometallics* **1993**, *12*, 589-592.
(24) Davan, T.;Corcoran Jr., E.W., and Sneddon, L.G. *Organometallics* **1983**, *2*, 1693-1694.
(25) Satoh, M.;Nomoto, Y.;Miyaura, N., and Suzuki, A. *Tetrahedron Lett.* **1989**, *30*, 3789-3792.
(26) Burgess, K. and Jaspars, M. *Organometallics* **1993**, *12*, 4197-4200.
(27) Burgess, K. and Jaspars, M. *Tetrahedron Lett.* **1993**, *34*, 6813-6816.
(28) Marks, T.J. and Harrison, K.N. *J. Am. Chem. Soc.* **1992**, *114*, 9220-9221.
(29) Molander, G.A. and Pfeiffer, D. *Org. Lett.* **2001**, *3*, 361-363.
(30) Evans, D.A.;Muci, A.R., and Stürmer, R. *J. Org. Chem.* **1993**, *58*, 5307-5309.

(31) Kettler, P.B. *Org. Process Res. Dev.* **2003**, *7*, 342-354.
(32) Evans, P.A., ed. *Modern Rhodium-Catalyzed Organic Reactions*. 2005, Wiley-VCH: Grünstadt. 473.
(33) Jardine, F.H., *Chlorotris(triphenylphosphine)rhodium(I): Its Chemical and Catalytic Reactions*, in *Progress in Inorganic Chemistry*, S.J. Lippard, Eds.; 1981, John Wiley & Sons: Toronto. p. 63-202.
(34) Kono, H.;Ito, K., and Nagai, Y. *Chem. Lett.* **1975**, 1095-1096.
(35) Evans, D.A.;Fu, G.C., and Anderson, B.A. *J. Am. Chem. Soc.* **1992**, *114*, 6679-6685.
(36) Burgess, K.;van der Donk, W.A.;Westcott, S.A.;Marder, T.B.;Baker, R.T., and Calabrese, J.C. *J. Am. Chem. Soc.* **1992**, *114*, 9350-9359.
(37) Baker, R.T.;Westcott, S.A.;Blom, H.P., and Marder, T.B. *J. Am. Chem. Soc.* **1992**, *114*, 8863-8869.
(38) Marder, T.B.;Baker, R.T., and Westcott, S.A. *Organometallics* **1993**, *12*, 975-979.
(39) Marder, T.B.;Baker, R.T.;Westcott, S.A.;Blom, H.P., and Calabrese, J.C. *Inorg. Chem.* **1993**, *32*, 2175-2182.
(40) Evans, D.A.;Fu, G.C., and Hoveyda, A.H. *J. Am. Chem. Soc.* **1992**, *114*, 6671-6679.
(41) Baldwin, J.E.;Barden, T.C.;Pugh, R.L., and Widdison, W.C. *J. Org. Chem.* **1987**, *52*, 3303-3307.
(42) Blum, J.;Rosenman, H., and Bergmann, E.D. *Tetrahedron Lett.* **1967**, 3665-3668.
(43) Birch, A.J. and Subba Rao, G.S.R. *Tetrahedron Lett.* **1968**, 2917-2918.
(44) Jun, C.-H. and Lee, J.H. *Pure Appl. Chem.* **2004**, *76*, 577-587.
(45) Osborn, J.A.;Jardine, F.H.;Young, J.A., and Wilkinson, G. *J. Chem. Soc. A* **1966**, 1711.
(46) Ogle, C.A.;Masterman, T.C., and Hubbard, J.L. *J. Chem. Soc., Chem. Commun.* **1990**, 1733-1734.
(47) Dunbar, K.R. and Haefner, S.C. *Inorg. Chem.* **1992**, *31*, 3676-3679.
(48) Burgess, K.;van der Donk, W.A., and Kook, A.M. *J. Org. Chem.* **1991**, *56*, 2949-2951.
(49) Geoffroy, G.L. and Keeney, M.E. *Inorg. Chem.* **1977**, *16*, 205-207.
(50) Bennett, M.J. and Donaldson, P.B. *Inorg. Chem.* **1977**, *16*, 1585-1589.
(51) Carvalho, M.;Wieserman, L.F., and Hercules, D.M. *Appl. Spectrosc.* **1982**, *36*, 290-296.
(52) Vaska, L. *J. Am. Chem. Soc.* **1960**, *83*, 756.
(53) Vaska, L. and DiLuzio, J.W. *J. Am. Chem. Soc.* **1961**, *83*, 2784-2785.
(54) Vaska, L. and DiLuzio, J.W. *J. Am. Chem. Soc.* **1962**, *84*, 679-680.
(55) Vaska, L. and DiLuzio, J.W. *J. Am. Chem. Soc.* **1965**, *87*, 4970-4971.
(56) Vaska, L. and Catone, D.L. *J. Am. Chem. Soc.* **1966**, *88*, 5324-5325.
(57) Bennett, M.A. and Milner, D.L. *J. Am. Chem. Soc.* **1969**, *91*, 6983-6994.
(58) Cotton, S.A., *Chemistry of Precious Metals*. **1997**, Bristol: Blackie Academic and Professional. 374.
(59) Westcott, S.A.;Marder, T.B.;Baker, R.T., and Calabrese, J.C. *Can. J. Chem.* **1993**, *71*, 930-936.
(60) Knorr, J.R. and Merola, J. *Organometallics* **1990**, *9*, 3008-3010.

(61) Ohmura, T.;Yamamoto, Y., and Miyaura, N. *J. Am. Chem. Soc.* **2000**, *122*, 4990-4991.
(62) Hartwig, J.F.;Nolan, S.P., and Rablen, P.R. *J. Am. Chem. Soc.* **1994**, *116*, 4121-4122.
(63) Widauer, C.;Grutzmacher, H., and Ziegler, T. *Organometallics* **2000**, *19*, 2097-2107.
(64) Hayashi, T.;Matsumoto, Y., and Ito, Y. *J. Am. Chem. Soc.* **1989**, *111*, 3426-3428.
(65) Masuda, Y.;Watanabe, S., and Murata, M. *Tetrahedron Lett.* **1999**, *40*, 2585-2588.
(66) Masuda, Y.;Murata, M.;Kawakita, K.;Asana, T., and Watanabe, S. *Bull. Chem. Soc. Jpn.* **2002**, *75*, 825-829.
(67) Rose, S.H. and Shore, S.G. *Inorg. Chem.* **1962**, *1*, 744-748.
(68) Woods, W.G. and Strong, P.L. *J. Am. Chem. Soc.* **1966**, *88*, 4667-4671.
(69) Fish, R.H. *J. Org. Chem.* **1973**, *33*, 158-159.
(70) Fish, R.H. *J. Am. Chem. Soc.* **1968**, *90*, 4435-4439.
(71) Brown, H.C. and Gupta, S.K. *J. Am. Chem. Soc.* **1971**, *93*, 1816-1818.
(72) Brown, H.C. and Gupta, S.K. *J. Am. Chem. Soc.* **1975**, *97*, 5249-5255.
(73) Brown, H.C. and Gupta, S.K. *J. Am. Chem. Soc.* **1972**, *94*, 4370-4371.
(74) Lane, C.F. and Kabalka, G.W. *Tetrahedron* **1976**, *32*, 981-990.
(75) Miyaura, N. and Suzuki, A. *Chem. Rev.* **1995**, *95*, 2457-2483.
(76) Corey, E.J.;Link, J.O., and Bakshi, R.K. *Tetrahedron Lett.* **1992**, *33*, 7107.
(77) Kabalka, G.W. *Org. Prep. Proced. Int.* **1977**, *9*, 131-147.
(78) Brown, H.C.;Kanth, J.V.B., and Periasamy, M. *Org. Process Res. Dev.* **2000**, *4*, 550-553.
(79) Morrill, T.C.;D'Souza, C.A.;Yang, L., and Sampognaro, A.J. *J. Org. Chem.* **2002**, *67*, 2481-2484.
(80) Kollonitsch, J. *J. Am. Chem. Soc.* **1961**, *83*, 1515.
(81) Fu, G.C. and Garrett, C.E. *J. Org. Chem.* **1996**, *61*, 3224-3225.
(82) Knochel, P.;Tucker, C.E., and Davidson, J. *J. Org. Chem.* **1992**, *57*, 3482-3485.
(83) Edwards, D.R.;Crudden, C.M., and Yam, K. *Adv. Synth. Catal.* **2005**, *347*, 50-54.
(84) Brinkman, J.A. and Sowa Jr., J.R., *New Rhodium Catalysts for the Regioselective and Enantioselective Hydroboration of Styrene*, in *Catalysis of Organic Reactions*, F.E. Herkes, Eds.; 1998, Marcel Dekker Inc.: New York. p. 642.
(85) Coapes, R.B.;Souza, F.E.S.;Thomas, R.L.;Hall, J.J., and Marder, T.B. *Chem. Commun.* **2003**, 614-615.
(86) Murata, M.;Oyama, T.;Watanabe, S., and Masuda, Y. *J. Org. Chem.* **2000**, *65*, 164-168.
(87) Zhu, W. and Ma, D. *Org. Lett.* **2006**, *8*, 261-263.
(88) Ishiyama, T.;Murata, M.;Ahiko, T.-a., and Miyaura, N. *Org. Synth.* **2000**, *77*, 176-179.
(89) Ishiyama, T. and Miyaura, N. *Chem. Rec.* **2004**, *3*, 271-280.
(90) Lawerence, J.D.;Takahashi, M.;Bae, C., and Hartwig, J.F. *J. Am. Chem. Soc.* **2004**, *126*, 15334-15335.
(91) Westcott, S.A.;Vogels, C.M.;O'Connor, P.E.;Phillips, T.E.;Watson, K.J.;Shaver, M.P., and Hayes, P.G. *Can. J. Chem.* **2001**, *79*, 1898-1905.

(92) Vogels, C.M.;Hayes, P.G.;Shaver, M.P., and Westcott, S.A. *Chem. Commun.* **2000**, 51-52.
(93) Nöth, H.;Lang, A., and Thomann-Albach, M. *Chem. Ber. Recl.* **1997**, *130*, 363-369.
(94) Nozaki, K.;Yoshida, M., and Takaya, H. *Bull. Chem. Soc. Jpn.* **1996**, *69*, 2043-2052.
(95) Arase, A.;Nunokawa, Y.;Masuda, Y., and Hoshi, M. *J. Chem. Soc., Chem. Commun.* **1991**, 205-206.
(96) Darmency, V.;Scanlan, E.M.;Schnaffner, A.P., and Renaud, P. *Org. Synth.* **2006**, *83*, 24.
(97) Suseela, Y.;Prasad, A.S.B., and Periasamy, M. *J. Chem. Soc., Chem. Commun.* **1990**, 446.
(98) Brown, J.M. and Lloyd-Jones, G.C. *Tetrahedron Asymmetry* **1990**, *1*, 869-872.
(99) Brown, J.M. and Lloyd-Jones, G.C. *J. Chem. Soc., Chem. Commun.* **1992**, 710-712.
(100) Brown, J.M. and Lloyd-Jones, G.C. *J. Am. Chem. Soc.* **1994**, *116*, 866-878.
(101) Brown, H.C. and Ramachandran, P.V. *Pure Appl. Chem.* **1991**, *63*, 307-316.
(102) Matteson, D.S.;Sadhu, K.M., and Peterson, M.L. *J. Am. Chem. Soc.* **1986**, *108*, 810.
(103) Crudden, C.M.;Chen, A., and Ren, L. *J. Org. Chem.* **1999**, *64*, 9704-9710.
(104) Crudden, C.M.;Chen, A.C., and Ren, L. *Chem. Commun.* **1999**, 661-612.
(105) Bal, B.S.;Childers Jr., W.E., and Pinnick, H.W. *Tetrahedron* **1981**, *37*, 2091-2096.
(106) Fernandez, E.;Hooper, M.W.;Knight, F.I., and Brown, J.M. *Chem. Commun.* **1997**, 173-174.
(107) Fernandez, E.;Maeda, K.;Hooper, M.W., and Brown, J.M. *Chem. Eur. J.* **2000**, *6*, 1840-1846.
(108) Rieu, J.-P.;Boucherle, A.;Cousse, H., and Mouzin, G. *Tetrahedron* **1986**, *42*, 4095-4131.
(109) Green, G.A. *Clin. Corner.* **2002**, *3*, 50-59.
(110) Green, M.;Kuc, T.A., and Taylor, S.H. *J. Chem. Soc. (A)* **1971**, 2334-2337.
(111) Schrock, R.R. and Osborn, J.A. *J. Am. Chem. Soc.* **1971**, *93*, 3089-3091.
(112) Schrock, R.R. and Osborn, J.A. *J. Am. Chem. Soc.* **1971**, *93*, 2397-2407.
(113) Slack, D.A.;Greveling, I., and Baird, M.C. *Inorg. Chem.* **1979**, *18*, 3125-3132.
(114) van Leeuwen, P.W.N.M.;Kamer, P.C.;Reek, J.N., and Dierkes, P. *Chem. Rev.* **2000**, *100*, 2741-2769.
(115) Burgess, K. and van der Donk, W.A. *Inorg. Chim. Acta* **1994**, *220*, 93-98.
(116) Sanger, A.R. *J. Chem. Soc., Dalton Trans.* **1977**, 120-129.
(117) Segarra, A.M.;Daura-Oller, E.;Claver, C.;Poblet, J.M.;Bo, C., and Fernández, E. *Chem. Eur. J.* **2004**, *10*, 6456-6467.
(118) Wiesauer, C. and Weissensteiner, W. *Tetrahedron: Asymmetry* **1996**, *7*, 5-8.
(119) Sanger, A.R. *J. Chem. Soc., Dalton Trans.* **1981**, 228-233.
(120) Sanger, A.R. *J. Chem. Soc., Dalton Trans.* **1977**, 1971-1976.
(121) Perez Luna, A.;Bonin, M.;Micouin, L., and Husson, H.-P. *J. Am. Chem. Soc.* **2003**, *124*, 12098-12099.

(122) Lesley, G.;Nguyen, P.;Taylor, N.J.;Marder, T.B.;Scott, A.J.;Clegg, W., and Norman, N.C. *Organometallics* **1996**, *15*, 5137-5154.
(123) Brunel, J.M.;Faure, B., and Maffei, M. *Coord. Chem. Rev.* **1998**, *178-180*, 665-698.
(124) Moteki, S.A.;Wu, D.;Chandra, K.L.;Reddy, D.S., and Takacs, J.M. *Org. Lett.* **2006**, *8*, 3097-3100.
(125) Togni, A.;Breutel, C.;Schnyder, A.;Spindler, F.;Landert, H., and Tijani, A. *J. Am. Chem. Soc.* **1994**, *116*, 4062-4066.
(126) Blume, F.;Zemolka, S.;Fey, T.;Kranich, R., and Schmalz, H.-G. *Adv. Synth. Catal.* **2002**, *344*, 868-883.
(127) Brown, J.M.;Hulmes, D.I., and Layzell, T.P. *J. Chem. Soc., Chem. Commun.* **1993**, 1673-1674.
(128) Brown, J.M.;Hulmes, D.I., and Guiry, P.J. *Tetrahedron* **1994**, *50*, 4493-4506.
(129) Valk, J.M.;Whitlock, G.A.;Layzell, T.P., and Brown, J.M. *Tetrahedron: Asymmetry* **1995**, *6*, 2593-2596.
(130) McCarthy, M. and Guiry, P.J. *Polyhedron* **2000**, *19*, 541-543.
(131) McCarthy, M.;Hooper, M.W., and Guiry, P.J. *Chem. Commun.* **2000**, 1333-1334.
(132) Connolly, D.J.;Lacey, P.M.;McCarthy, M.;Saunders, C.P.;Carroll, A.-M.;Goddard, R., and Guiry, P.J. *J. Org. Chem.* **2004**, *69*.
(133) Kwong, F.Y.;Yang, Q.;Mak, T.C.W.;Chan, A.S.C., and Chan, K.S. *J. Org. Chem.* **2002**, *67*, 2769-2777.
(134) Crudden, C.M. and Edwards, D. *Eur. J. Org. Chem.* **2003**, 4695-4712.
(135) Brown, J.M., *Rhodium-Catalyzed Hydroborations and Related Reactions*. Modern Rhodium-Catalyzed Organic Reactions, ed. P.A. Evans. **2005**, Grünstadt: Wiley-VCH. 473.
(136) Doucet, H.;Fernandez, E.;Layzell, T.P., and Brown, J.M. *Chem. Eur. J.* **1999**, *5*, 1320-1330.
(137) Noyori, R., *Asymmetric Catalysis in Organic Synthesis*. **1994**, New York: Wiley-Interscience.
(138) Morimoto, T.;Nakajima, N., and Achiwa, K. *Tetrahedron:Asymmetry* **1995**, *6*, 23-26.
(139) Burckhardt, U.;Baumann, M., and Togni, A. *Tetrahedron: Asymmetry* **1997**, *8*, 155-159.
(140) Daura-Oller, E.;Segarra, A.M.;Poblet, J.M.;Claver, C.;Fernandez, E., and Bo, C. *J. Org. Chem.* **2004**, *69*, 2669-2680.
(141) Burgess, K.;van der Donk, W.A., and Ohlmeyer, M.J. *Tetrahedron Asymmetry* **1991**, *2*, 613-621.
(142) Burgess, K.;Ohlmeyer, M.J., and Whitmire, K.H. *Organometallics* **1992**, *11*, 3588-3600.
(143) Uozumi, Y.;Tanahashi, A.;Lee, S.-Y., and Hayashi, T. *J. Org. Chem.* **1993**, *58*, 1945-1948.
(144) Junge, K.;Hagemann, B.;Enthaler, S.;Oehme, G.;Michalik, M.;Monsees, A.;Riermeier, T.;Dingerdissen, U., and Beller, M. *Angew. Chem. Int. Ed. Eng.* **2004**, *43*, 5066-5069.

(145) Junge, K.;Hagemann, B.;Enthaler, S.;Spannenberg, A.;Michalik, M.;Oehme, G.;Monsees, A.;Riermeier, T., and Beller, M. *Tetrahedron: Asymmetry* **2004**, *15*, 2621-2631.
(146) Enthaler, S.;Hagemann, B.;Junge, K.;Erre, G., and Beller, M. *Eur. J. Org. Chem.* **2006**, 2912-2917.
(147) Boaz, N.W.;Debenham, S.D.;Mackenzie, E.B., and Large, S.E. *Org. Lett.* **2002**, *4*, 2421-2424.
(148) Demay, S.;Volant, F., and Knochel, P. *Angew. Chem. Int. Ed. Eng.* **2001**, *40*, 1235-1238.
(149) Burckhardt, U.;Hintermann, L.;Schnyder, A., and Togni, A. *Organometallics* **1995**, *14*, 5415-5425.
(150) Schnyder, A.;Hintermann, L., and Togni, A. *Angew. Chem. Int. Ed. Eng.* **1995**, *34*, 931-933.
(151) Schnyder, A.;Togni, A., and Wiesli, U. *Organometallics* **1997**, *16*, 255-260.
(152) Blaser, H.-U.;Brieden, W.;Pugin, B.;Spindler, F.;Studer, M., and Togni, A. *Top. Catal.* **2002**, *19*, 3-16.
(153) Hayashi, T.;Matsumoto, Y., and Ito, Y. *Tetrahedron Asymmetry* **1991**, *2*, 601-612.
(154) Kurosawa, H. and Ikeda, I. *J. Organomet. Chem.* **1992**, *428*, 289-301.
(155) Gevorgyan, V.;Rubina, M., and Rubin, M. *J. Am. Chem. Soc.* **2003**, *125*, 7198-7199.
(156) Brown, J.M. and Chaloner, P.A. *J. Chem. Soc., Chem. Commun.* **1980**, 344-346.
(157) Chan, A.S.C.;Pluth, J.J., and Halpern, J. *J. Am. Chem. Soc.* **1980**, *102*, 5952-5954.
(158) Jendralla, H.;Li, C.H., and Paulus, E. *Tetrahedron Asymmetry* **1994**, *5*, 1297-1320.
(159) Yudin, A.K.;Martyn, J.P.;Pandiaraju, S.;Zheng, J., and Lough, A. *Org. Lett.* **2000**, *2*, 41-44.
(160) Nugent, W.A. and McKinney, R.J. *J. Org. Chem.* **1985**, *50*, 5370-5372.
(161) Musaev, D.G.;Mebel, A.M., and Morokuma, K. *J. Am. Chem. Soc.* **1994**, *116*, 10693-10702.
(162) von Ragué Schleyer, P. and Dorigo, A.E. *Angew. Chem. Int. Ed. Eng.* **1995**, *34*, 115-118.
(163) Baker, R.T.;Nguyen, P.;Marder, T.B., and Westcott, S.A. *Angew. Chem. Int. Ed. Eng.* **1995**, *34*, 1336-1338.
(164) Dai, C.;Robins, E.G.;Scott, A.J.;Clegg, W.;Yufit, D.S.;Howard, J.A.K., and Marder, T.B. *Chem. Commun.* **1998**, 1983-1984.
(165) Morgan, J.B.;Miller, S.P., and Morken, J.P. *J. Am. Chem. Soc.* **2003**, *125*, 8702-8703.
(166) Trudeau, S.;Morgan, J.B.;Shrestha, M., and Morken, J.P. *J. Org. Chem.* **2005**, *70*, 9538-9544.
(167) Guiry, P.J.;Carroll, A.-M., and O'Sullivan, T.P. *Adv. Synth. Catal.* **2005**, *347*, 609-631.
(168) Thomas, A.F., *Deuterium Labeling in Organic Chemistry*. **1971**, New York: Meredith Corporation. 518.
(169) Martin, M.L. and Martin, G.J., *Deuterium NMR in the Study of Site-Specific Natural Isotope Fractionation (SNIF-NMR)*, in *NMR Basic Principles and Progress*, P. Diehl, et al., Eds.; 1991, Springer-Verlag: New York. p. 1-61.

(170) Evans, D.A. and Fu, G.C. *J. Org. Chem.* **1990**, *55*, 2280-2282.
(171) Evans, D.A. and Fu, G.C. *J. Am. Chem. Soc.* **1991**, *113*, 4042-4043.
(172) Brown, J.M. and Kent, A.G. *J. Chem. Soc., Perkin Trans. 2* **1987**, 1597-1607.
(173) Hayashi, T.;Tanaka, M., and Ogata, I. *J. Mol. Catal.* **1981**, *13*, 323-330.
(174) Yu, J. and Spencer, J.B. *J. Am. Chem. Soc.* **1997**, *119*, 5257-5258.
(175) Werner, H. and Feser, R. *J. Organomet. Chem.* **1982**, *232*, 351-370.
(176) Werner, H.;Schäfer, M.;Nürnberg, O., and Wolf, J. *Chem. Ber.* **1994**, *127*, 27-38.
(177) Fryzuk, M.D.;McConville, D.H., and Rettig, S.J. *J. Organomet. Chem.* **1993**, *445*, 245-256.
(178) Stuhler, H.-O. and Pickardt, J. *Z. Naturforsch* **1981**, *36b*, 315-321.
(179) Brown, H.C. and Subba Rao, B.C. *J. Am. Chem. Soc.* **1959**, *81*, 6434-6437.
(180) Brown, H.C. and Zweifel, G. *J. Am. Chem. Soc.* **1966**, *88*, 1433-1439.
(181) Augustine, R.L. and van Peppen, J.F. *Chem. Commun.* **1970**, 495-496.
(182) Cipot, J.;Vogels, C.M.;McDonald, R.;Westcott, S.A., and Stradiotto, M. *Organometallics* **2006**, *25*, 5962-5968.
(183) Klei, S.R.;Golden, J.T.;Tilley, T.D., and Bergman, R.G. *J. Am. Chem. Soc.* **2002**, *124*, 2092-2093.
(184) Herde, J.L.;Lambert, J.C., and Senoff, C.V. *Inorg. Synth.* **1974**, *15*, 18-21.
(185) Lin, Y.;Nomiya, K., and Finke, R.G. *Inorg. Chem.* **1993**, *32*, 6040-6045.
(186) Lipshutz, B.H.;Frieman, B., and Birkedal, H. *Org. Lett.* **2004**, *6*, 2305-2308.
(187) Robinson, S.D. and Shaw, B.L. *J. Chem. Soc.* **1965**, 4997-5011.
(188) Shaw, B.L. *Chem. Commun.* **1968**, 464.
(189) Winkhaus, G. and Singer, H. *Chem. Ber.* **1966**, *99*, 3610-3618.
(190) Cramer, R. *J. Am. Chem. Soc.* **1966**, *88*, 2272-2282.
(191) Kuznetsov, V.L.;Mudrakovskii, I.L.;Romanenko, A.V.;Pashis, A.V.;Mastikhin, V.M., and Yermakov, Y.I. *React. Kinet. Catal. Lett.* **1984**, *25*, 137-141.
(192) Usui, Y.;Wakai, C.;Matubayasi, N., and Nakahara, M. *Chem. Lett.* **2004**, *33*, 394-395.
(193) Eberhardt, G.G. and Vaska, L. *J. Catal.* **1967**, *8*, 183-188.
(194) Strathdee, G. and Given, R. *Can. J. Chem.* **1975**, *53*, 106-113.
(195) Wilkinson, G. *Bull. Soc. Chim. Fr.* **1968**, 5055-5058.
(196) O'Connor, C. and Wilkinson, G. *J. Chem. Soc. (A)* **1968**, 2665-2671.
(197) Evans, D.;Yagupsky, G., and Wilkinson, G. *J. Chem. Soc. (A)* **1968**, 2660-2665.
(198) Callaghan, P.L.;Fernández-Pacheco, R.;Jasim, N.;Lachaize, S.;Marder, T.B.;Perutz, R.N.;Rivalta, E., and Sabo-Etienne, S. *Chem. Commun.* **2004**, 242-243.
(199) Frosin, K.M. and Dahlenburg, L. *Inorg. Chim. Acta* **1990**, *167*, 83-89.
(200) Itoh, K.;Nagashima, H.;Ohshima, T.;Oshima, N., and Nishiyama, H. *J. Organomet. Chem.* **1984**, *272*, 179-188.
(201) Pertici, P.;Vitulli, G.;Paci, M., and Porri, L. *J. Chem. Soc., Dalton Trans.* **1980**, 1961-1964.
(202) Miyaura, N.;Ishiyama, T.;Ishida, K., and Takagi, J. *Chem. Lett.* **2001**, 1082-1083.
(203) Morgan, J.B. and Morken, J.P. *J. Am. Chem. Soc.* **2004**, *126*, 15338-15339.
(204) Hoel, E.L. and Hawthorne, M.F. *J. Am. Chem. Soc.* **1974**, *96*, 4676-4677.
(205) Hoel, E.L.;Talebinasab-Savari, M., and Hawthorne, M.F. *J. Am. Chem. Soc.* **1977**, *99*, 4356-4367.

(206) Emerson, W.S. *Chem. Rev.* **1949**, *45*, 347-383.
(207) Rybtchinski, B.;Cohen, R.;Ben-David, Y.;Martin, J.M.L., and Milstein, D. *J. Am. Chem. Soc.* **2003**, *125*, 11041-11050.
(208) Fu, G.C. and Netherton, M.R. *Org. Lett.* **2001**, *3*, 4295-4298.
(209) Corey, E.J. and Fuchs, P.L. *Tetrahedron Lett.* **1972**, *36*, 3769-3772.
(210) Morris, J. and Wishka, D.G. *Synthesis* **1994**, 43-46.
(211) Cram, D.J. and Allinger, N.L. *J. Am. Chem. Soc.* **1955**, *78*, 2518-2524.
(212) Horino, Y.;Kimura, M.;Tanaka, S.;Okajima, T., and Tamaru, Y. *Chem. Eur. J.* **2003**, *9*, 2419-2438.
(213) Buchwald, S.L.;Nielsen, R.B., and Dewan, J.C. *Organometallics* **1989**, *8*, 1593-1598.
(214) Fu, G.C. and Arp, F.O. *J. Am. Chem. Soc.* **2005**, *127*, 10482-10483.
(215) Wolkoff, P. *J. Org. Chem.* **1982**, *47*, 1944-1948.
(216) Steiner, U. and Schinz, H. *Helv. Chim. Acta* **1951**, *34*, 1176-1183.
(217) Hollywood, F. and Suschitzky, H. *Synthesis* **1982**, *8*, 662-665.
(218) Simoni, D.;Rossi, M.;Rondanin, R.;Mazzali, A.;Baruchello, R.;Malagutti, C.;Roberti, M., and Invidiata, F.P. *Org. Lett.* **2000**, *2*, 3765-3768.
(219) Patney, H.K. and Margan, S. *Tetrahedron Lett.* **1996**, *37*, 4621-4622.
(220) Ho, T.-L.;Ho, H.C., and Wong, C.M. *J. Chem. Soc., Chem. Commun.* **1972**, 791.
(221) Sabot, C.;Kumar, K.A.;Antheaume, C., and Mioskowski, C. *J. Org. Chem.* **2007**, *asap*, asap.
(222) Kampfen, U. and Eschenmoser, A. *Helv. Chim. Acta* **1989**, *72*, 185-195.
(223) Tour, J.M.;Bedworth, P.V., and Wu, R. *Tetrahedron Lett.* **1989**, *30*, 3927-3930.
(224) Still, W.C.;Kahn, M., and Mitra, A. *J. Org. Chem.* **1978**, *43*, 2923-2925.
(225) Armarego, W.L.F. and Perrin, D.D., *Purification of Laboratory Chemicals 4th Edition*. **1997**, New York: Pergamon.
(226) Honore, T.;Jacobsen, P.;Nielsen, F.E., and Naerum, L. 5,026,704. **1991.**
(227) Detert, H. and Sugiono, E. *J. Prakt. Chem.* **1999**, *341*, 358-362.
(228) Johnson, W.S. and Schnieder, W.P. *Org. Synth.* **1950**, *30*, 18.
(229) Chavan, S.P.;Soni, P.B.;Kale, R.R., and Pasupathy, K. *Synth. Commun.* **2003**, *33*, 879-883.